Republic of Iraq
Ministry of Higher Education and Scientific Research
University of Babylon
College of Engineering
Electrical Engineering Department

Implementation of Electro-Plasmonics Chip for Detection Alzheimer Disease

A Thesis

Submitted to the College of Engineering of the University of Babylon in Partial Fulfillment of the Requirements for the Degree of Doctor of Philosophy in Engineering / Electrical Engineering / Electronics and Communications

By
Hussam Jawad Kadhim Abood Al-Janabi

Supervised by
Asst. Prof. Dr.Haider Al-Mumen
Asst .Prof. Dr.Hussein Hadi Nahi

2023 A.D. **1444 A.H.**

بِسۡمِ ٱللَّهِ ٱلرَّحۡمَٰنِ ٱلرَّحِيمِ

﴿يُؤْتِي الْحِكْمَةَ مَن يَشَاءُ ۚ وَمَن يُؤْتَ

الْحِكْمَةَ فَقَدْ أُوتِيَ خَيْرًا كَثِيرًا ۗ وَمَا يَذَّكَّرُ

إِلَّا أُولُو الْأَلْبَابِ﴾

صدقَ اللهُ العليُّ العظيم

سورة البقرة (٢٦٩)

To

My Father and Mother

To

My Wife

My Sun Radhwan

My Daughter Zainab

Acknowledgment

In the name of Allah, the Most Gracious and the Most Merciful

Firstly, I would like to thank and praise ALLAH for blessing and providing me with a great opportunity to complete my Ph.D. project and for granting me the ability to proceed with this thesis.

I would like to warmly thank my father, mother, brothers, and sisters for their material and spiritual support throughout my academic career.

I thank my wife for her support and encouragement during my Ph.D. studies. Also, I offer my lovely for my nice children Radhwan and Zainab.

I want to express my thanks, respect, and gratitude to my supervisors Dr. Haider Al-Mumem and my co-advisor Dr. Hussein Hadi for their guidance through my work in the thesis.

Also, I want to express my thanks, respect, and gratitude to Prof. Dr. Seyyedeh Mehri Hamidi at Shahid Beheshti University, Tehran, Iran for her guidance through my work in the Magnet and Plasmonics Lab.

I would like to thank the department of electrical engineering and the college of engineering.

I would like to thank all my friends who support me through my studies.

Hussam Jawad Kadhim Aljanabi

2023

اقرار لجنة المناقشة

نحن أعضاء لجنة المناقشة، نشهد بأننا اطلعنا على اطروحة الدكتوراه الموسومة (**تطبيق شريحة كهروبلازمونية لكشف مرض الزهايمر**) وقد ناقشنا الطالب في محتوياتها وفيما له علاقة بها، نؤيد أنها جديرة بالقبول لنيل درجة دكتوراه فلسفة في الهندسة الكهربائية / ألكترونيك واتصالات.

رئيس اللجنة
التوقيع :
الاسم : ا.د. ابراهيم عبد الله مرداس
التاريخ :

عضو اللجنة
التوقيع :
الاسم : ا.د. ايهاب عبد الرزاق حسين
التاريخ :

عضو اللجنة
التوقيع :
الاسم : ا.د. حيدر جبار عبد نصار
التاريخ :

عضو اللجنة
التوقيع :
الاسم : ا.د. عبد الستار سلمان حمزة
التاريخ :

عضو اللجنة
التوقيع :
الاسم : ا.م.د. حيدر مهدي عبد الرضا
التاريخ :

عضو اللجنة (مشرفا)
التوقيع :
الاسم : ا.م.د. حيدر صاحب منجي
التاريخ :

عضو اللجنة (مشرفا)
التوقيع :
الاسم : ا.م.د. حسين هادي ناهي
التاريخ :

مصادقة رئيس القسم
التوقيع :
الاسم : أ.د. قيس كريم عمران
التاريخ :

مصادقة عميد الكلية
التوقيع :
الاسم : ا.د. ليث علي عبد الرحيم
التاريخ :

Supervisor Certification

I certify that this thesis (**Implementation of Electro-Plasmonics Chip for Detection Alzheimer's Disease)** and submitted by the student (**Hussam Jawad Kadhim Al-Janabi)** was prepared under my supervision at the Department of Electrical Engineering, College of Engineering, University of Babylon as part of requirements for the degree of Doctor of Philosophy in Engineering / Electrical Engineering / Electronics and Communications.

Signature:
Supervisor: Asst. Prof. Dr. Hayder Sahib Manji
Date: / / 2023

Signature:
Co-Supervisor: Asst. Prof. Dr. Hussein Hadi Nahi
Date: / / 2023

I certify that this thesis mentioned above has been completed in Electronics and Communications Engineering in the College of Engineering / University of Babylon

Signature:

Head of Department:
Prof. Dr. Qais Kareem Omran
Date: / / 2023

Examining Committee Certificate

We certify that we have read this thesis entitled **"Implementation of Electro-Plasmonics Chip for Detection Alzheimer's Disease**" and as an examining committee, examined the student, "**Hussam Jawad Kadhim Al-Janabi**", in its contents and that in our opinion it meets the standard of a thesis for the degree of Doctor of Philosophy in Engineering / Electrical Engineering / Electronics and Communications.

Signature:
Name: Prof. Dr. Ibrahim A. Murdas
(Chairman)
Date: / / 2023

Signature:
Name: Prof. Dr. Ehab A. Hussein
(Member)
Date: / / 2023

Signature:
Name: Prof. Dr. Haider Jabber Abd Nasar
(Member)
Date: / / 2023

Signature:
Name: Prof.
Dr. Abdulsattar Salman Hamzah
(Member)
Date: / / 2023

Signature:
Name: Asst. Prof.
Dr. Hayder Mahdi Abdulridha
(Member)
Date: / / 2023

Signature:
Name: Asst. Prof. Dr. Haider Sahib Manji
(Supervisor))
Date: / / 2023

Signature:
Name: Asst. Prof. Dr. Hussein Hadi Nahi
(Co-Supervisor)
Date: / / 2023

Approval of Head of Department
Signature:
Name: Prof. Dr. Qais Kareem Omran
Date: / / 2023

Approval of Dean of college
Signature:
Name: Prof. Dr. Laith Ali Abdul-Rahaim
Date: / / 2023

Abstract

The human brain contains of billions of neurons that control the central nervous system. Many techniques have been used for recording neural signals and mapping such as EEG (electroencephalogram), MEG (Magnetoencephalography), MRI (Magnetic Resonance Imaging), fMRI (Functional magnetic resonance imaging), CT scan (computed tomography), and fiber-optic techniques…etc. The recording of neuronal activity with low spatial and millisecond temporal resolutions at arbitrary depths in the brain tissues is the most difficult challenge for all of that methods. Therefore, these challenges required novel neural recording techniques in the fields of optics, electronics, magnetics, and other technologies to increase the spatial and millisecond temporal resolutions.

One of the modern technologies for sensing neuron activity with high spatial and millisecond temporal resolutions is the plasmonics technique. This technology uses surface plasmon resonance (SPR) sensing to detect neuron activity. Using plasmonics technology with neuron sensing is called Neuroplasmonics technology. This technology combines biosensing with nanotechnologies in both in-vitro and in-vivo conditions. Furthermore, it is providing advantages such as label-free detection, real-time analysis, Biocompatible, small sample, low detection limit, and high throughput.

In this thesis, an electro-plasmonic chip has been fabricated. It consists of grading layers of polycarbonate as a dielectric coated by a thin layer of gold (35nm). The prepared chip is connected with two terminals (wires) to apply an external voltage and then induce a one-dimensional (1D) electro-plasmonic nanograting chip. The fabricated chip has been evaluated physically by use of a suitable setup and then evaluated biologically to sense a different concentration of dopamine. The second step was to culture the electro-plasmonic chip with neuron cells extracted from rats and stimulated

by dopamine. This step was to evaluate the ability of the electro-plasmonic chip for detecting the activity of cultured neuron cells. Finally, the electro-plasmonic chip was cultured with human nucleus pulposus cells (HNPC) and then injected with streptozotocin (STZ). This step was to evaluate the ability of the proposed chip for sensing the inhibition of the cultured neuron cells.

The results show a nice physical phenomenon known as a plasmonic induce transparency (PIT). This physical phenomenon is produced by surface plasmon resonance (SPR) and it is proper for sensing neuron activity. By applying an external DC voltage, the amplitude (light intensity) increased, which means generating a tunable plasmon-induced transparency. The generating of tunable PIT means increasing the proposed chip sensitivity. The proposed chip shows excellent results for sensing different concentrations of dopamine (300 and 700 ppm). A very clear difference was observed in the amplitude of concentration at the wavelength range of 580nm to 600nm.

In the next step, twelve samples were cultured with neuron cells (rats) and then stimulated by different concentrations of dopamine. The results show the high ability of the proposed chip for sensing the neuron cells' activity with high concentration (700ppm) and low concentration about 0.5ppm. Also, the high sensitivity with low concentration at the time range of 2 – 10 min.

Lastly, the proposed chips (8 samples) were cultured with HNPC cells and injected with Streptozotocin (STZ) in three different concentrations (0.5, 1, and 2 mM). This step was to induce Alzheimer's disease and to measure the cell's inhibition. The results show the cell's activity decreased (inhibition) with increasing the STZ dose. These indicate the high sensitivity of the electro-plasmonic chip for sensing the cultured neuron cells' activity.

Table of Contents

List of Symbols

θ	angle of the incident light
ω	angular frequency
φ	azimuth coordinates on the plane
Cl^-	chloride ions
Cr	Chromium
E_{φ}^{SPP}	components of the oscillation in azimuthal
E_{ρ}^{SPP}	components of the oscillation in radial
E_{z}^{SPP}	components of the oscillation in the *z* directions on the sample
K_{zm}	diffracted wave vector in the grating plane
$\boldsymbol{m}$	diffraction integer
n_{eff}	effective refractive index
t_{01}^{m}	Fresnel reflection
h	grating depth
Λ	grating period
$\boldsymbol{G}$	grating wave vector
E_i	incident amplitude for the electric-field
P	Parallel plane polarization
ε_D	permittivity of the dielectric material
ε_M	permittivity of the metal
K^+	Potassium ions
B	propagation constant
β^{ew}	propagation constant for the evanescent wave
ρ	radial coordinates on the plane
n_d	refractive index of the dielectric constant
S	Senkrecht polarization
Ag	Silver
Na^+	Sodium ions
I^{SPP}	the amplitude intensity of the electric field of the sample
r_{10}^{m}	transmission coefficient
$T(\lambda_0)$	transmission spectrum of the system

c	velocity of light
K	wave vector
λ	Wavelength

List of Abbreviations

SNR	signal-to-noise ratio
EEG	Electroencephalography
CT scan	computed tomography scanning
MEG	Magnetoencephalography
fMRI	functional magnetic resonance imaging
MRI	magnetic resonance imaging
PIT	Plasmon induce-transparency
EIT	electromagnetically induced transparency
SPR	surface plasmon resonance
SPP	surface plasmon polaritons
STZ	Streptozotocin
AD	Alzheimer’s disease
Aβ	amyloid beta
CNS	central nervous system
LSP	localized surface plasmon
ATR	attenuated total reflection
IOS	Intrinsic optical signal
SP	surface plasmons
TM	Transverse magnetic
TE	transverse electric
SiO_2	Silicon dioxide
NaCl	Sodium chloride
FDTD	Finite-Difference Time-Domain
CCD	Charged-Coupled Device camera
INS	Infrared neural stimulation
GNRs	Gold nanorods
KCl	Potassium chloride
DA	Dopamine
HNPC	Human nucleus pulposus cells
EOS	Extrinsic optical signal
BBB	blood-brain barrier

EOT	Extraordinary optical transmission
DMEM	Dulbecco’s modified eagles’ medium
FBS	Fetal Bovine Serum
GLIT	glucose transporters
IGF-1	insulin-like growth factor 1
IR	Insulin resistance
GSK3β	glycogen synthase kinase 3 beta
MAPT	microtubule-associated protein tau
NA	Numerical Aperture
DI	Deionized water
SEM	scanning electron microscopy
ATP	Adenosine triphosphate
T-PIT	tunable plasmonic induce transparency

List of Figures

List of Tables

List of Publications

1- Kadhim, Hussam Jawad, et al. "Tunable plasmon induced transparency in one-dimensional gold nano-grating as a new kind of neuro-transmitter sensor." ***Optik*** 269 (2022): 169907. **(Clarivate Q2)**

2- Kadhim, Hussam Jawad, et al. "Streptozotocin-induced Alzheimer's disease investigation by one-dimensional plasmonic grating chip." ***Scientific Reports*** 12.1 (2022): 21878. **(Clarivate Q1)**

3- Kadhim, Hussam Jawad, et al. "Dopamine-induced neural activity detection onto a cell-cultured plasmonic nanograting platform." Applied Physics A 129.5 (2023): 323. **(Clarivate Q2)**

Chapter One

General Introduction

1.1 Overview

There are billions of neurons in the human brain, which control the central nervous system. Even though the brain plays a crucial biological function, there are still many obstacles to understanding the causes of cerebral neuropathy as people age and developing new medical technology to improve the detection, diagnosis, and treatment of brain disorders [1]. In order to provide better recording and mapping, a variety of techniques have been used, including (EEG), (CT scan), thermal imaging, (MEG), (MRI), (fMRI), fiber-optic techniques, etc. However, the most challenging part of all of these techniques is recording the activity of neurons in the brain tissues with lowering the spatial and temporal resolutions by a millisecond. The need for novel neural recording techniques in the fields of optics, electronics, magnetics, and other technologies is thus highlighted by this challenge [2].
One of the modern technologies for sensing is plasmonics which resulted from the interaction of electromagnetic fields with free electrons on metal surfaces [3]. The plasmonics technology has attracted more attention because of its ability to break the limitation of classical optics [4], optimize plasmonic filters [5], extremely highly sensing [6], suitable wavelength division multiplexing devices (WDMD), isolator [7], modulator [8], and so on. The interaction of these modes would provide new insights into novel physical phenomena like Plasmon induce transparency. This amazing physical phenomenon is produced by surface plasmon resonance (SPR), which acts as a sharp transparency window within a rather large absorption spectrum, resulting from very destructive interference between the wideband and the narrowband in the plasmonic nanostructures. Due to its crucial functions in the nonlinear phenomenon, integrated devices, slow light, modulators, and

sensors, it has attracted a significant amount of attention [9]. There are several ways to set up the PIT as sensors in a nanostructure. For example, metamaterials, waveguides made of dielectric material coupled to a metallic grate, metallic nanoparticle arrays …etc. [10].

On the other hand, the PIT window's capability to be tuned is an important factor in the design and manufacture of practical sensors, however, there are several reports that suggest tuning this window using external parameters such as creating a tunable metasurface furthermore using guided-mode resonance [11].

An innovative optical method called Neuroplasmonics uses SPR sensing to detect neuron activity and then record the brain signals and images [12]. Whenever the cell membrane is in direct touch with a metal surface, the sensor's dielectric constant will change based on the ion redistribution. The free electrons' oscillation activity is affected by the ion redistribution (K^{+}, Na^{+2}) around the bilayer, which produces the SPR signals [13]. SPR sensing depends on the detection of changes in the layer thickness or reflective index. As a result, little change in the cellular volume and the refractive index of the membrane are used to detect brain activity [14].

The advantages of Neuroplasmonics are that it is non-toxic, real-time, extremely high sensing, label-free detection, and provides both qualitative and quantitative information about the sensitivity of the sensor. High spatial and temporal resolution data for individual neurons are provided by this method both in vivo and in vitro [15].

In order to determine if streptozotocin (STZ) can cause Alzheimer's disease in cultured cells, this technology was utilized to evaluate the activity of healthy cells before and after stimulating the cells with dopamine. One type of dementia that affects older individuals frequently is AD. AD is a brain disorder that impairs daily functioning. Dementia causes neuron death, which is followed by the patient's death in a period of three to nine years.

Almost 45 million people worldwide are affected by AD, which is the fifth worst dangerous disease in the world. [16]. Around 5.8 million Americans already have AD, and that range is predicted to grow to about 13.8 million by 2050 [17]. Additionally, by 2050, 18.9 million more people in Europe are predicted to have AD, as well as 36.5 million in East Asian nations [18]. This disorder occurred because of the aggregation of amyloid-beta and tau protein. Insulin regulates many processes in the central nervous system (CNS), including eating, behavior, learning, and cognitive abilities. Also protects the brain from redox stress and neuroinflammation [19]. So, neuronal insulin resistance IR might contribute to occur AD [20]. In experimental settings, AD is induced using streptozotocin.

1.2 literature review

Neoroplasmonics techniques are attractive for sensing the neuron cell's activity with high spatial and temporal resolutions. Therefore, many research papers on this topic have been presented and cited. So, these papers represented the base research on this field.

Hyoungwon *et al*., (2005) [21], proposed a method to detect the neural action potential using SPR based on the optical recording. In this setup, the Kretschmann method has been used, and instead of neurons, they used a solution of a phosphate buffer. By applying an external electric field, the SPR would originate at the interface between metal and dielectric. Applying three voltages of 10nV, 30mV, and 50mV with a frequency of 1 kHz and using an oscilloscope to trace the signal. They conclude that the noise which originates from the photodiode and laser beam fluctuation has been improved. So, they stated that the development of SPR configuration would be a promising solution for recording neural signals.

Ae Kim *et al*., (2008) [21], developed an SPR sensor to record neural activity externally as shown in Figure (1.1). Because the sensitivity of an intensity-based SPR sensor was reportedly comparable to or greater than that of the phase-sensitive technique, it should be highlighted that this sensor was utilized. The drawback of this method is the requirement to contact the metal surface to the nerves.

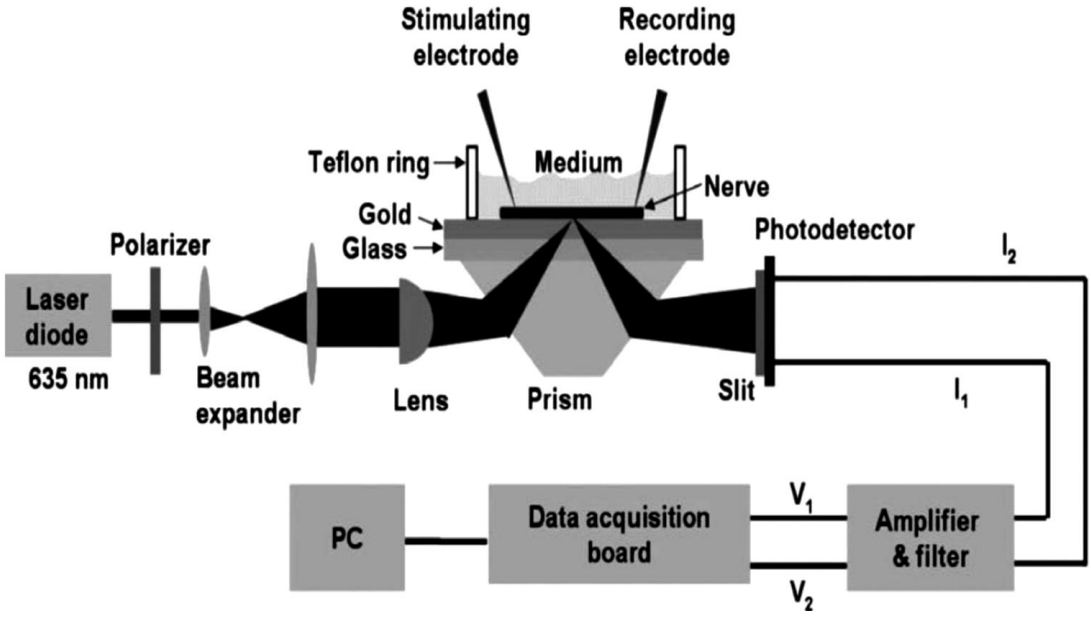

Figure (1.1): Illustration of the SPR system schematically [21]

Zhang *et al.* (2009) [23], demonstrated how to detect the spiking activity of the hippocampal neurons in real-time by using localized surface plasmon (LSP) resonance. The biological sample used in the experiment was tissue extracted from rats (hippocampus). ACSF had a glutamate injection to activate the cell. Figure (1.2) demonstrate the schematic of the setup. Briefly, this setup is used to optically probe neural activity. This technique detects the activity of neurons in the neural microcircuit according to plasmon probe geometry.

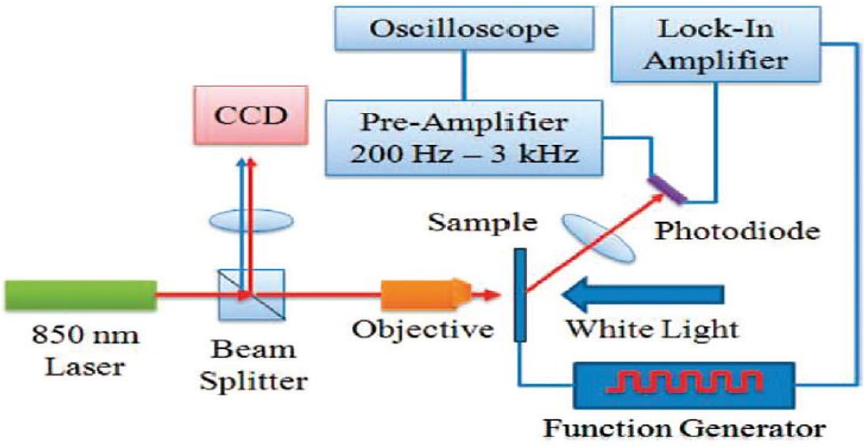

Figure (1.2): Demonstration of the schematic of the optical setup proposed by Zhang *et al.*[23]

Moirangthem *et al.* (2010) [24], Investigate the biomolecular interaction in the solution using a prism and SPR ellipsometry. Prism-based optical alignment and micro-fluidic cells reduce biological sample volume. Recording the data based on the ellipsometric parameters as sensor signals. By using this data it's possible to understand how biomolecules interact. Spectroscopy was used to measure the corresponding wavelength for maximum sensitivity. This method is better when compared with the SPR method because it's based on resonance angular detection.

Choi *et al.*, (2011) [25], by using the SPR phenomenon, describe the mechanism of neuron activation. They employ the Kretschmann ATR system with artificial cerebrospinal fluid (containing K^+, Na^+, and water molecules) and neural membrane taken from a rat sciatic nerve that is illuminated by TM-polarized light, as shown in Figure (1.3). This model represents the interaction between the nerve of the rat sciatic and the SPR. This method is used to understand the mechanism of electrons and the variation of ion concentration which is used to measure SPR neural signal numerically independent from electrical noise.

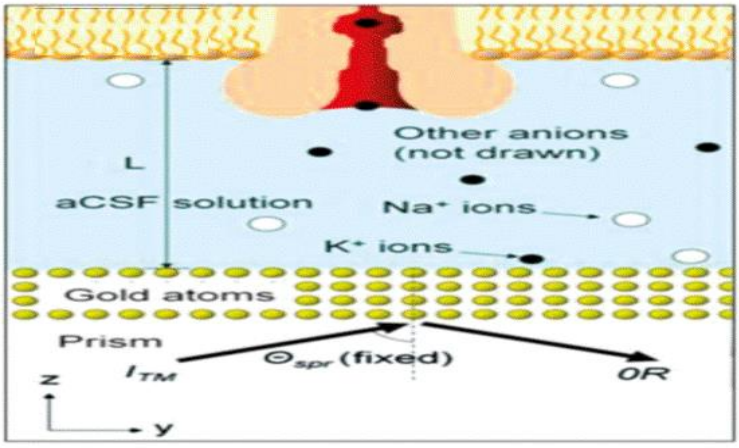

Figure (1.3): Illustration of a 2D model of the SPR recording system. The nerve membrane is close to the gold film (nanoscale distance) which the prism substrate has a coating of. A CSF fluid fills the space. [25].

Kim *et al*., (2012) [26], Explain the SPR sensor based on fiber optic to record neural activity. They used this technology to detect the brain activity of rats in vivo. This technique had more benefits because it could be potable and implantable with excellent sensitivity for monitoring neural activity. But the drawback of this technique is just one point that might be considered with tight contact with the neural cells. It's sufficient to study the neural function with a small region. The schematic were illustrated in detail in Figure (1.4).

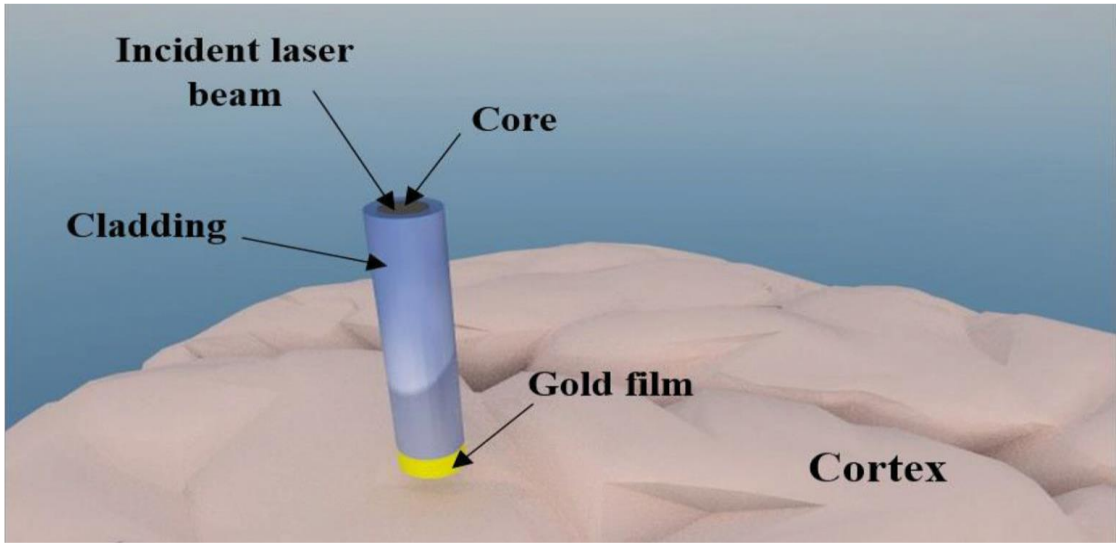

Figure (1.4): The schematic of the fiber optic sensor based on the SPR to record neural activity [26].

Chikara *et al*., (2012) [27], Prepared a plasmonic chip that has been soft lithographically coated by a thin layer of metal. The setup consists of the plasmonic chip, the grating substrate, the thin metal sheet, the four layers of Cr/Ag/Cr/SiO2 produced on the grating chip, the Si photodiode, the depolarizer, the photomultiplier tube, and finally the He-Ne laser source (633nm). Hippocampal nerve cells served as the sample, and Figure (1.5) illustrates the measurement system's schematic design. The fluorescent image of the dendrites in this experiment is brighter better than four times that given for a similar sample on a glass bottom dish, and the results demonstrate excellent spatial resolution.

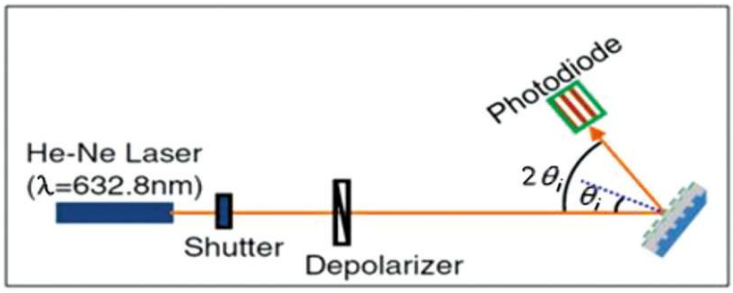

Figure (1.5): Illustration the setup of the SPR measurement system [27]

Huang *et al*., (2013) [28], Analyzed theoretically the design of SPR sensors based on fiber optic for voltage detection in the optimal case. They investigate a simple, effective method for measuring a single wavelength that uses contrast analysis to identify voltage. To increase the sensitivity, coated the fiber sensor probe with gold which is used as an electrode to detect the voltage. The electrolyte (0.1NaCl), which served as the culture medium for the cells, came into direct contact with the side film. The setup is shown in Figure (1.6) and could be used to measure low voltage. Also, this setup could be used as a portable sensor.

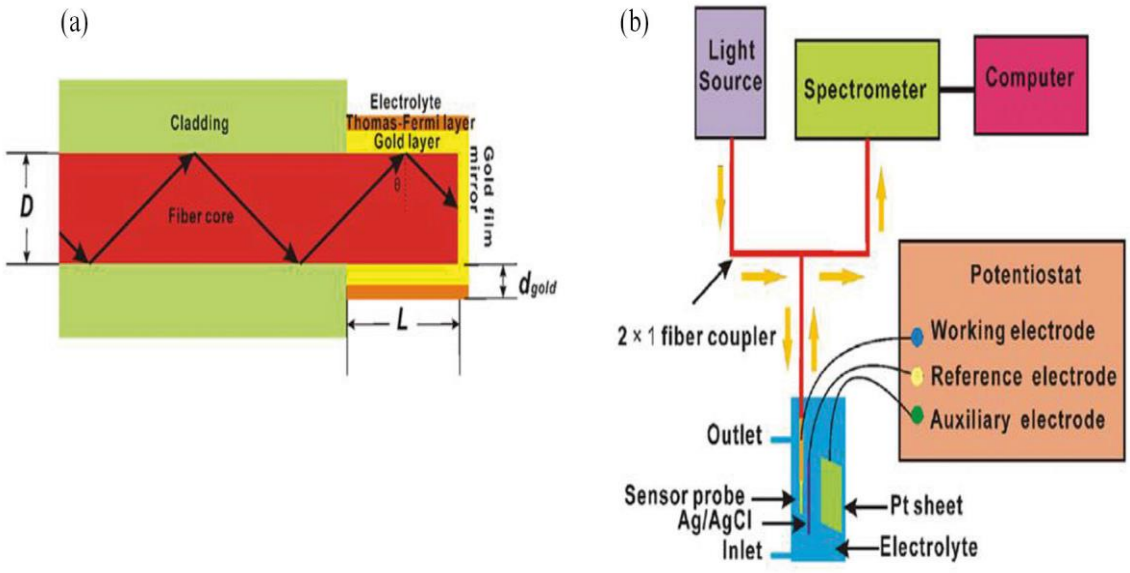

Figure (1.6): The schematic explains (a) a four-layer stack is used in the voltage-sensitive fiber-optic SPR sensor (B) The schematic of the optical measurement setup and the cell structure [28].

Le *et al*., (2013) [29], Propose an imaging technique that accompanied the bandpass filter with plasmonic crystal. The benefit of the bandpass filter was to improve the contrast of the image and the sensitivity.

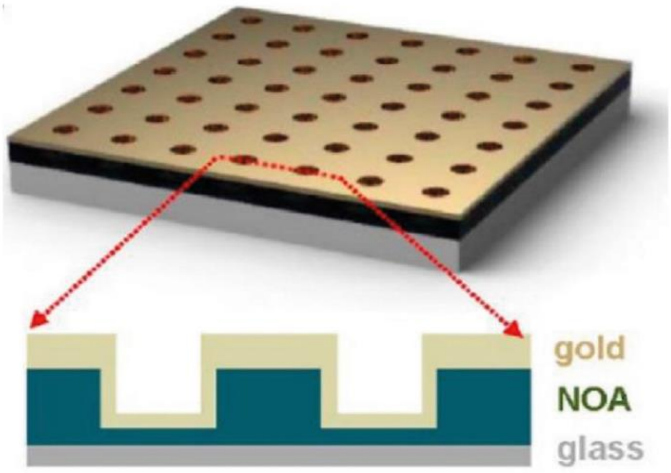

Figure (1.7): The schematic of the plasmonic crystal fabricated by Le *et al.* [29].

The plasmonic crystal used soft NIL in its fabrication and comprised a square array of a polymer (NOA) coated by gold and placed on a glass substrate as shown in Figure (1.7). Additionally, they stimulated the suggested structure by applying the FDTD approach, contrast calibration, and image processing, all of which were carried out using Matlab and ImageJ. These methods had the ability to measure the surfacing depths at the nanoscale over substantial areas in physiochemical-varied settings induced by physical or chemical changes and in real time. In general, it is a useful method for researching cell dynamics or morphology.

Choi *et al*., (2014) [30], present the idea of a plasmonic-based multicolor imaging system that uses a white light source as illumination rather than a laser beam. They were made out of a (45nm) thick gold film with a dielectric SiO2 grating that was designed by NIL. A 5nm Ti adhesion layer and SF10 glass were present under that gold film. The setup includes a polarizer, beam splitter, mirror, and camera (CCD) as shown in Figure (1.8). Their set-up was suggested as an analytical tool for both imaging the structure and tracking or monitoring the activity of the cells (hippocampal cells).

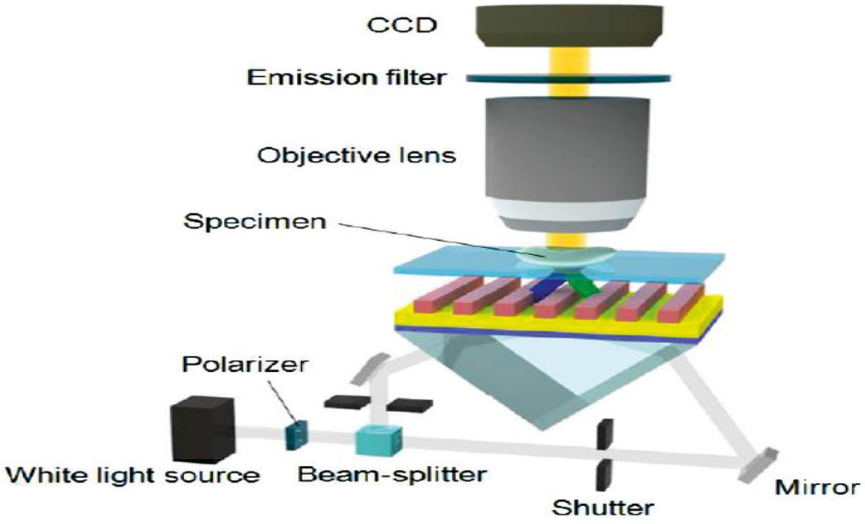

Figure (1.8): Illustration the setup of a multicolor imaging system with the plasmonic splitter [30].

Eom *et al*., (2014) [31], Proposed remote the activation of neurons by Infrared neural stimulation (INS) and gold nanorods (GNRs). As illustrated in Figure (1.9), the system includes a laser diode, stimulation probe, tungsten microelectrode, pre-amplifier, differential amplifier, and recorded controller.

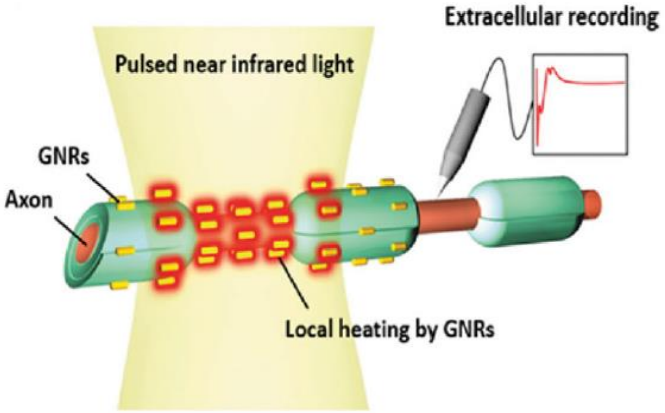

Figure (1.9): The schematic design of a plasma membrane for a nerve tissue that contains gold nanorods distributed in its vicinity to absorb light (980nm) [31].

This system was done with in vivo rats. The nanorods were embedded in the plasma membrane of the axon. Monitor the action potential of the nerve cells in real time by using an electrical recording system to record the response to the optical stimulation. This method used nanorods and lasers to stimulate more neurons. Moreover, the radiant exposure level for the cells tissue decreased and then decreased the damage.

Foozieh *et al*. (2017) [32], Explain the plasmonics sensing based on the physical mechanism of voltage sensitivity and recording the response. A strong sensitivity approach for voltage-sensitive plasmonics was proposed using ellipsometry measurements. Different voltages were applied to the biological solution. Artificial Cerebrospinal (Fluid) and brain tissue are included in the biological solution together with phosphate buffer

(cerebellum tissue). The results refer to a good response for stimulating the brain tissue by the external potential. This causes the charges at the metal/dielectric constant interface to be redistributed. Furthermore, the surface plasmon resonance varied according to this phenomenon.

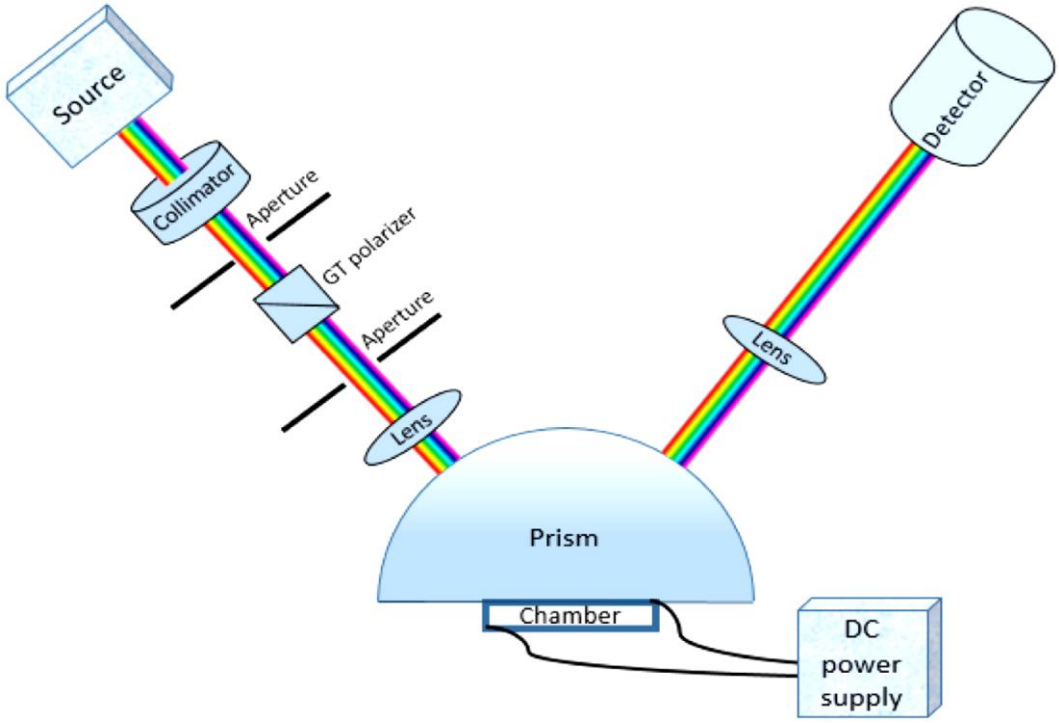

Figure (1.10): The schematic diagram of the ellipsometry setup for the detection of brain activity [32].

Sajede *et al*. (2019) [33], Proposed a two-dimensional plasmonic chip to sense cellular activity using laser stimulation. This method eliminates some disadvantages of the conventional plasmonic biosensor, such as lack of mass, high price and inflexibility. Two different types of cells were used (Hep G2 and mesenchymal stem cells) which had different membrane potentials. An infrared laser was used to excite these cells. The authors use the ellipsometry parameter to measure the cell's activity.

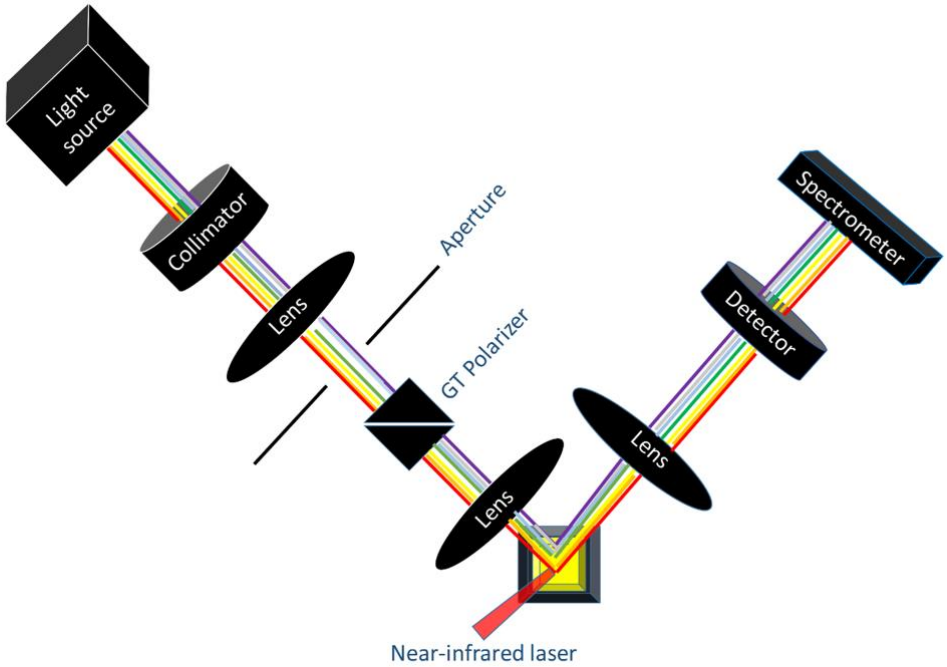

Figure (1.11): The schematic of the cellular activity detection under the effecting of laser [33].

Sohrabi *et al*. (2020) [34], demonstrate the ability of an integrated plasmonic ellipsometry chip to detect the activity of three types of cells (SH-SY5Y cells, HEK293, and primary hippocampal neurons). Using KCl solution as a chemical stimulus. With the ellipsometry technique measures the neuron activities by measuring the amplitude and the phase difference of the reflected light which leads to enhancing the sensitivity of the plasmonic technique.

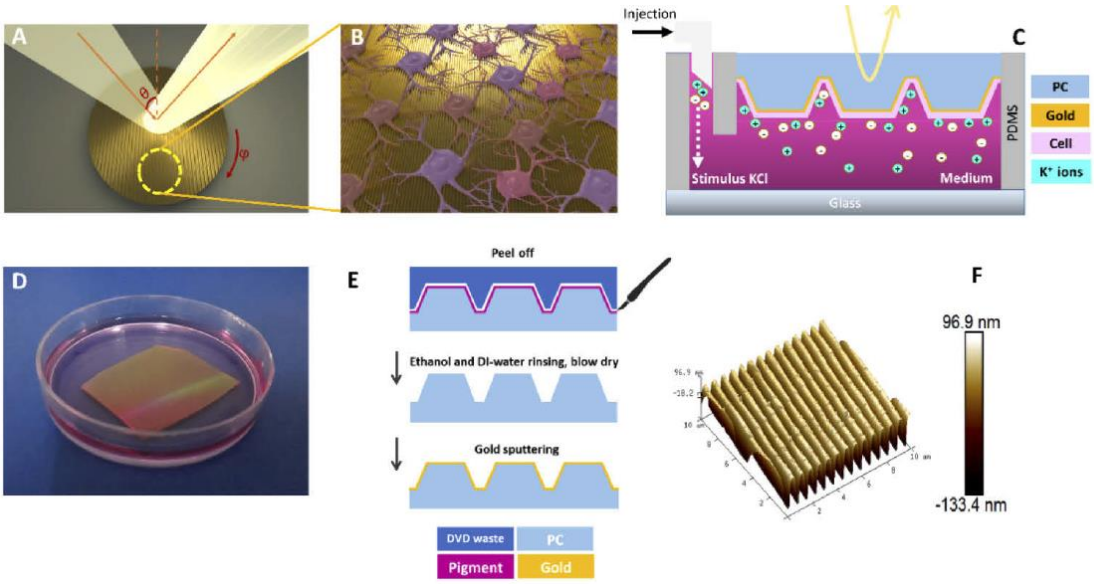

Figure (1.12): The schematic of the membrane activity detection [34].

S. Akbari *et al*. (2021) [35], Proposed a new generation of wearable small, flexible, and light heart rate recorders based on a two-dimensional plasmonic nanostructure chip as the main chip onto Kapton substrate. To reach the portable recorder, a miniaturized optical setup was used near the heart surface of the toad. Based on the results, very good agreement was observed between the input and output signals of heartbeats in the toad and the ability to distinguish between different signals. Finally, the thermoplasmonic effect due to gold nanorods onto our main chip under the green laser pump could affect the T and P shape of the heart signal, which was confirmed by the aid of the simulation part.

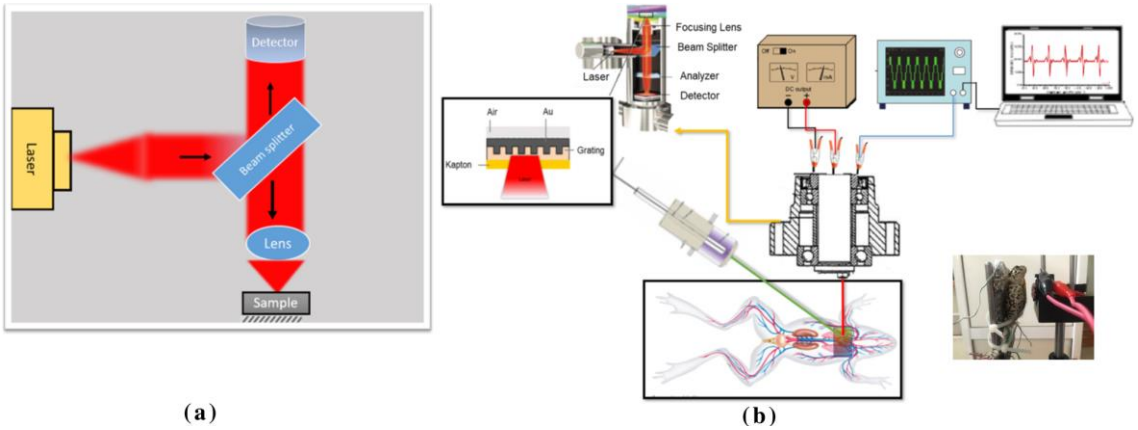

Figure (1.13): (a) optical setup of the microchip and (b) main experimental setup use for signal recording with and without green laser pumping and in the inset: real pic of the experimental setup with toad [35].

Chemerkouh *et al.* (2021) [36], A high-sensitive SPR biosensor is investigated based on 2D materials with the angle interrogation method and integrated ellipsometry SPR approach. It is shown that using STO as an interlayer can protect the Ag from being oxidized and significantly increase the conventional SPR sensor and biosensor sensitivity. The quality factor of the proposed SPR biosensor is improved with Ψ, which can be calculated with numerical modeling of ellipsometry. As a result, Ag-based SPR biosensor performance has been enhanced dramatically. Ultra-high-sensitive approach can be used to measure a very slight change in biomolecules samples and has a wide variety of biomedical applications like DNA and RNA (or any other analytes) detection, biomolecule interaction analysis, environmental monitoring, and food safety.

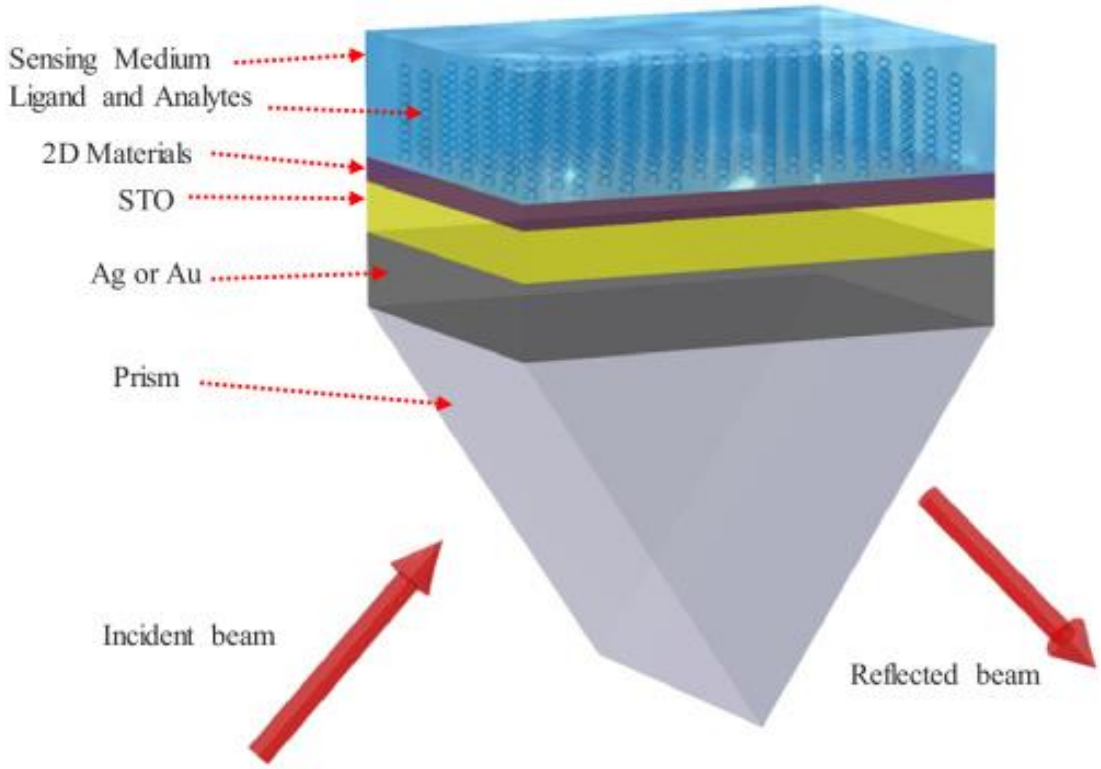

Figure (1.14): Schematic diagram of the Proposed SPR biosensor [36].

The setup and the plasmonic chip that is proposed in this thesis are preferred by the following facilities:

The electro-plasmonic chip is fabricated from a biocompatible substrate (polycarbonate) and coated with a thin layer of gold (35nm). This chip was connected by two terminals (wires) to apply an external power supply. The fabricated chip was placed on a homemade chamber that was fabricated from glass to fix the chip through the measurement steps. Using an objective lens in the setup induces a nice physical phenomenon known as Plasmon induces transparency (PIT). Applying an external voltages on the chip terminals from 1V to 3V increases the intensity that refers to generating tunable plasmon-induced transparency and then increases the sensor sensitivity. The high sensitivity may refer to inducing another physical phenomenon known as extraordinary transmission (EOT). The proposed

chip shows high sensitivity for sensing different concentrations of dopamine. Furthermore, the results show high sensitivity for stimulation and inhibition of the cultured neuron cells.

1.3 Problem statement

- Recording the neuron cell's activity with a high spatial and temporal resolution
- Investigating the effect of the suggested drugs on the neuron cell's activity.
- Monitoring the dopamine concentration is very important, if the dopamine levels are abnormal in the brain, it will contribute to making neurological disorders such as Alzheimer's disease.

1.4 Aim of the thesis

Based on the facts mentioned in the introduction:-

1. Fabricate an electro-plasmonic chip that supports SPR as a new kind of neuroplasmonic sensor.
2. Study the electro-plasmonic chip characteristics
3. Investigate the performance of the plasmonic chip for sensing and monitoring the different concentrations of dopamine (DA) as a kind of neurotransmitter.
4. Investigating the ability of the plasmonic chip to sense the activity of the cultured neuron cells extracted from rat cortex.
5. Investigated the ability of the electro plasmonics chip to detect inhibits in cultured HNPC cells by using streptozotocin (STZ) which introduces Alzheimer's disease.

1.5 Structure of the Thesis

The dissertation consists of five chapters divided as:-

- **Chapter One** presents an introduction to plasmonic technology, neurons cells activities, and Alzheimer's disease. Also, explain in detail the motivation of this research and demonstrate the significance of using neuroplasmonic technology to improve the performance of recording the neurons cell's activities. In addition, this chapter includes a recent literature survey, the aim of the thesis, and the thesis structure.

- **Chapter two** contains the theoretical part of the thesis which includes the introduction, SPR sensor, neuroplasmonics, extraordinary optical transmission, and plasmon-induced transparency, the neural activity of HNPC cells, the proposed experiment setup, and the results.

- **Chapter three** presents the material and methodology of the thesis which contains the chip preparation, the setup components, the excitation of the sample, and neuronal cell culture on a plasmonic chip.

- **Chapter four** explains the results and discussions of the thesis.

- **Chapter five** illustrates the conclusions and the future works

Chapter Two

Theoretical Background

2.1 Introduction

This chapter explains the theoretical background of all the concepts used in the experiment part. Plasmonics and the benefits of their use for monitoring neuronal activity will be discussed first, then the physics behind neuroplasmonic phenomena such as tunable PIT and EOS will be discussed. Also, the neuroplasmonics and the main types of neuroplasmonics will definition in detail. Furthermore, the neuron cells and the action potential concept with the Hodgkin–Huxley model are explained in detail. Lastly, brain dementia as Alzheimer's disease and how to generate this disease by using Streptozotocin will define with suitable diagrams.

The detail of building the setup and the devices required for this setup.

2.2 Plasmonic

There is great interest in plasmonic behavior because of its several applications. A plasmon is a collective oscillation of free electrons (charges) at the nanostructure surface which was suggested for the first time by Pines and Bohm in 1952 [37]. Also, it can be defined as a quantum of oscillating plasma. [38, 39]. Plasmons were created when light and free charges interacted. [40]. In the past, the devices were bulky and slow. The semiconductor scaling the electronic devices to nanoscale in dimensions. The challenges were the realization of the electronic devices operating speeds of more than 10 GHz. Photonic devices carry enormous data (bandwidth), but the challenge was with the limited size. Finally, plasmonics technology offers precise scale which electronic and photonics can't realize

to it. Figure (2.1) shows the critical dimensions and the operating speeds of the chip scale technologies [41].

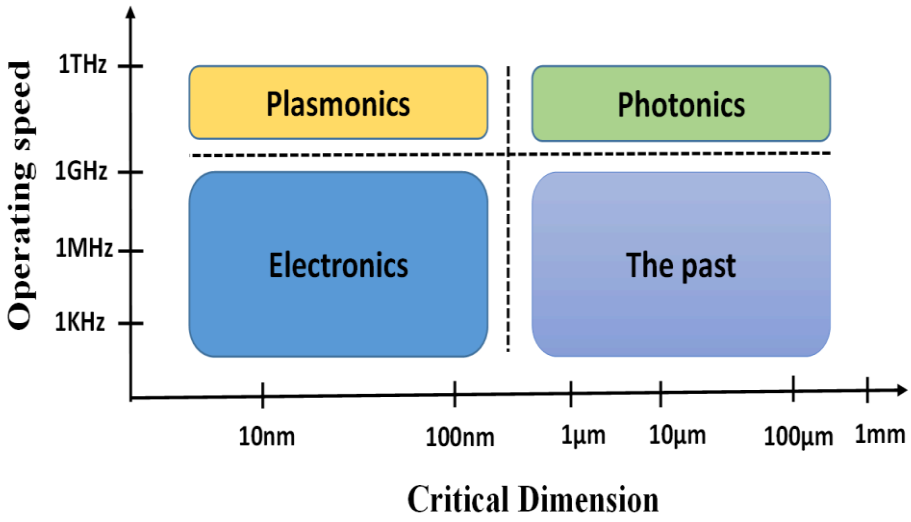

Figure (2.1): Demonstration of the different technologies of the chip scale depending on the critical dimensions and the operating speed [41].

Plasmons are classified into two categories which are known as surface plasmon (SP) and volume plasmon. Surface plasmons (SP) represent the oscillations of free electrons on the surface of the metal and an electromagnetic mode surrounding it is called surface plasmon polariton (SPP). Electromagnetic waves that propagate at the interface (dielectric/metal) are referred to the surface plasmon polaritons (SPPs) [48]. SPPs have attracted a lot of interest because of their capability to confine light and so break the limitation of traditional optics [42], enhance plasmonic filters [43], high-sensitivity sensors [44], the wavelength division multiplexing devices [45], modulators [46], and isolators [47] and so on.

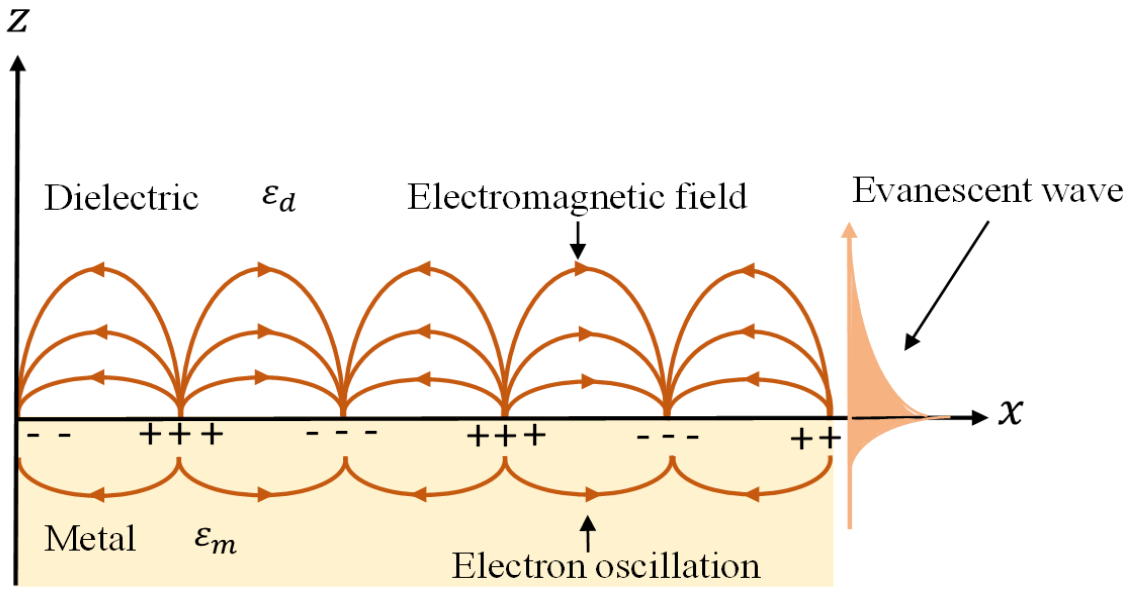

Figure (2.2): The distribution of charge along the x-axis in between the metal-dielectric surface with an electric and magnetic field component of the SPPs [48].

Figure (2.2) illustrates the SPP propagation. The electromagnetic field intensity appears highest at the surface with exponentially decays away at the interface. The engineering viewed the SPP as a special type of light wave that propagates along the metal surface.

Light represents an electromagnetic wave which means it consists of electric and magnetic fields. These fields oscillated along as they propagated. In the nanoscale, metal behaves differently when interacting with light which depends on the size, shape, and surrounding medium. A nanostructure of the metallic surface contains positive ions covered by a cloud of free electrons (gas). The optical properties of metal in nanostructure differ from those in bulk structure. Light's electric field can cause the conducting free electrons to oscillate when it interacts with the material. When the light passes through the surface of the metal, electromagnetic waves penetrate the interface locate between the metal and are dielectric caused by the oscillation of these electrons in the metal and propagate parallel to the surface. The depth of

penetration in metal is about 20 – 30 nm and 200 – 400 nm in a dielectric, and the propagation length is about a few micrometers. These surface waves are known as surface plasmons (SP) [49].

Surface plasmons (SPs) were discovered for the first time by Wood in 1902 [50]. This technique spans 66 years of development and the Kretschmann configuration was designed in 1966 [51]. The surface plasmons produce a local electric field surrounding the surface. A resonant behavior appears with surface plasmonics that occur at specific frequencies of light. These frequencies are known as surface plasmon resonance (SPR) [52].

2.3 SPR sensors

SPR phenomenon is a type of chemical and biological sensor [53]. That use surface plasmon waves propagate at the interface located between metal (negative permittivity) and the dielectric (positive permittivity). The electromagnetic field penetrates as mentioned previously a few hundred nanometers into the dielectric side and tens of nanometers into the metal side. So, the propagation constant of the plasmon wave on the surface will vary in reaction to a change in the refractive index medium of the dielectric or any other change in an optical property, which will subsequently result in a change in the characteristics of the incident light.

2.3.1 Excitation of surface plasmon polariton

Couple the incident light in P-polarized to SPP at the interface (metal/dielectric), and the incident light's wave vector components parallel to the interface must match the SPP's wave vector. [54]. In comparison to incoming light in the dielectric, the SPP constant of propagation is greater at the interface. Therefore, the excitation of the SPP will not be available by incident light directly on the metal surface. So, there are two methods for improving the incident light's wave vector to match that of the SPP.

The first method by using a prism (dielectric medium), because it has a greater refractive index than the dielectric found on the metal's opposite side. The second method, increasing the roughness of the metal side. This method is known as coupling. There are several ways to do the coupling such as optical waveguide coupling, prism coupling, and gratings coupling as shown in Figure (2.3)

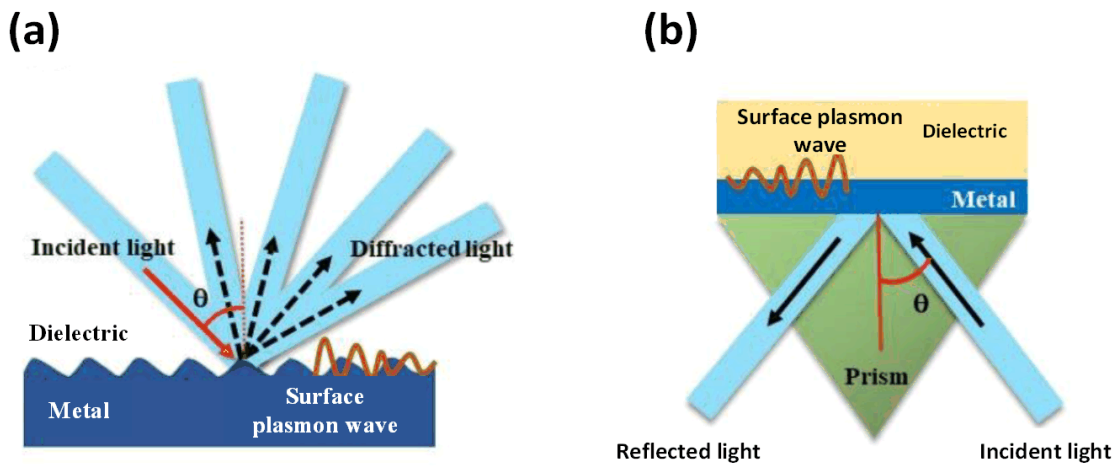

Figure (2.3): Illustration the schematic of (a) grating coupling, (b) prism [18].

The propagation constant is determined by the following equation [55]

$$\beta = \frac{\omega}{c}\sqrt{\frac{\varepsilon_M \varepsilon_D}{\varepsilon_M + \varepsilon_D}}, \qquad (2.1)$$

- Where β refers to the propagation constant, ω represents the angular frequency, crepresentst the velocity of light, ε_M the metal's permittivity, and ε_D the material's dielectric permittivity.

2.3.1.1 Kretschmann configuration

The Kretschmann configuration is one of the earliest settings, in which the resonances of the surface plasmon polariton were observed. In this setting, the metal and then the dielectric is deposited on the base of a prism as shown in Figure (2.3(b)). By directing the incident light via a high refractive index prism, such as BK7, the incident light's wave vector is improved. This way is known as attenuated total reflection (ATR) [51]. Based on the ATR method, there are two setups known as the Kretschmann configuration and the Otto configuration.

In the Kretschmann method, there is a thin film of metal that is placed between the prism (high refractive index) and the dielectric (Lower refractive index). On the other hand, a space layer is founded between the metallic surface and the prism. The disadvantage of this technique is the difficulty of placing the thin layer of air between the metal and the prism. Therefore, the practical application of this method is limited [56]. So, we discussed the Kretschmann configuration in this thesis as shown in Figure (2.4).

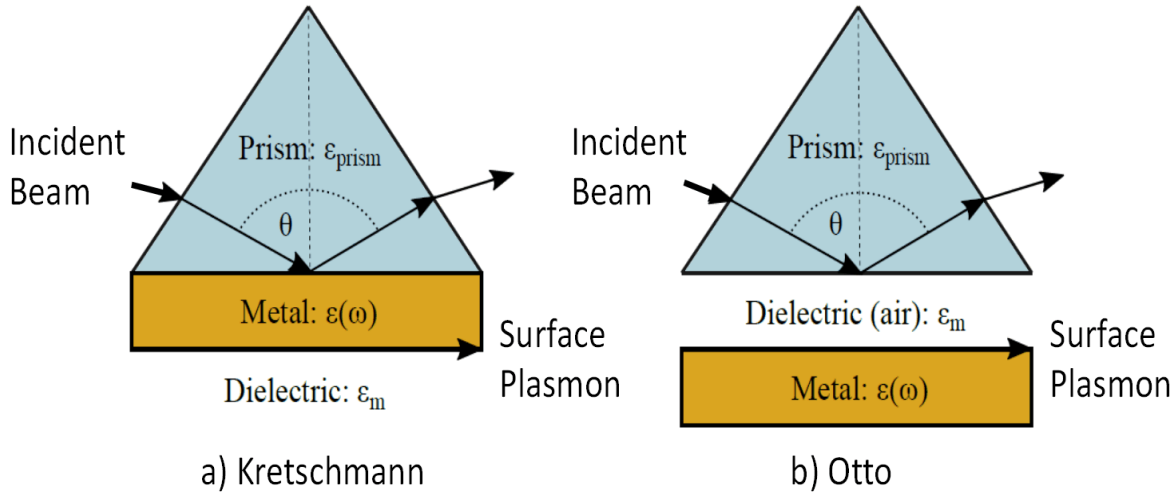

Figure (2.4): Illustration of the schematic of Kretschmann and Otto configurations [51].

The incident light in the Kretschmann setup passes through the prism to the thin metal film. When the incident light's angle exceeds the critical angle, it is reflected back and a portion of it propagates at the metal, generating an electromagnetic wave (inhomogeneous) at the interface (metal/dielectric). This electromagnetic wave is known as an evanescent wave because it decays exponentially to the interface, as illustrated in Figure (2.2).

When the metal film's thickness is ideal, the evanescent wave penetrates it and couples with the surface plasmons on the interface. The constant of propagation in metal (for surface plasmon) must be equal to the constant of propagation of the evanescent wave [56].

The constant of propagation for the evanescent wave β^{ew} is:

$$\beta^{ew} = \sqrt{\varepsilon_p}\sin(\theta) \tag{2.2}$$

The coupling condition calculated as [21]

$$\sqrt{\varepsilon_p}\sin(\theta) = \mathrm{Re}\left\{\sqrt{\frac{\varepsilon_M \varepsilon_D}{\varepsilon_M + \varepsilon_D}}\right\}, \tag{2.3}$$

Where θ is the incident light's angle.

The coupling that occurs between the surface plasmon (SP) and evanescent wave at a specific incident angle is called a resonant angle.

2.3.1.2 Plasmon excitation grating

This technique requires an increase in the incident light's wave vector by using a rough surface of a metal film or using a diffraction grating surface which is the most common method. In the grating coupling when the incident light with the wave vector (K) passes through the dielectric medium to the grating surface. The dielectric constant (ε_D) causes the incident light wave to diffract into several beams and at different angles away from the interface as shown in Figure (2.3 a). Therefore, the wave vector for the diffracted light ($\boldsymbol{K_m}$) is expressed as:

$$K_m = K + mG, \tag{2.4}$$

Where ***K*** is the wave vector of the incident light on a grating surface, ***m*** is the diffraction integer and ***G*** is a grating wave vector for the grating plane which is expressed as

$$G = 2\pi/\Lambda. \tag{2.5}$$

Where Λ is a grating period and h is a grating depth.

Therefore, the grating plane's component of the diffracted wave vector Kzm is:

$$K_{zm} = K + m2\pi/\Lambda \tag{2.6}$$

Furthermore, the coupling condition is that the constant of propagation of the diffracted wave must be equal to the constant of propagation of surface plasmon.

$$\frac{2\pi}{\lambda} n_d \sin\theta + m\frac{2\pi}{\Lambda} = K_{zm} = \pm Re\{\beta\}, \tag{2.7}$$

Where n_d is the refractive index of dielectric constant, θ is an angle of the incident light wave, λ is the wavelength, and the constant of propagation of the surface plasmon can be rewritten as shown in equation (2.1).

After submission, the coupling equation equals:

$$n_d \sin\theta + m\frac{\lambda}{\Lambda} = Re\left\{\sqrt{\frac{\varepsilon_M \varepsilon_D}{\varepsilon_M + \varepsilon_D}}\right\}. \tag{2.8}$$

In SPR cases when using a grating coupling, the stability of the system depend on the prism coupler. So, to avoid unnecessary reflections, the grating coupler tools are kept mostly larger in height than the reflected evanescent waves. Therefore, the prism couplers approach is most commonly used [106].

2.3.1.3 Plasmon excitation by near-field optical

In this technique, the near-field optical allows a local SPP excitation over the surface of the metal film as shown in Figure (2.5). The SPPs propagating can be imaged by the collecting of leakage radiation into the substrate with n refractive index that occurs at the angle θ_{SPP}. The light due to this technique radiates outside the cone of air light. So, a high numerical aperture objective lens is used to gather this radiation or by using a suitable arrangement of mirrors. Figure (2.5 (b,c)) shows two representative images of the SPPs propagation away from the illuminating area. [56].

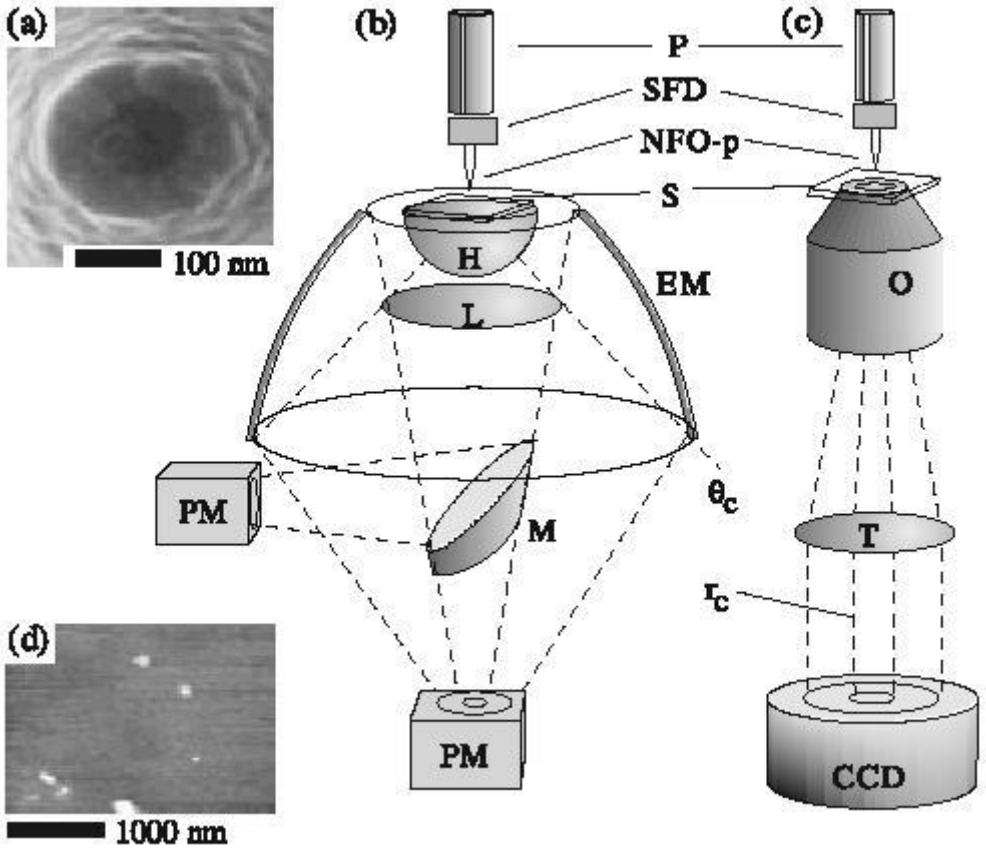

Figure (2.5): Illustration the excitation of SPP by using near-field optical (a) The SEM image of a near-field fiber probe's aperture (b) and (c) represents the two configurations for SPP optical excitation. Moreover, the light collected radiated into the substrate (d) the silver film's topography that was utilized as a sample (height of protrusions 40 nm and roughness 1 nm,) [56].

Furthermore, a high numerical aperture objective lens can be used to excite the SPP. The spatial resolution is improved if the excitation of the SPP is localized over a small area.

The propagation constant for the SPPs excitation on the metal surface is known as written in equation (2.1).

To calculate the constant propagation of light in the air as follows:

$$k_{\text{light}}(\omega) = \frac{\omega}{c}\sqrt{\varepsilon_2(\omega)} \qquad (2.9)$$

Where (ω) indicates the angular frequency, and (c) indicates the light speed in a vacuum. Additionally, $\mathcal{E}2$ (ω) is the relative permittivity of the air.

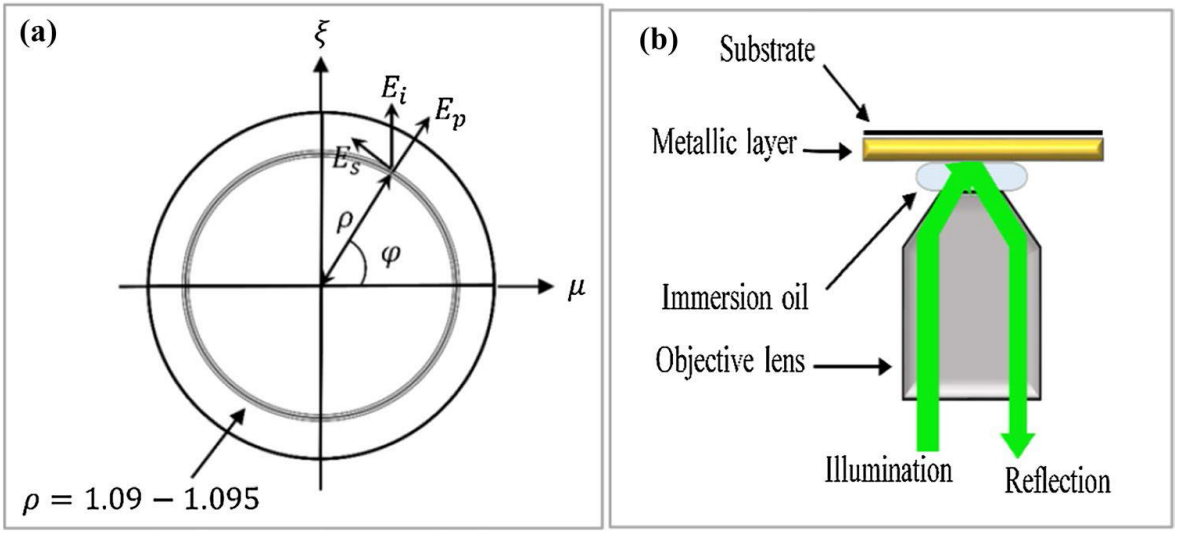

Figure (2.6): The schematic of (a) using a high numerical aperture to excite SPP (b) the objective lens pupil plane

The evanescent wave is generated by using an objective lens with high numerical aperture. In Figure (2.6), when the polarized light incident the objective lens, electric field components are presented at the pupil plane.

$$E_p(\rho,\varphi) = E_i cos\varphi(\ 1.09 < \rho < 1.095)$$
$$E_s(\rho,\varphi) = E_i sin\varphi(\ 1.09 < \rho < 1.095)$$
$$E_p(\rho,\varphi),\ E_s(\rho,\varphi) = 0 \quad \text{(otherwise)} \qquad (2.10)$$

Where (E_i), (ρ), and (φ) indicate the electric field's incidence amplitude plus radial and azimuth coordinates, respectively.

The incident light illuminates the sample after passing through the plane at (ρ,φ) and converting to the matching plane wave. There are several reflections produced by each plane wave. The amplitude transmission coefficient of a three-layered system is introduced in this explanation and is obtained by:

$$T_m(\rho) = \frac{t_{01}^m(\rho)t_{12}^m(\rho)\exp[ik_{1z}(\rho)d_1]}{1-r_{10}^m(\rho)r_{12}^m(\rho)\exp[i2k_{1z}(\rho)d_1]} m = p,s. \qquad (2.11)$$

Where t_{01}^m and r_{10}^m indicate the Fresnel reflection and the transmission coefficient at the interface of medium (a) and (b), respectively. They are based on the relative permittivity of the materials on both surfaces. Also, within this equation k_{1z} refers to the wave vector's z component in the gold grating and d_1 indicates the thickness of that.

From Equations 2.10 and 2.11, the elements of the amplitude produced by light passing through the plane at position $(\rho,\varphi)$are determined. So, the functions E_ρ^{SPP}, E_φ^{SPP}, and E_z^{SPP} explain the components of oscillation in radial, azimuthal and the *z* directions on the sample shown in Figure (2.6 a), respectively.

Moreover, according to the oscillation's direction, the sample's electric field's amplitude intensity in each plane wave is determined as:

$$I^{\mathrm{SPP}}(x,y) = \left|\int E_x^{SPP}(x,y,\rho,\varphi)\rho \mathrm{d}\rho \mathrm{d}\varphi\right|^2 + \left|\int E_y^{SPP}(x,y,\rho,\varphi)\rho \mathrm{d}\rho \mathrm{d}\varphi\right|^2 + \left|\int E_z^{SPP}(x,y,\rho,\varphi)\rho \mathrm{d}\rho \mathrm{d}\varphi\right|^2 \quad (2.12)$$

These computations were measured both with and without the addition of external voltage [57].

2.4 Neuroplasmonics

2.4.1 Definition of Neuroplasmonics

An innovative optical method called neuroplasmonics uses SPR sensing to record neural signals and images [59]. Plasmonics is a research field that studies the interaction of electromagnetic fields with the free electrons on a metal surface, which links with biosensors that depend on the resonance changes in the external environments [60]. When the cell membrane comes into direct contact with the metal surface, the sensor surface's dielectric constant varies. The oscillation activity of free electrons is subsequently influenced by the redistribution of ions (Na^{2+}, K^{+}) within the bilayer, and this results in the SPR signals [61]. SPR sensing depends on the detection of changes in the thickness of the layer or the reflective index [62,63]. The smallest variations in cellular volume and membrane refractive index are therefore utilized to detect neural activity [64-72]. The advantages of neuroplasmonics are that it is real-time, biocompatible, non-toxic, extremely sensitive, small in size, label-free in detection, and provide both qualitative and quantitative information about the sensitivity of the sensor [73-77]. High spatial and temporal resolution data for individual neurons are provided by this method both in vivo and in vitro [78].

2.4.2 Sensors based on neuron plasmon

There are four main categories of neuroplasmonics techniques-

2.4.2.1 Neuroplasmonics technique based on prism methods that divided into two types: -

a- The simple configuration

With this technique, many studies were done in the field of neuro-plasmonics. Kretschmann's method is the most traditional SPR sensor which offers great sensitivity although with their difficulty with integration and miniaturization [79]. Furthermore, the absence of some facilities such as corrosion resistance, portability, remote monitoring, and anti-electromagnetic interferences are the disadvantages of this method and limit its applications [80].

b- Optical fiber technique with SPR sensing

In this technique, the bottom of the probe is coated with gold to support SPR sensing at the surface between the coated gold and the brain. So, it combines the facilities of optical technology and SPR sensing [81-83]. The intrinsic optical signal is one of the main divisions of this technique. It doesn't use labeling tools to measure the physiological changes related to the activities of neurons [84,85]. The IOS measurement is done by a few alterations in optical properties that are affected by the changes in the volume of a cell, the potential of the membrane, the flowing of the blood, and the oxidation of hemoglobin [86,87]. However, signal integration over the measurement volume is a problem with this approach, resulting in a poor SNR [88].

2.4.2.2 The Neuroplasmonics method combines fluorescence microscopy and SPR sensing.

In this technique, EOS utilizes calcium indicators and voltage-sensitive fluorescence proteins to support the detection of neuronal activities both in vivo and in vitro [88,89]. The optical probe was developed because it can the generation of fluorescence from physiological signals and then detect them using the appropriate equipment. Investigate the neurological signal from the studied neurons in living cases and in cultured [90,91]. These resources contribute to making the EOS measurement more useful in the field of neuroscience [88].

Fluorescence microscopy is a 2-D optical imaging technique used to investigate the cellular structure and its biological processes. It is a key subset of EOS recording [92,93]. This approach can produce a brighter, higher-contrast image, which can aid with cell diagnosis immediately away [94,95]. However, attaching the fluorescent labels to live cells without affecting their physiology or morphology is still difficult. [96,97].

2.4.2.3 Neuroplasmonics technique using nanorods

In order to improve a cochlear implant probe with exceptional penetration depth and high spatial selectivity, pulsed mid-IR laser light has been found to activate neurons in the direct optical path [98,99]. Also, the action potential was generated by local thermal heating delivered by the infrared neural stimulation (INS) approach at the neuronal plasma membrane. This might be because temperature-sensitive ion channels can be activated by the thermal heating of neurons and/or changes in membrane conductance or capacitance [100-102].The drawback of this approach is that it may limit neuronal stimulation and cause tissue damage when used in continuous wave mode for a long time [103].

2.4.2.4 Neuroplasmonics technique using plasmonic crystals

This method is divided into two subsets: -

a- Structures using nanoparticle arrays

Neuroscience uses nanoparticles to deliver drugs over the blood-brain barrier (BBB) to the central nervous system (CNS) for the purpose of transferring gene materials, integrating gene materials into the nucleus, and other uses, including the treatment of neurological disorders [104,105]. The size of noble metal nanoparticles that sustain LSPs is limited to that of a subwavelength [106,107], and the light waves interact with them to enhance the electromagnetic field at the surface [108,109]. Minimum changes in the dielectric constant affected the absorption spectrum [110]. This property of the metallic nanoparticles can be used to create a sensor with high sensitivity which permit to record intrinsically the activity of neural cell at the level of a single neuron [111-113]. Gold nanoparticles are biocompatible and can be used to fabricate a substrate for growth neural cells [111]

Electron beam lithography or chemical processes can be used to create nanoparticle arrays [111]. Also, an ion beam can be used to prepare the nanoparticle arrays on the fiber optics facet, which can be used to implant into the brain [114].

b- **Structures using nanohole arrays**

This method allows for the calculation of the thickness of thin-film structures that are present in a model complex biological structure after growth in culture. It does this by using plasmonic crystals and bandpass filters. The sensitivity and contrast of the image might be enhanced by these bandpass filters. Because it doesn't need special operating conditions or long scanning times, it may be possible to use this plasmonic reflection imaging technique for live-cell imaging [115].

2.5 Extraordinary optical transmission (EOT)

EOT is an optical phenomenon discovered in 1998 which refers to electromagnetic resonances passing through sets of sub-wavelength apertures of geometry (circle or square) in a metal film, then providing transmission of electromagnetic fields larger than would be expected from a small aperture size. This way, SPPs can be exited through grating coupling and an enhanced electromagnetic field on the top of the aperture.

This phenomenon has an interesting research field to enhance optical transmission and its applications for sensing, metamaterials, color filters, lenses, enhancing nonlinear effects...etc. [116]. Also, it has high sensitivity when compared with the Kretschmann SPR setup. The principle working of the EOT phenomenon is shifting the resonance wavelength peaks of the EOT spectrum to the higher wavelength end. This shifting occurs when the dielectric constant change at the metallic interface. The changing of the dielectric constant induces changes in the refractive index. Based on this phenomenon, researchers succeeded in developing many sensors for molecules and neuron sensors via the changing of the refractive index.

In line with these facts, the activities of the neuron cells make a shift in the spectrum of the transmitted light (resonance peaks).

Detection of low concentration is important for researchers and applications. The key aspect of developing a method to detect a single molecule is based on its fluorescent measurements.

In practical implementation, the presence of parasitic signals restricts single molecule sensitivity such as the media surrounding the molecule's fluorescence.

Melentiev et al. (2018) [58], presented a method for measuring ultra-low concentration and ultra-small volume based on the phenomenon of Ebbesen effect through an array of nano-holes. This technique significantly increased

sensor sensitivity while reducing the parasitic fluorescence of the sensor substrate. In this method, the excited plasmonic waves' dispersion changes when the media adjacent to the nanohole array's refractive index varies slightly. Therefore, the resonant wavelength of the EOT is shifting through the optical transmission.

Figure (2.7) shows a design of the plasmonic sensor which was built to measure the single drop of Cy-5 molecule's fluorescence in the solution. The sensor is based on nanoholes (diameter =175 nm and thickness of silver = 100 nm) to sense ultra-high quality.

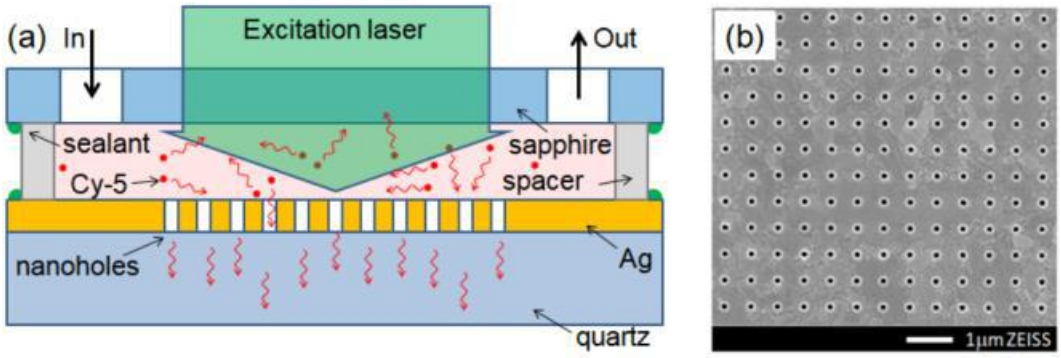

Figure (2.7): The schematic of (a) the plasmonic sensor based Ebbesen effect (b) the electron microscope image of the plasmonic nanoholes film (silver) [58].

A diode laser with a power output of roughly 10 mW illuminated the plasmonic sensor with laser light at a wavelength of 628 nm. The sensor is placed in the microscope's object plane. As shown in Figure (2.8), a nanohole array is used to excite Cy-5 molecules using laser energy, and a microscope objective then collects the excited molecules.

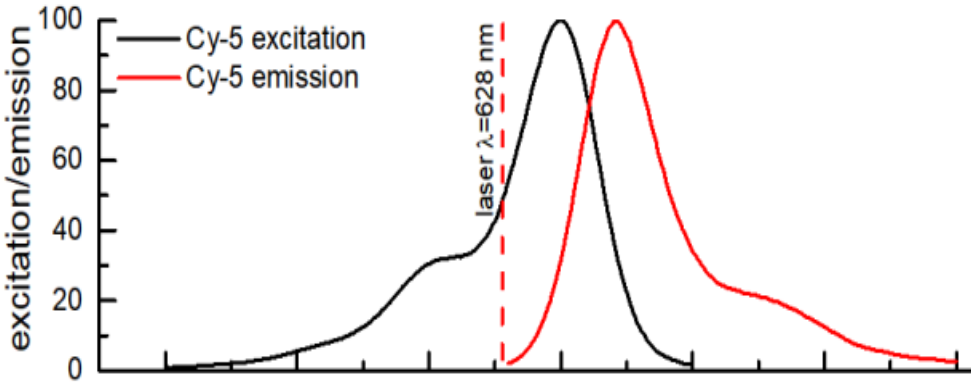

Figure (2.8): Shows the excitation spectrum of the plasmonic sensor for Cy-5 based on the Ebbesen effect [58].

Figure (2.9) demonstrates the optic image captured by a CCD camera without adding Cy-5 molecules to the sensor. The resulting image shows the luminance of the substrate (quartz) that is used to build the sensor. The parasitic luminance in Figure (2.9 a), which indicates the smallest detectable concentration of the dye molecules in the sensor, is represented by the amplitude.

According to the image in Figure (2.9 b), the recorded signal increased when Cy-5 molecules solution, at a concentration of about 40 pg/ml, was added to the sensor. Also, the different concentration of the molecule is measured by the plasmonic sensor shown in Figure (2.9 c).

In summary, the plasmonic sensor based on the EOT effect has an ultrasensitive sensor to the Cy-5 molecule.

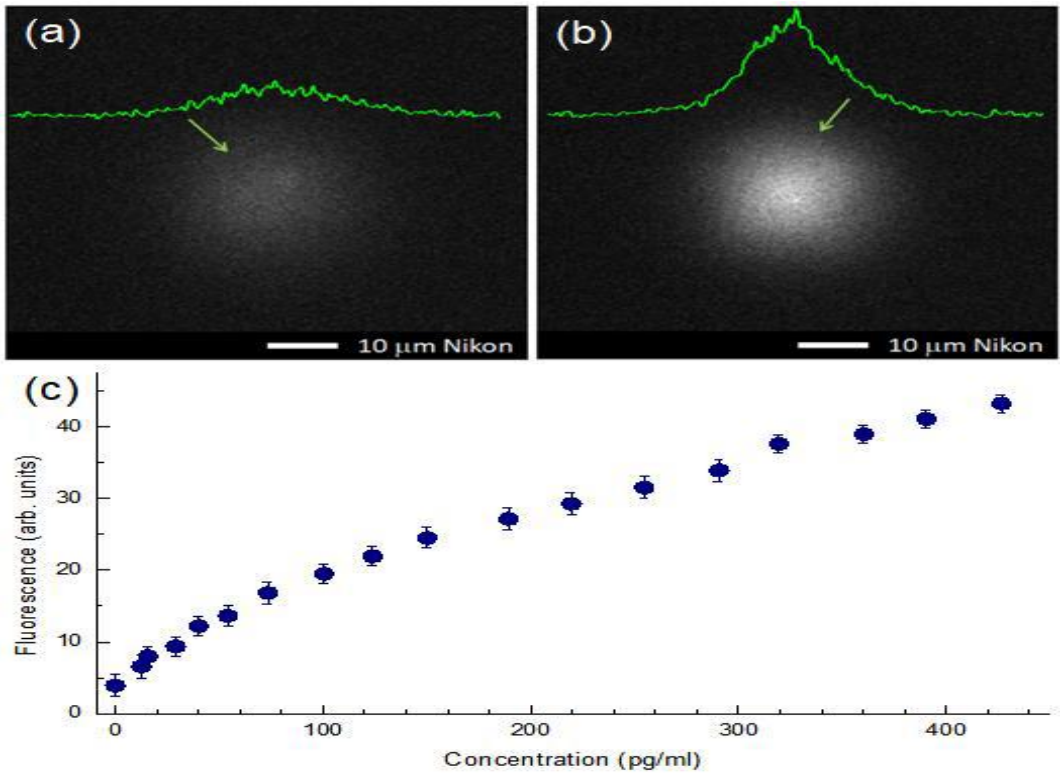

Figure (2.9): Illustration of the detection of Cy-5 molecules by the plasmonic sensor (a) measured the solution's luminescence without Cy-5 molecules, (b) measured the solution's luminescence with Cy-5 molecules, (c) a CCD camera measured the fluorescence of the solution at various Cy-5 molecule concentrations [58].

2.6 Plasmon Induce Transparency (PIT)

The physical phenomenon of Plasmon-induced transparency (PIT) is analog to the classical phenomenon of electromagnetically induced transparency (EIT). The physical phenomenon (EIT) is a quantum interference effect that eliminates light absorption and renders the metamaterials transparent within narrow spectra. Also, steep dispersion is created within the transparency that leads to slow light. This phenomenon permits the light to propagate through an opaque atomic medium.

In the atomic system, there are three levels known as ground state 1, bright state 2, and dark state 3. Dipoles are allowed when moving from ground state 1 to bright state 2, and they are also allowed when moving from

bright state 2 to dark state 3. However, the transition from ground state 1 to dark state 3 is not permitted (forbidden). Hence, there are double pathways shown from |1> → |2> →|1> and |1> → |2> →|3> → |2>. That means there are two coupling paths that caused interferes destructively that causes sharp and narrow peaks in the transmission spectrum. In plasmonic induce transparency the interference destructively caused between light emerging for two coupling states. This phenomenon results in a positive variation in refractive index and rapid change in absorption, thus in this form, light has a very low group velocity and could be employed as delay lines in photonic circuits [117].

In this thesis, externally applied voltage is used to enhance the modulation of PIT and then get tunable PIT.

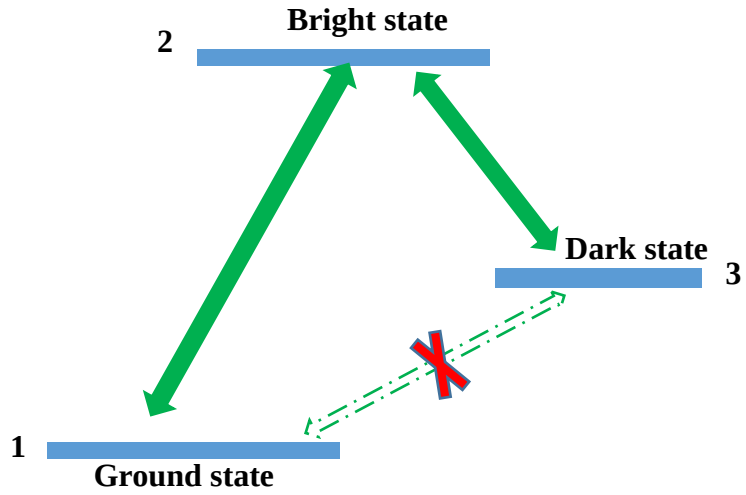

Figure (2.10): Illustration of the three levels of Plasmonic analogue of electromagnetically induced transparency system [117].

Nowadays, novel techniques have been used to fabricate microstructures in optical physics. The plasmonic technique which applied electromagnetic waves on the metal-dielectric interface caused the propagating of metals' free electron oscillations. This phenomenon is referred to as surface plasmon polaritons, which is considered to be a promising candidate to design sensors.

The EIT phenomenon could achieve inside the SPP waveguide configuration and the transparency peak could be tunable by adjusting the space between bright and dark states [137].

Zhang et al. (2014) [137], explain the EIT phenomenon that achieves inside the SPP waveguide configuration. The SPP waveguide is formed using air as a core and metallic (silver) as cladding which illustrates in Figure (2.11 a). To achieve the EIT phenomenon, the bright and dark states must be constructed in the SPP waveguide system. So, the rectangle cavity and line slot are arranged to increase or decrease the distance denoted by c. When decreasing the distance c, the rectangular cavity is excited by the transverse magnetic wave (TM) due to near-field coupling. As a result, Figure (2.11 b) shows the transmission spectrum of the SPP coupled with a single cavity. The different dips indicated to the different resonant frequencies with different values of c.

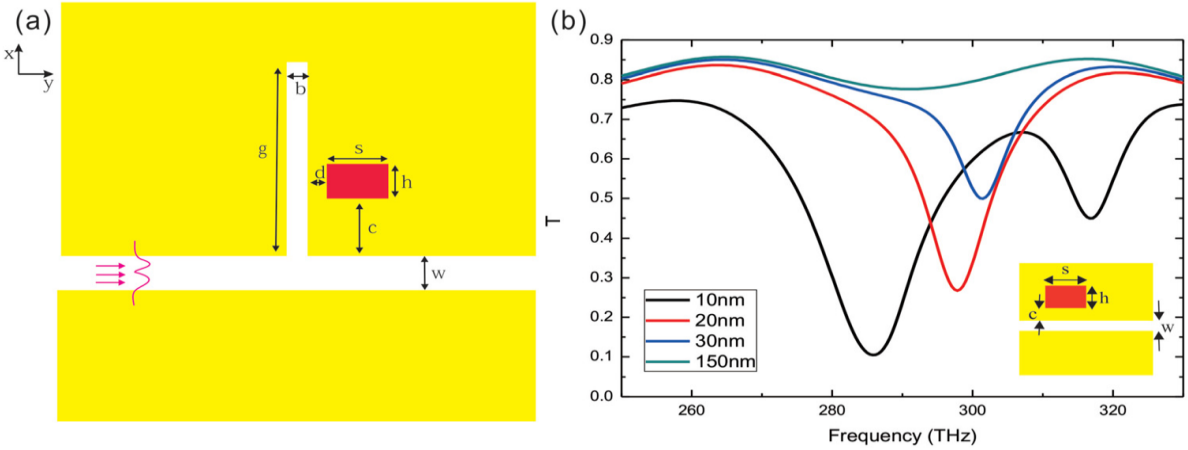

Figure (2.11): Illustration of (a) the schematic of a plasmonic resonator system in a nanoscale, (b) the SPP transmission spectra with a rectangular cavity with different values of c [137].

Figure (2.12) demonstrates a bright resonator with a high broadband resonance excitation and a dark resonator with a weak narrowband resonance excitation on the other side. Thus, the EIT transmission demonstrated the structure shown in Figure (2.11 b).

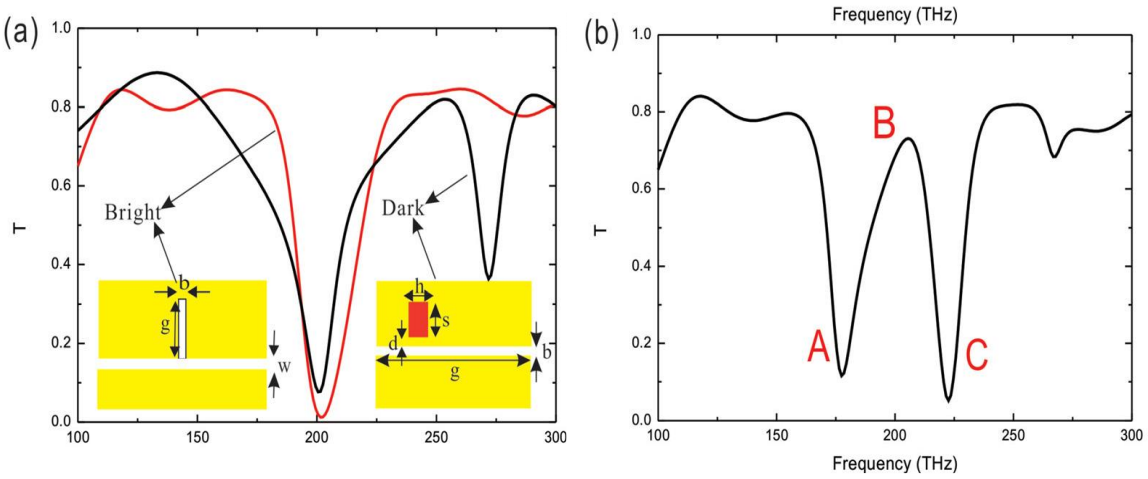

Figure (2.12): Illustration (a) the transmission spectra of both the dark and light states, (b) the EIT transmission spectra of the plasmonic resonator system [137].

However, when c=150nm, the electric field's strength in the line slot is weak. Hence, the dark resonator is weakly excited. Moreover, a bright resonator reflects the majority of the optical wave's incident light. As a result, the distance between the bright and dark states determines the width of the transmission spectra and can be enhanced by reducing the coupling distance.

2.7 Neuron cells

2.7.1 Physics of neuron activity

2.7.1.1 Neurons

The fundamental elements of the nervous system are represented by neurons, which are specialized cells. The number of neurons in the human brain is approximately 10^{11} neurons. These neurons transmit information via electrical and chemical signals. Furthermore, the neuron consists of three main parts known as soma, dendrites, and axon as shown in Figure (2.13). The soma represents the cell body that contains the nucleus and organelles to maintain the cell and to keep the functions of neurons. Soma neurons are

surrounded by dendrites, these dendrites received signals from thousand neighbor neurons. So, dendrites represent the input to the neuron which can be excitatory or inhibitory. The dendrites are covered by synapses that received signals as chemical signals from the neighbor neurons and converted them into electrical signals to the cell body. When the electrical signals are transmitted toward the cell body, an action potential will generate and a signal will transmit to the axon. The axon is an extended fiber from the cell body on one side to the ending of the cell on the other side. The neuron signals are transmitted through the axon. Some axons are covered by insulators called myelin. The myelinated axons could be transmitted information faster than other types of neurons and protect neurons. The axon is connected to other neuron cells by junctions called synapses [135].

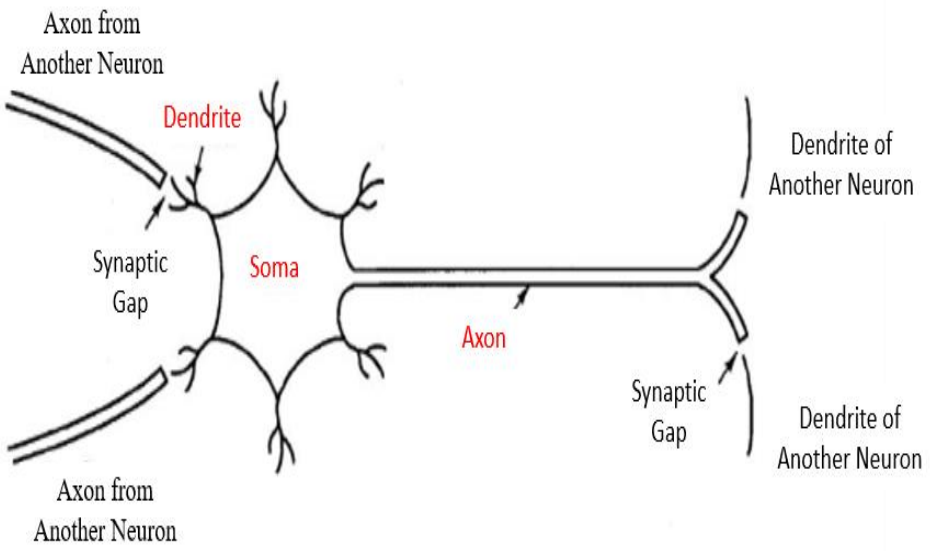

Figure (2.13): Illustrate the neuron's main parts

2.7.1.2 The Action Potential

A.L. Hodgkin and A.F. Huxley (1939) recorded the membrane potential change of a squid giant axon for the first time because of its large size (its diameter was approximately 0.5 mm, and it had a length of several

centimeters). The change of the membrane potential means the action potential (AP) which is illustrated in Figure (2.14). They measured the rest state of around -60mV by using a micro-electrode connecting with the axon [113, 114]. The action potential results from the transient change of sodium (Na^+) and potassium (K^+) ions across the membrane during 2 msec and reversal in polarity of the trans-membrane potential.

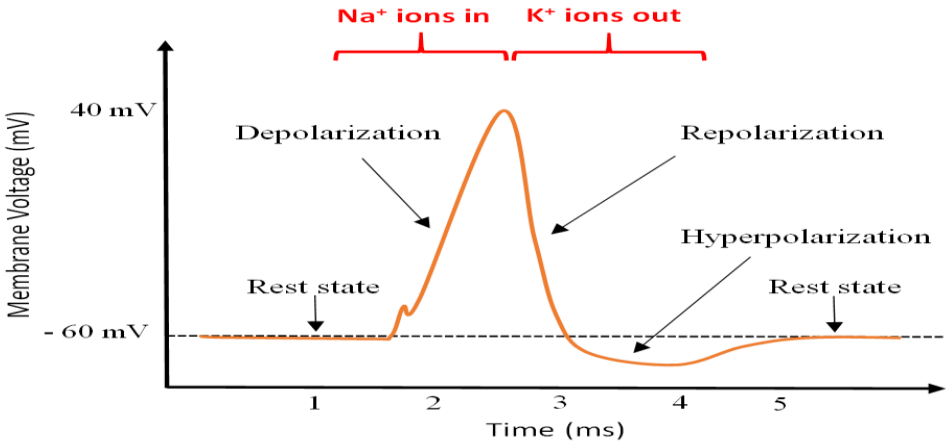

Figure (2.14): Illustrate the action potential of the intracellular using micro-electrode [115]

As shown in Figure (2.15), in the extracellular space the concentrations of the positive ions of Na^+ are more than in the intracellular space. Oppositely, the concentrations of K^+ ions in the intracellular are more than in the extracellular space. The action potential is powered by an imbalance between the ion concentrations and the membrane resting potential. This mechanism allows the membrane to be permeable to flow the ions and respond to stimulation. The cell membrane contains an ionic pathway called ion channels which allow the ions to flow through it in response to electrical or chemical stimuli. In the depolarization case, the sodium channels in the cell membrane are activating and resulting in a large influx of sodium ions. On the other hand, repolarization results from the inactivation of the sodium channel at the same time the potassium channels are activated which results

in the efflux of large ions of potassium. The potassium channels stay open for a little then they needed to back to their resting potential. In this case, the membrane potential dips briefly lower than its resting potential. The membrane contains the sodium-potassium pump that allows the movement of three ions of sodium to extracellular space and two ions of potassium to intracellular space in each pumping cycle. By sodium-potassium pump channels, the distribution of the ions back to normal cases [115].

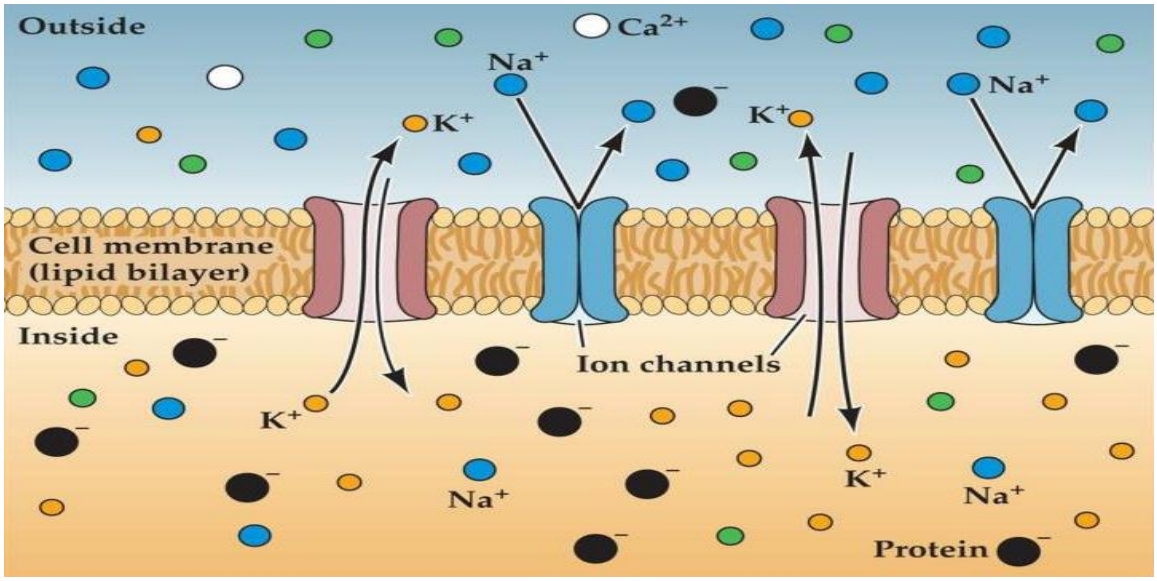

Figure (2.15): Illustrate the ion concentrations for a mammalian neuron [115]

2.7.1.3 Hodgkin-Huxley model

One of the models that represent the ionic membrane conductance, which varies with time and voltage, is Hodgkin and Huxley. This model supposes to segment the axon into several simples of the electrical circuit as shown in Figure (2.16). The electrical circuit describes the activity of the axon.

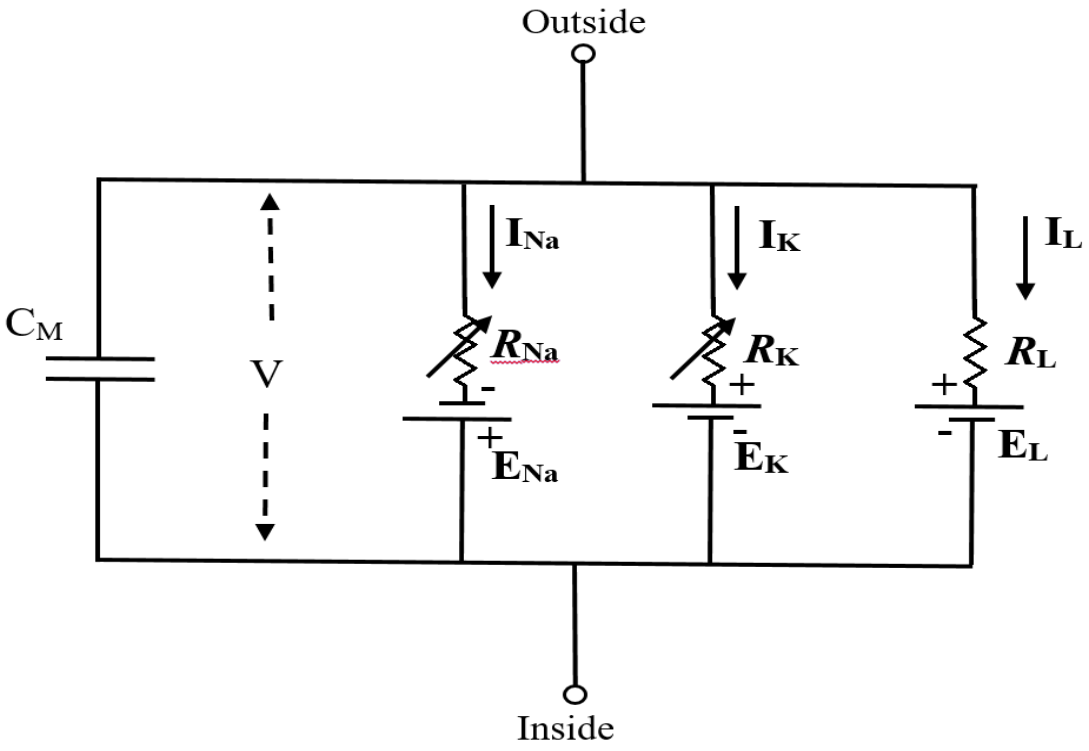

Figure (2.16): The illustration of the equivalent electrical circuit of the H-H model for squid axon [138].

According to the Hodgkin-Huxley model, the membrane of the neuron cell, which divides the cytoplasm from the extracellular space, could be represented as a capacitor. The value of the membrane capacitance is about 10 μF/cm^2. Consider parallel paths that pass three different types of ionic currents for the ionic current channels. They are referred to the sodium current (I_{Na}), the potassium current (I_K), and leakage current (I_L). The membrane ion channels are represented by the variable resistance with the sodium and potassium currents. Furthermore, the total current is represented by the summation of the capacitive and ionic currents. The rate of charge accumulation on the opposing sides of the cell membrane is represented by the capacitive current and is equal to $C\frac{dv}{dt}$.

Where v represents the membrane potential.

So, the total current is calculated as the following equation:-

$$I = C\frac{dv}{dt} + I_{Na} + I_K + I_L \tag{2.13}$$

The ionic current calculated by Ohm's law *(I=gV)*

$$\begin{aligned} I_{Na} &= g_{Na} \cdot (v - E_{Na}), \\ I_K &= g_K \cdot (v - E_K), \\ I_L &= g_L \cdot (v - E_L), \end{aligned} \tag{2.14}$$

Where g is the conductance of the ionic membrane and in the cases of sodium and potassium, it is varied.

In this model, Hodgkin-Huxley deduced the ionic membrane conductance could be formed as:-

$$\begin{aligned} g_{Na} &= x_1 m^3 h, \\ g_K &= x_2 n^4, \\ g_L &= x_3. \end{aligned} \tag{2.15}$$

Where x_1, x_2, and x_3 represent the value of the highest conductance for sodium, potassium, and leakage current, respectively. These values are constant as shown in table (2.)

Table (2.) Illustrate the parameter values assumed by Hodgkin-Huxley [138]

Ionic current	Reversal potential (mV)	Maximal conductance (mS/cm^2)
Sodium	$E_{Na} = -115$	$x_1 = 120$
Potassium	$E_K = 12$	$x_2 = 36$
Leakage	$E_L = -10.613$	$x_3 = 0.3$

In the sodium ion channel, the activation variable *m(v,t)* and the inactivation variable *h(v,t)* regulate the conductance. For potassium, only activation variable *n(v,t)* affects conductance. Furthermore, these variables represent the degree relevant to the ion channel that is open.

The ion channel for sodium is activated whit the probability of m^3h and the ion channel for potassium is activated with the probability of n^4. Furthermore, the activation and inactivation variables varied with time and are represented in the following equations

$$\begin{aligned} \frac{dm}{dt} &= \alpha_m(v)(1-m) - \beta_m(v)m, \\ \frac{dn}{dt} &= \alpha_n(v)(1-n) - \beta_n(v)n, \\ \frac{dh}{dt} &= \alpha_h(v)(1-h) - \beta_h(v)h. \end{aligned} \tag{2.16}$$

Where α represent the transition of the ion channel from the close state to the open state and β represent the transition of the ion channel from the open state to the close state [138].

2.7.2 The human cells

The human nucleus pulposus cells (HNPC) are jelly-like substances extracted from the intervertebral disc of a healthy human. Its function is to distribute the pressure on the disk in all directions when the disk is under load. This nucleus pulposus consists of nucleus pulposus cells, proteoglycan aggregations, and collagen fibrils.

The HNPC cells were purchased from the Royan Institute. The plasmonics chip must the first time coated with laminin (33 g/mL) and poly-L-lysine to support the cell's adherence before being used to culture neuron cells [118]. Dulbecco's modified eagles' medium (DMEM), which provides glucose for neuron cell growth, is what is required for cultured neuron cells.

Streptomycin (100 mg/mL) and fetal bovine serum (FBS) (20%) was added to this medium, which was kept at (37 °C) similar to the human temperature in an incubator with 5% CO2. For the first time, Human Nucleus Pulposus Cells (HNPC) cultured neuron cells were cultured on small dishes with a medium. This medium, which contains Neurobasal, penicillin/streptomycin (100 U/mL), B-27 supplemented (2% w/v) at (37^0C) in the incubator with 5% CO_2, and then L-glutamine (500 M). Streptozotocin is utilized in three doses (0.5, 1, and 2 mM). The samples (8) are divided into four groups each group with two chips. The first group remains healthy only neurons without the effecting of STZ. The second sample injured with Alzheimer's disease by injecting the cultured cells with a low dose of STZ equal to 0.5 mM. The third sample was injured with Alzheimer's disease by injecting the cultured cells with a middle dose of STZ equal to 1 mM. Furthermore, the remaining samples were injured with Alzheimer's disease by injecting the cultured cells with a high dose of STZ equal to 2 mM.

The resonance of the plasmonic sensor can detect neural activity based on the membrane refractive index and the minimal change in cellular volume. The sensor surface's dielectric constant is changed when neuron cells are cultured on a gold surface, which affects the refractive index. The basis for sensing is the detection of changes in the layer thickness or reflective index.

2.7.3 Neuronal insulin

2.7.3.1 Glucose transporters

Neurons cells consume high energy. This energy was spent to generate actions and biosynthesis for neurotransmitters. Glucose acts as the main energy for the brain, and glucose transporters (GLITs) are a special type of membrane protein. This energy is transported across the plasma of the membrane. There are several isoforms of GLUT that contribute to homeostasis and the functions of the brain.

The insulin transporters GLUT1 and GLU3 respectively regulate the absorption of glucose by glial neuron cells.

Furthermore, GLUT2 is found in the hypothalamus, which regulates food consumption. The presence of GLUT4 in the neocortex, cerebellum, and hippocampus suggests that GLUT4 is important in the uptake of glucose by neurons. Also, there are GLUT5, GLUT6, and GLUT 13 which have a weak affinity for glucose [119].

2.7.3.2 Insulin affects the brain.

Insulin and insulin-like growth factor 1 (IGF-1) are closely related and widely distributed in the brain. Also, their biological effects are done by two kinase receptors known as IR and IGF-1 receptors. The signaling machinery is shared intracellular by IR and IGF-1R and every significant part of the brain is signaling similar to that presented in peripheral tissue such as IR substrate 1 and IR substrate 2.

The molecules involved in this signaling have key roles in brain functions. The glycogen synthase kinase 3 beta (GSK3β) regulates the growth and plasticity of brain progenitor cells, and when it is activated, tau protein undergoes hyperphosphorylation, which is thought to be a key factor in the pathogenesis of AD.

Insulin controls many actions through the central nervous system (CNS), including eating, learning, behavior, and cognitive abilities. Also, protects against neuroinflammation and redox stress in the brain [120, 121]. Hence, neuronal insulin resistance may play a role in the development of Alzheimer's disease [122].

2.7.4 Dopamine

Dopamine (DA) is a neurotransmitter located in the central nervous system of the human brain. Dopamine acts as a chemical messenger and is essential for regulating intentional movement, learning, sleeping, attention, and reward in addition to playing a major role in the feeling of happiness. On the other side, if dopamine levels become abnormally regular in the brain, it will contribute to causing brain disorders such as Alzheimer's disease. Therefore, it is essential to understand how dopamine affects brain functions and to create a sensor to track the level of dopamine in brain cells. Therefore, several techniques have been used to trace the level of dopamine for the diagnosis, monitoring, and treatment of neurological disorders. The commercial techniques used to detect dopamine include chromatography, chemiluminescence, visible spectrophotometry, colorimetric probes, chromatography/mass spectrometry, fluorometry, and electrophoresis [123]. All the mentioned techniques had limits of detection at a nanomolar level. So, one of the novel techniques with high sensitivity is surface plasmon resonance. The SPR technique offers a promising way that overcomes the limitation of the previous methods.

The effect of dopamine is exerted by binding to the cell surface receptors and its activation. In mammals, there are five subtypes of receptors that are labeled D1 to D5. These receptors are divided into D1-like and D2-like families. The ultimate effect of D1-like on the neurons located in the nervous system is to activate the receptors (D1 and D5). These receptors can be

exciting (open the sodium channels) or inhibit (open the potassium channels). On the other hand, the effect of D2-like activation represented by D2, D3, and D4 inhibits the targeted neuron. Furthermore, its effects on the neuron are based on the receptors located on the neuron's membrane. The series of receptors from D1 to D5 represent the dopamine level which is the highest at D1 and lowest at D5.

2.8 Alzheimer disease

Alzheimer's disease (AD) is a brain dementia that injured older people over the age of 65. It affects the ability of the human to carry out their daily activities such as memory, learning, thinking... etc. Because of this dementia, the neuron cell died and the patient can still be alive between 3 to 9 years. This dementia causes damage to the neuron cells and then the patient died takes around three to nine years. Nearly 45 million people worldwide are affected by this dementia and ranked as the fifth most deadly disease in the world [124]. In the USA, there are approximately 5.8 million patients with AD, and it is predicted that number would increase to 13.8 million by 2050 [125]. Furthermore, by the year 2050, 18.9 million people in Europe are expected to have the disease.0 [126], as well as 36.5 million in East Asian nations [124]. Amyloid beta (A) and tau protein aggregation caused this disease to form.

2.8.1The Features of Alzheimer's disease

2.4.2.5 Amyloid Beta Aβ

The term "Aβ " referred to the length of the amino acid sequence in the cerebral and peripheral tissue. The sequences range from 36 to 43 amino acids, and Aβ -42 is the worst one for causing amyloid plaques to aggregation [127]. The pathophysiology of Alzheimer's disease is characterized by the aggregation of Aβ-42. The diameter of Aβ-42 is about 70 to 100 A^0 and its insoluble as shown in Figure (2.17) [128].

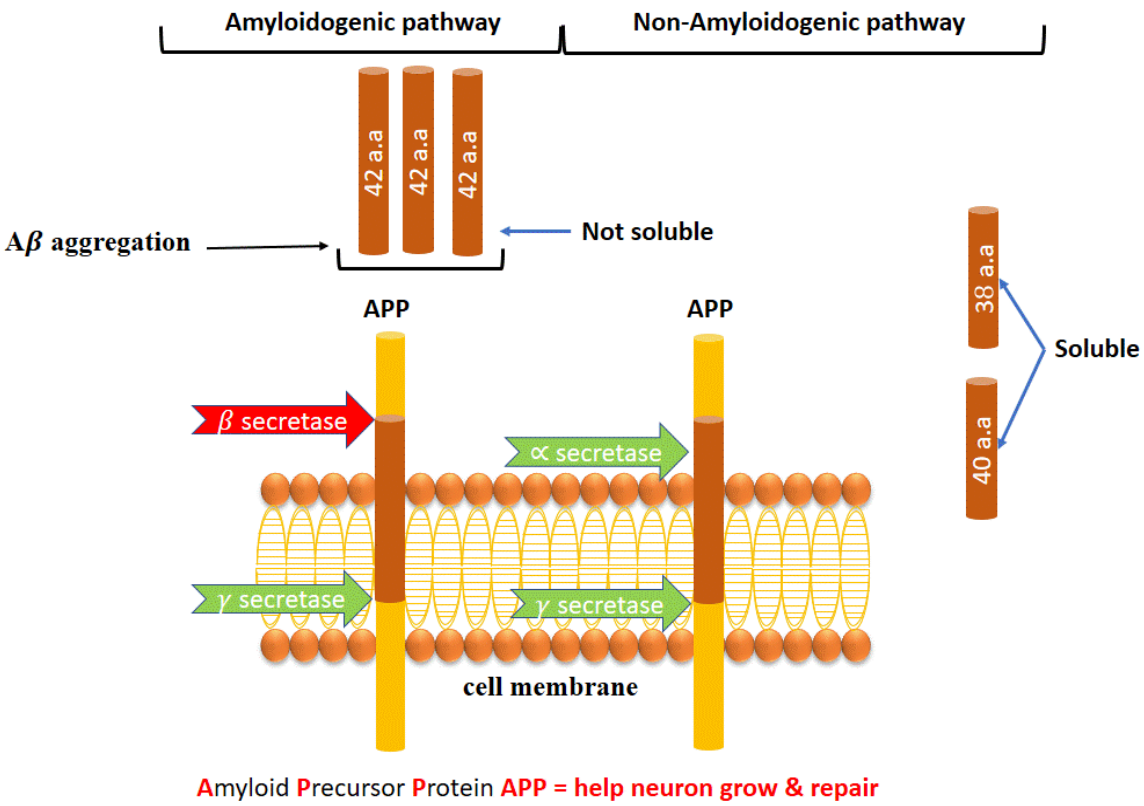

Figure (2.17): The schematic of amyloid beta aggregation [128].

2.4.2.6 Tau Proteins

The accumulation of tau proteins is the second characteristic of AD. This particular protein is produced by the gene for microtubule-associated protein tau (MAPT) and belongs to the soluble protein family. It is based on the axons of the neuron cells to maintain stability and to enhance polymerization. As shown in Figure (2.18), neurofibrillary tangles are an insoluble form of tau protein aggregation that develops in AD [129].

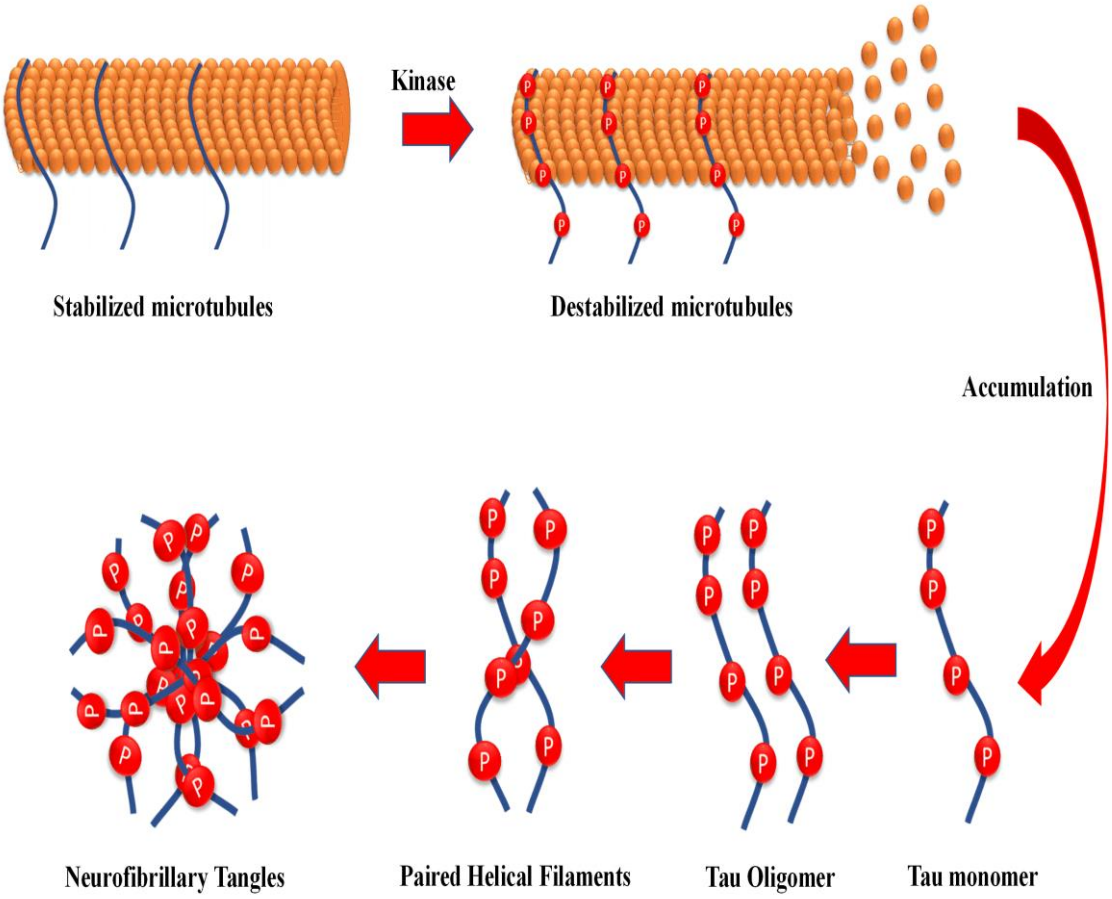

Figure (18): Illustration the tau protein aggregation called neurofibrillary tangles [129].

2.8.2 Streptozotocin

Streptozotocin, also known as streptozocin (STZ), is a glucosamine-nitrosourea compound originally used as an antibiotic. This compound is toxic to the pancreas's insulin and is used in the research field to induce a model of Alzheimer's disease in vivo and in vitro. As shown in Figure (2.19), adding STZ intraperitoneal or intracerebroventricular led to induce the aggregation of amyloid-beta (Aβ) and tau protein. Additionally cause oxidative stress, neuroinflammation, and metabolic changes. The primary characteristics of the pathological disease, which results in a loss of cognitive function and causes neuronal death, are A-aggregation and tau proteins [130]. In order to create β-amyloidogenic in vivo and in vitro models, Zhang

et al. report that STZ produced deficiency in the insulin with AD transgenic mouse model [134]. STZ utilized in vitro research to model the cellular mechanisms causing Alzheimer's disease [135-136]. Additionally, Kamat et al. discovered that STZ is related to pancreatic beta cells damage, which results in an insulin deficiency. Moreover, STZ affects glycogen synthase kinase by affecting insulin receptors in the brain (GSK3β) [130]. Affecting GSK3 activity, which is associated with brain disorders such as Alzheimer's disease, type 2 diabetes, and other brain disorders [131]. A large dose of STZ injection has a negative impact on the pancreatic beta cells' GLUT-2, which results in loss of insulin secretion [132]. STZ is used to introduce diabetes type II in small doses [133].

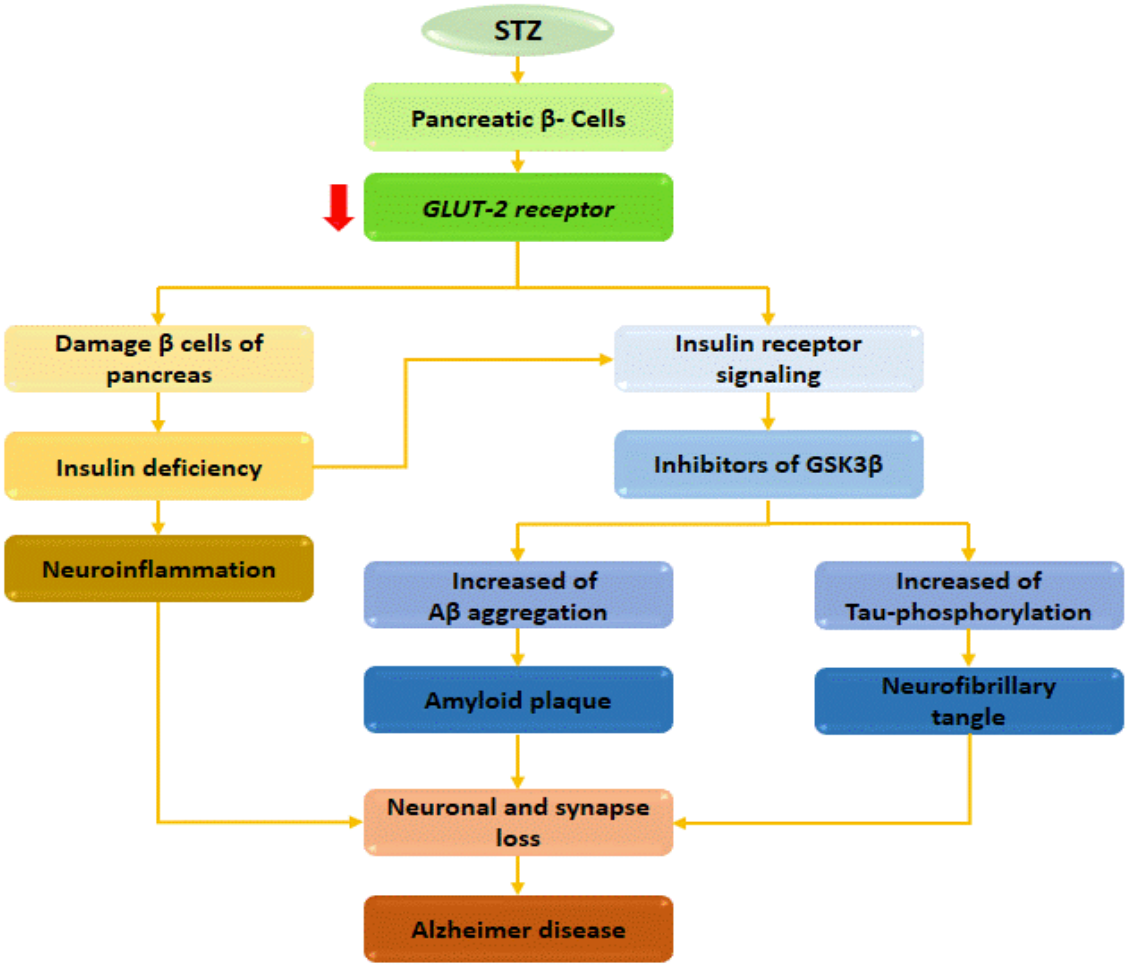

Figure (2.19): The diagram that illustrated how streptozotocin damages the pancreatic beta cells and induces Alzheimer's disease [130].

Chapter Three

Material and methods

3.1 Introduction

This chapter explained how to prepare a one-dimensional plasmonic chip from the polycarbonate (dielectric) as a substrate and coated with a thin layer of gold. Also, explained in detail the setup and all components used in this setup. The first experiment includes the preparation of the electro-plasmonic chip and then measuring the plasmonic spectrum and the generating of plasmonic induce transparency by using an objective lens. Furthermore, applying external voltage and measuring the tunable plasmonic induce transparency by increasing the voltage applied. The next step investigated the electro-plasmonic chip as a new kind of neurotransmitter sensor by adding dopamine and measuring its effect on the plasmonic chip by using spectroscopy.

The second part was done by culturing the plasmonic chip with neuron cells extracted from rats and explaining in detail the dissection and culturing of neuron cells. To investigate the plasmonic chip's ability in measuring the cell’s activities using chemical stimulus (dopamine). So, the first sample was measured with no dopamine and then different concentrations of dopamine were used to measure the cell’s performance.

The third part of this chapter, explains how to prepare eight samples of the plasmonic chips cultured with HNPC. These samples were divided into four groups each with two samples. The first group kept healthy without STZ. The second group was injected with a low dose of STZ equal to 0.5 mM. The third group was injected with a middle dose of STZ equal to 1 mM. The final group was injected with a high dose of STZ equal to 2 mM.

Then, investigation of the ability of streptozotocin (STZ) to inhibit the cell’s activity and induce Alzheimer's disease.

3.2 Sample preparation

Fabrication of one-dimensional (1D) plasmonics chips utilizing commercial DVD grating polycarbonate (pc). The outer layer and inner layer are first separated using a sharp instrument. Utilizing the inner layer with the lattice groove and discarding the outer layer. The next step is to use ethanol to remove the purple color before washing it with DI and drying it with a drier. The prepared layer was divided into specialized pieces facilitated with a one-dimensional pattern. The substrate needed to be protected from any pollutants or fingerprints that could interfere with the measurements. As shown in Figure (3.1), the substrate is connected to two wires before being coated with a 35nm-thick layer of gold using a desk sputter coater. The advantages of the produced structure include a fast and cheap manufacturing process, small dimensions, biocompatible, and good strength. A voltage within the specified range of 1–3 volts should be applied to the sample's surface to create electro-plasmonic properties in the plasmonic sample. Due to the coating of a thin layer of gold on the plasmonic sample, the two electrodes should be connected to the substrate with conductive silver adhesives.

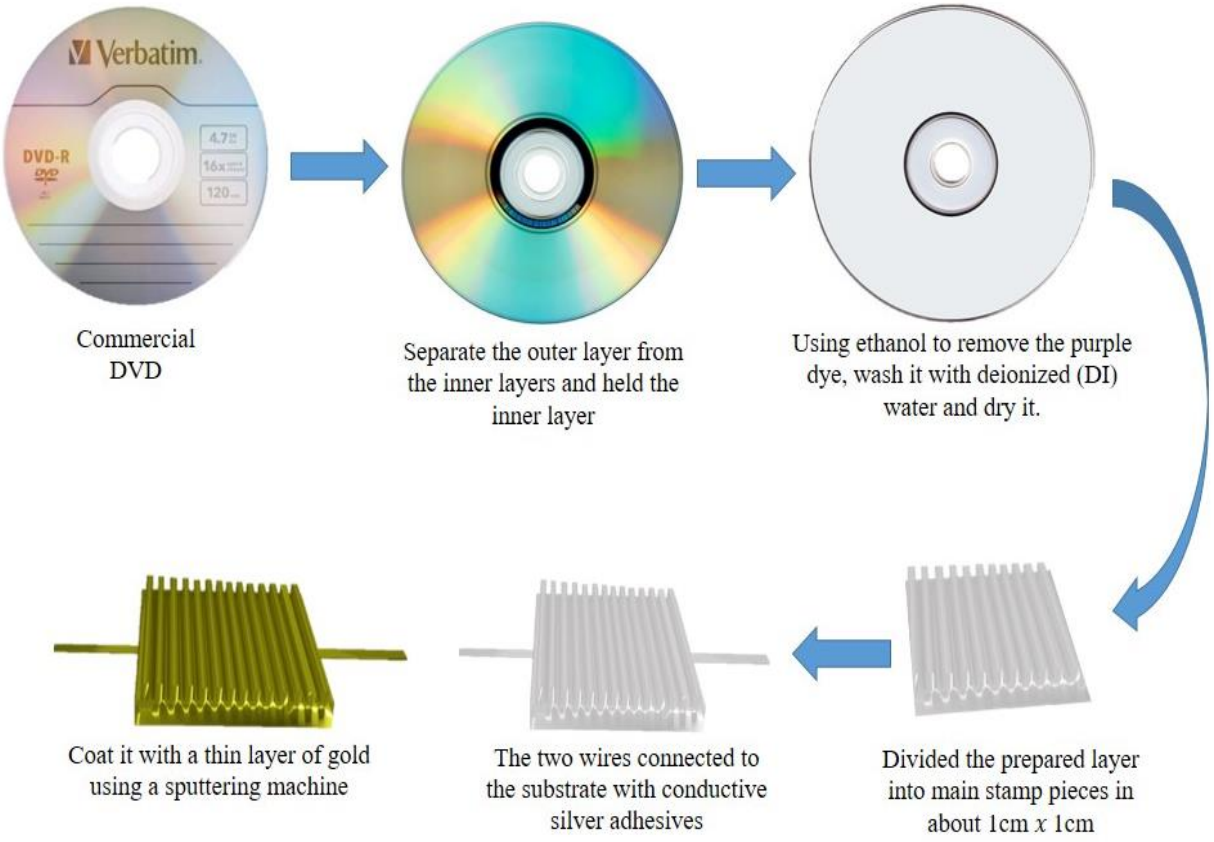

Figure (3.1): The schematic of preparing a one-dimensional nanograting chip from the commercial DVD and with a thin layer of gold was coated.

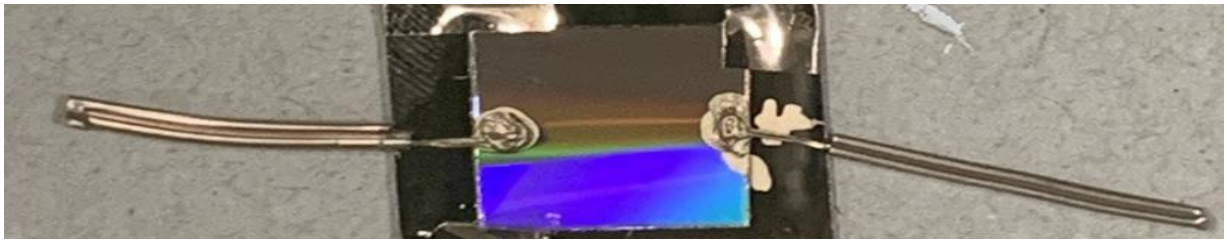

Figure (3.2): A real image of the one-dimensional nanograting chip

3.3 Experimental setup

To build the experiment setup, several components are required such as:-

1. **A light source.**

The light source used in the experimental setup is a broadband halogen illuminator. The wavelength range of the light source is about 400–700 nm (white light). This band is safe for dealing with cultured neuron cells. The

illumination intensity of the light source is variable manually from 0 to 100%. This type of source was used to excite the plasmonic chip by the objective lens and measured by spectroscopy.

2. `Collimator.

The collimator is a device that consists of a tube and a convex lens. It is used to change the diverging light from a point source to a parallel beam. This beam of light is required to pass through the polarized and then measured by spectroscopy.

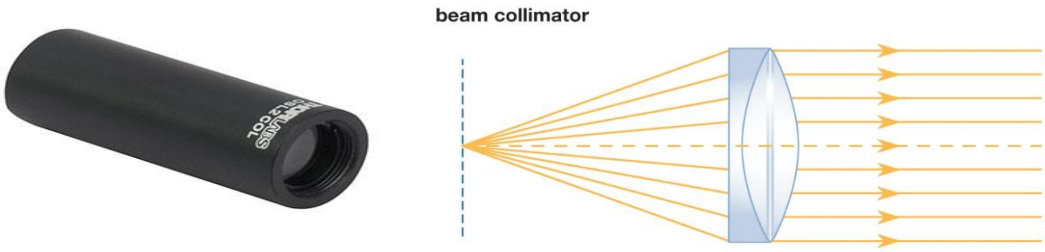

Figure (3.3): Illustration of the collimator functions

3. Polarization.

Polarization is an optical filter that permits to the passing of a specific polarization of light waves while blocking other polarizations. The polarization is required because of the wave propagating phenomena such as reflection, refraction, and diffraction. Polarization is the process of changing the scattered waves in a single proper direction. The polarization is applied to the transverse wave and cannot be applied to the longitudinal waves.

The polarization is divided into S and P polarizations which are essential properties for transmission waves in the medium. The S polarization refers to Senkrecht which is derived from the German word and means perpendicular. That is mean the S polarization is perpendicular to the

plane of the incident. The P polarization refers to the parallel plane of the incident.

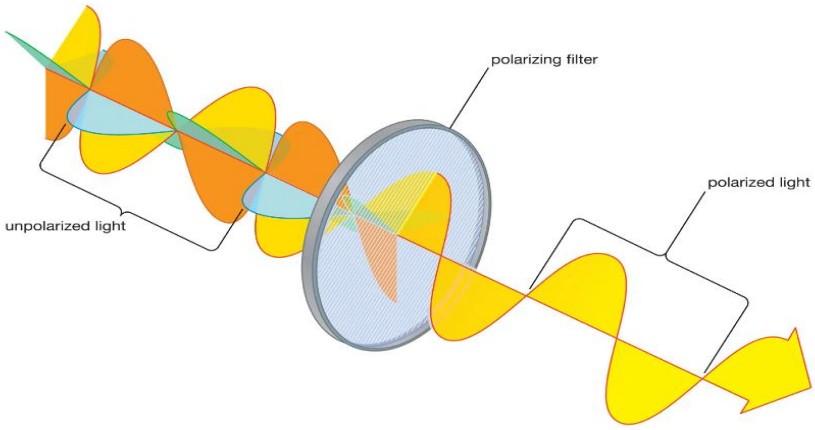

Figure (3.4): Illustration of the optical filter polarization

4. Optical lens.

The optical lens is a transparent component used to focus the light beam on a focal point. In our setup, the polarized light passes through the optical lens to focus on an optical mirror.

5. Mirror.

The optical mirror used to reflect the beam of light at a suitable angle depend on the setup. In our setup, the mirror is used to reflect the beam of light coming from the optical lens at an angle of about 45^0 to pass to the objective lens

6. Objective lens.

The objective lens is an optical element used to gather the beam of light and focus it on an objective and it's specified with a short focal length. The objective lens is designed normally with a cylindrical shape containing lenses made of glass to collect light and focus it on the sample point. The

objective lens with a numerical aperture (NA=0.65) was used to excite the SPP.

7. **An external voltage supply (DC).**

The power supply (DC) is used to apply an external voltage on the plasmonic chip to increase the sensor sensitivity. When the applied voltage increased from 1V to 3V the sensitivity increased and this physical phenomenon is known as tunable plasmonic induce transparency.

8. **Objective lens 2.**

The second objective is used to gather the transmitted light passing through the plasmonic chip and focus it in a narrow beam to the fiber adapter.

9. **Fiber adapter.**

The fiber adapter is used to pass the light beam to the optical fiber cable which is connected directly to the spectroscopy.

10. **Optical fiber cable.**

An optical cable is used to transmit the optical signal to the spectrometer device.

11. **Spectrometer**.

The spectrometer is a device used to measure the optical spectrum. Display the intensity of the light as a function of frequency or wavelength. Also, the spectrometer receives the optical signal, convert it to a digital signal, and displays it through specific software such as the ocean software installed on a computer.

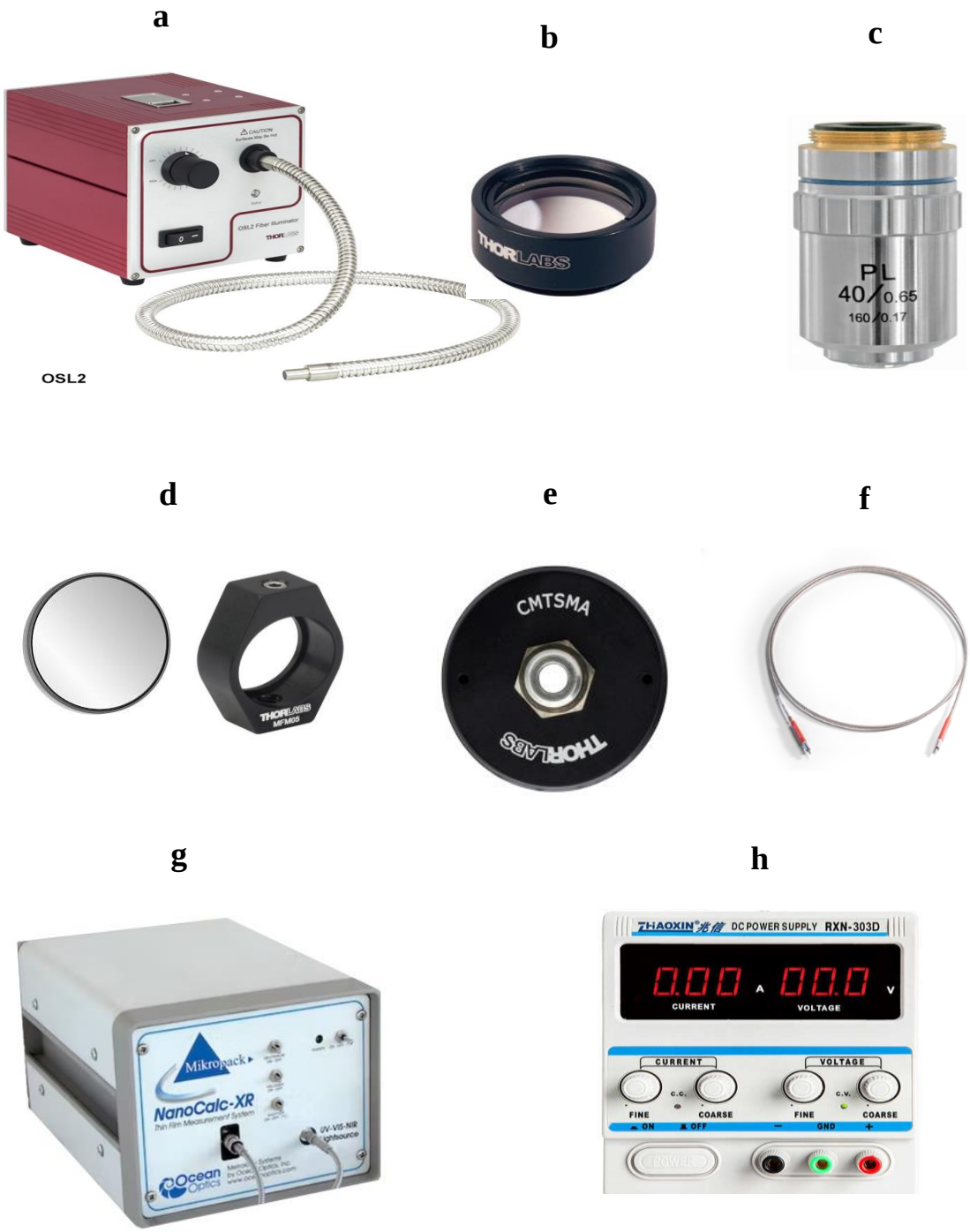

Figure (3.5) shows the experiment components (a) light source (broadband halogen), (b) Optical lens, (c) Objective lens, (d) Mirror, (e) Fiber adapter, (f) Optical fiber cable, (g) Spectrometer, (h) DC power supply.

12.Homemade chamber

The homemade chamber is fabricated from glasses to incubate the plasmonic chip throughout the experiment. Also, to keep the food of the culture neuron cells and make the injection of stimulus or inhibit liquid to the chip easy.

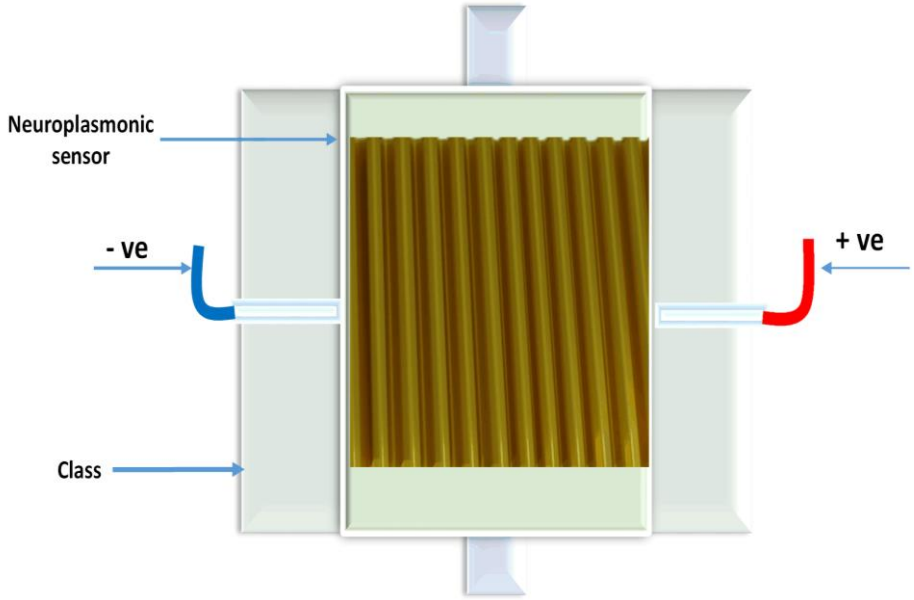

Figure (3.6): Illustration the homemade chamber used to incubate the plasmonic chip throughout the experiment

13.Ocean software.

The ocean software allows the performing of three spectroscopic experiments such as emission, absorbance, and reflectance. The spectroscopy acquired the data from the detector in real time and displays the data via ocean software which allows the user to evaluate the experiment setup and the parameters. Furthermore, when adjusted the setup and parameters saved the data to a specific location on the computer driver. The data is saved as ASCII files and plotted on another software such as OriginPro software.

Figure (3.7): Shows a screenshot for the ocean software that read the data from the spectrometer.

14. OriginPro software.

The OriginPro software is a computer program designed for data analysis and scientific graphing which support 2D and 3D plot. Various formats of data files could be imported in Origin such as Excel, ASCII text, NI TDM, SPC, DIADem, etc. On the other hand, graphs could be exported in various image formats such as GIF, JPEG, TIFF, etc.

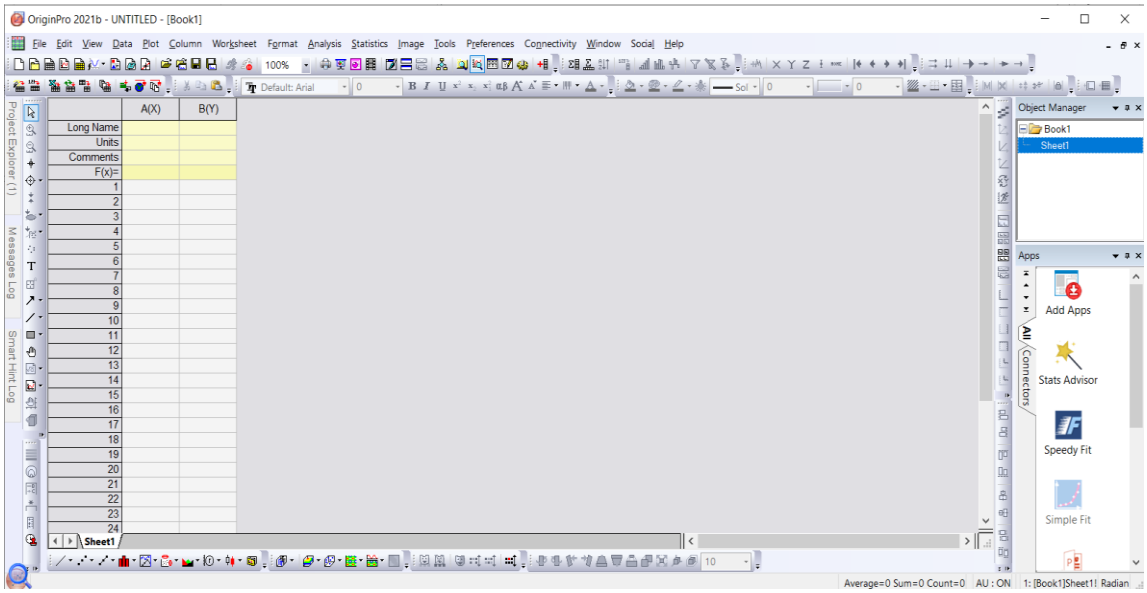

Figure (3.8): Shows the snap shot of the OriginPro software

Table (3.1) Show the setup components and their functions

No.	component	model	Made in	function
1	Light source broadband halogen illuminator	Thorlabs - OSL2	USA	*Deliver white light (*400 - 900 nm*)*
2	Collimator	Thorlabs - OSL2COL	USA	Device for changing the light passing through it from a point source to a parallel beam
3	Polarizer	Thorlabs - GT10-A	USA	Optical filter permit to passing of a specific polarization of light waves while blocking other polarizations.
4	Optical lens	Thorlabs - AC254-035-A1	USA	Focusing the light beam on a focal point
5	Reflected lens	Mirror		Reflect the light beam
6	Numerical objective (NA = 0.65)	Entatial	UK	Used for SPP excitation
7	XYZ Translation Stage	Thorlabs – PT3/M	USA	controlling the height of the chip from the objective lens
8	Fiber Adapter	Thorlabs – CMTSMA	USA	*adapters connector*
9	Fiber cable	Ocean Optics QP600-2-VIS-NIR	USA	Transmitted the optical signal to the spectrometer
10	Spectrometer	Ocean Optics XR model	USA	Receive the optical signal, convert it to a digital signal, and display it through the ocean software on a computer.
11	DC power supply	RXN -303D	China	Applied external voltage

3.4 Build the experiment setup

To build the experiment setup, a light source (halogen illuminator) was used to deliver white light. This band is safe for dealing with cultured neuron cells. The delivering light needs to pass through a collimator to convert from a point source to a parallel beam and then to a polarizer as an optical filter to pass only P or S polarizing light. The polarized light will pass through an optical lens to focus the light beam on the mirror and the mirror will reflect the light beam to the objective lens. The objective lens with 0.65 numerical aperture focuses on the plasmonics chip to excite the SPPs on the interface between the metal and the dielectric. Connect the two terminals of the plasmonic chip with an externally applied voltage (DC) to increase the chip sensitivity by getting tunable plasmonic induce transparency. Using another objective lens to focus the observing beam through the plasmonic chip to the fiber adapter and then transmitted the optical signal to the spectrometer. The spectrometer receives the optical signal, convert it to a digital signal, and finally displays it through the ocean software on a computer. The data set for each measurement is saved on the computer and by using originPro software which is used to draw the curves for each case. OriginPro software is a data analysis program that is used to plot in 2D and 3D. All the components detail of our experiment are explained in the following table (3.1) with their models and country. Also, shown schematically in Figure (3.1 a).

a

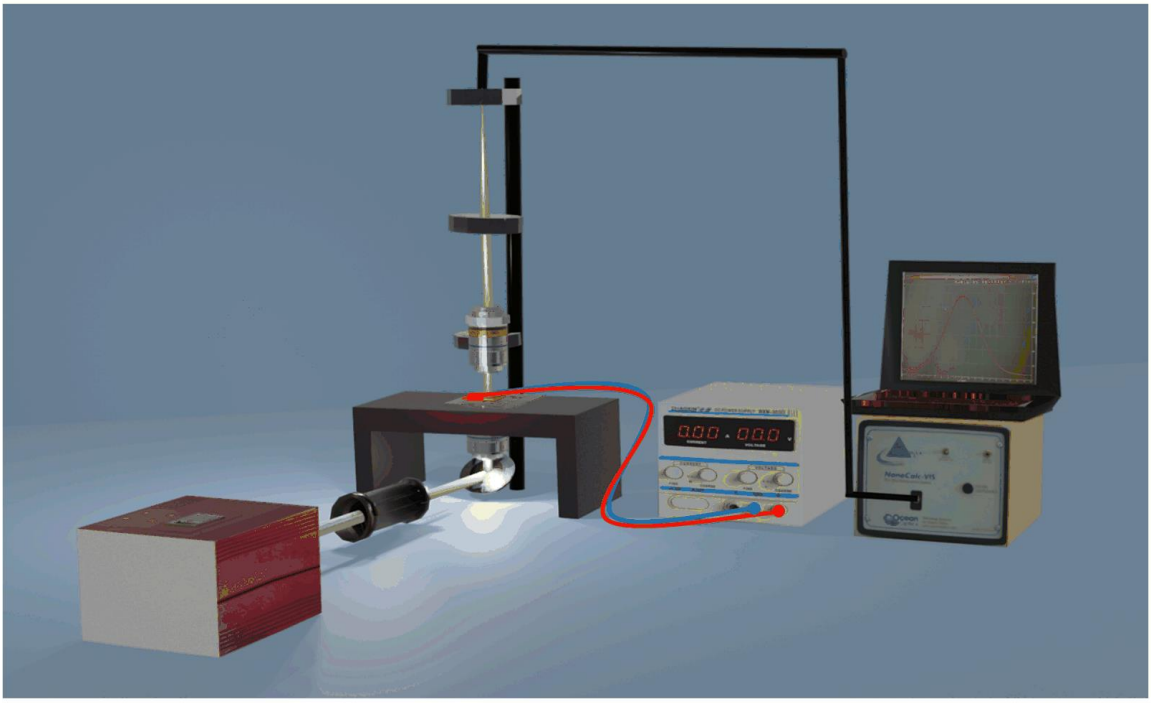

b

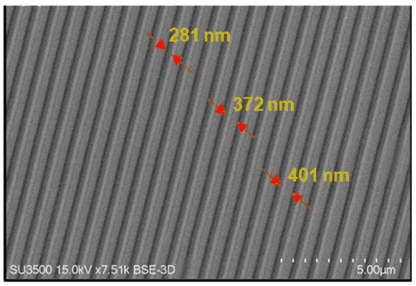

c

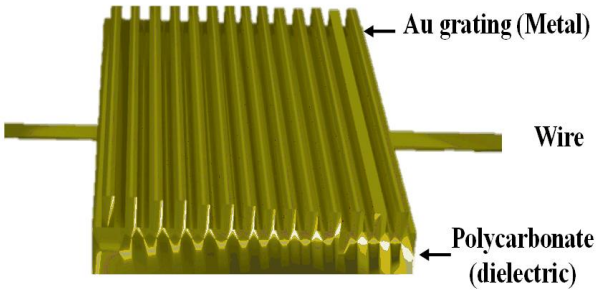

Figure (3.9): The schematic illustrate the setup connection that contain from (a) halogen illuminator, Collimator, Polarizer, Reflected lens, Numerical objective, XYZ Translation Stage, Fiber Adapter, fiber cable, Spectrometer, (b) scanning electron microscopy image, (c) the schematic of the prepared plasmonic chip.

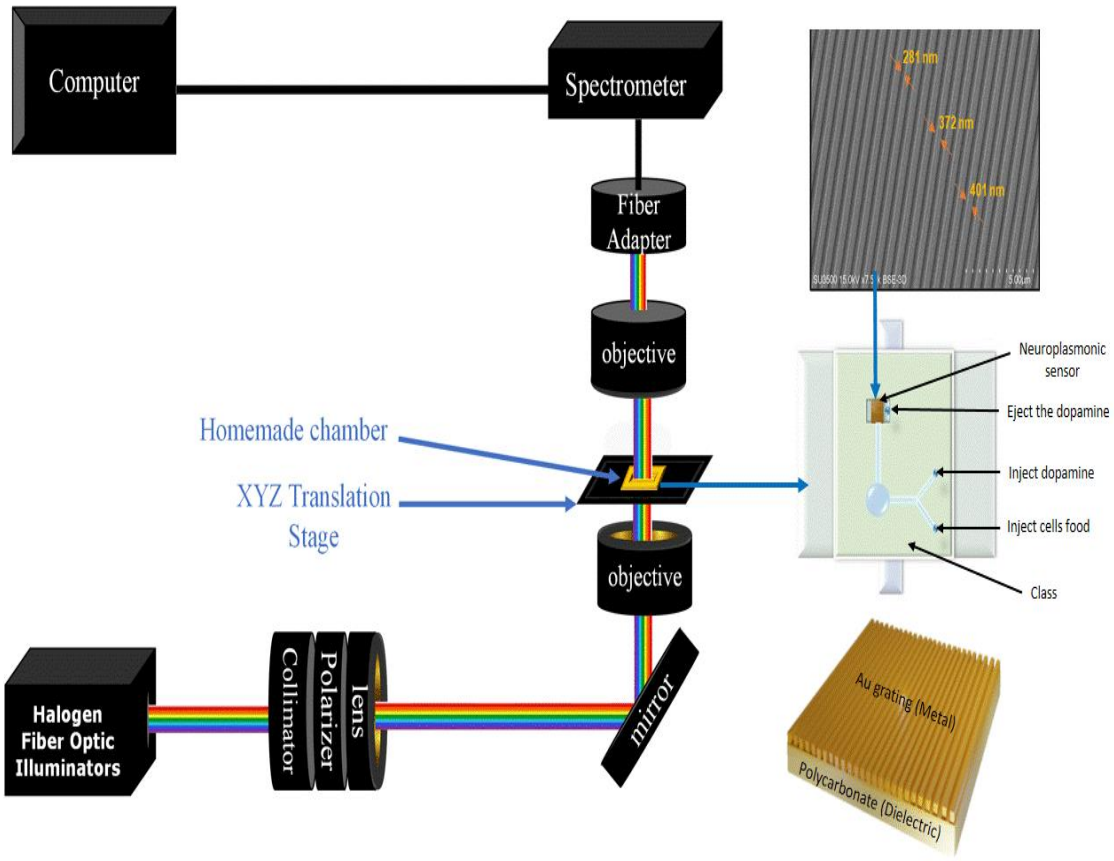

Figure (3.10): The schematic illustrates the details of the components that are shown in Figure (3.9)

3.5 Excitation of the sample

Figure 3.11 displays the arrangement of SPP excitation by the objective lens from the backside of the plasmonic sample. We used broadband light with a range of wavelength about 400–700 nm, a grating chip coated with a thin layer of gold equal to 35 nm, and an objective lens with NA= 0.65.

By illuminating light in P/S polarized components passing through the substrate to excite SPPs on the gold grating, we have two main horizontal and vertical SPPs in each groove. The SPPs would disrupt the localized electric field that is present at the objective lens' geometric focus. [35].

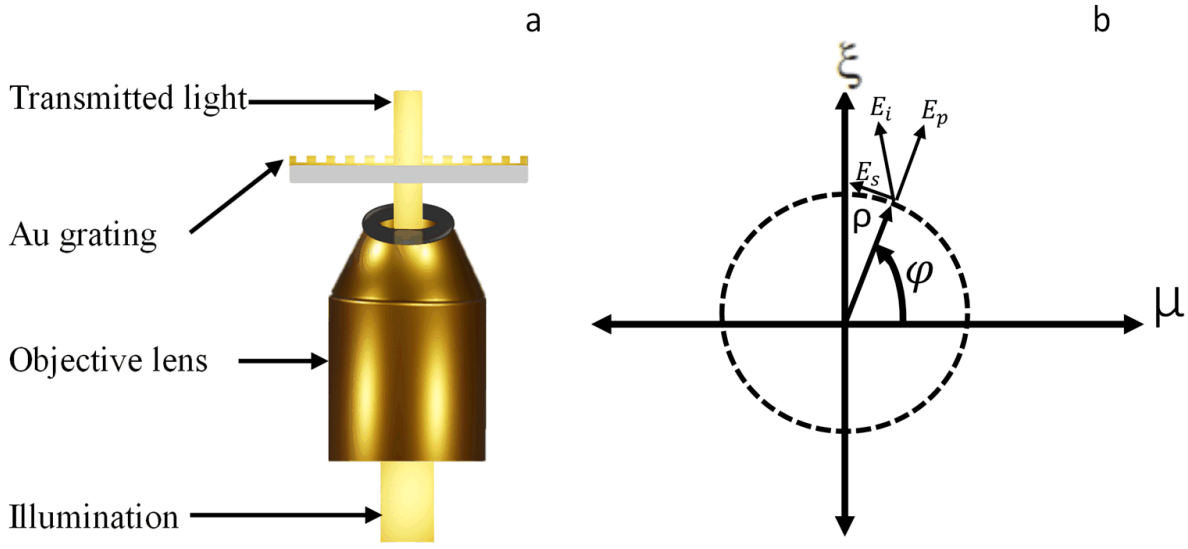

Figure (3.11): Illustration of (a) Schematic of SPP excitation using a high numerical objective lens (b) Coordinates used for calculation

3.6 Measurement system

A spectroscopy measurement system was used to measure and study the properties of the linear transmission spectrum in a one-dimensional gold/ Polycarbonate plasmonic nanostructure. The incident light from the halogen lamp passed through the polarizer; then using the objective lens, the light was focused on the sample and changed the polarizations to excite the surface plasmon polariton (SPP). Next, the transmitted light through the sample was collected by the microscope objective (40X, NA=0.65) and then coupled to microscopy (Model NANOCALC-XR, Ocean Optics, Germany) by another eyepiece.

The next step was done by applying external voltage from 1V to 3V in two different polarizations. After completing the measurements of all cases, the second measurement of sensing dopamine concentration was initiated in similar cases with S and P polarization, using three voltage levels from 1 V to 3 V. This measurement aimed to check and monitor the sensing performance with the electro-plasmonic sensor.

3.7 Preparing the concentration of dopamine

To prepare the dopamine concentration as listed in Table 3.2, the laboratory should be dark. The sample tubes must be washed with water, acetone, isopropanol, and deionized (DI) water respectively, followed by blow-drying.

Table 3.2: The concentration of dopamine is taken in three samples

Sample	dopamine	deionized (DI) water	Concentration
S_1	0.375ml	4.625cc	3mg/ml
S_2	0.625ml	4.375cc	5mg/ml
S_3	0.875ml	4.125cc	7mg/ml

3.8 Cultured neuron cells

3.8.1 Cultured neuron cells extracted from Rats

3.8.1.1 Prepare the chip for cultured neuron cells.

The plasmonic chip is coated with laminin (33 μg/mL) and poly-L-lysine which enables the cultured neuron cells to adhesion [34]. The Dulbecco's Modified Eagles' Medium (DMEM), which contains glucose and supports the growth of neuron cells, was used to culture the neuron cells. Fetal bovine serum (FBS), a necessary component for the growth and maintenance of the cultured cells, was supplied with 20% to this medium. In addition, 100 mg/mL of streptomycin and 100 /mL of penicillin are added at body temp (37 ^{0}C) in a humidified condition of 5% CO_2 as an antibiotic treatment to treat bacterial infection.

3.8.1.2 The protocol for culturing neurons of rat cortical

Cultured neuron cells of rat cortical are important for studying neural functions and development, drug discovery, neurotoxicity screening, and mechanisms disease of neurological. This protocol explains the instructor of dissecting and culturing neurons from postnatal (P1-P2) rats.

3.8.1.3 Dissection of the cortical tissue

1- Place the rat head in a petri dish (100 x 20 mm) containing cold PBS.
2- Cut through the skull of a rat with small scissors and keep cuts to avoid damaging the tissue.
3- Take out the brain and place it in a petri dish (60 x 15 mm) containing cold PBS. Keep it on ice.
4- Repeat the previous steps for the remaining ready heads.
5- Under the dissection microscope, the brain fissure and cuts as shown in Figure (3.12) by using Vannas-Tubingen scissors.
6- Peel off each hemisphere by using fine forceps and then reveal the mid-sagittal side of the brain.
7- By using Vannas-Tubingen scissors, remove the hippocampus and c-shaped region. Place the remaining tissue in a new petri dish containing cold PBS and then keep it on ice.
8- Cut the isolated tissue into small pieces of about $2mm^2$.

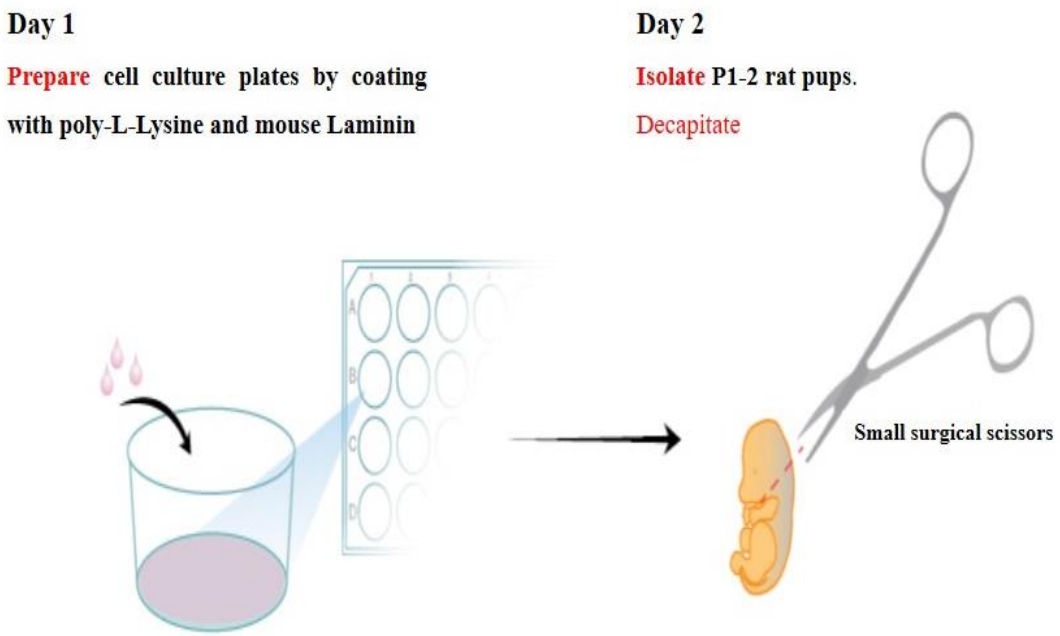

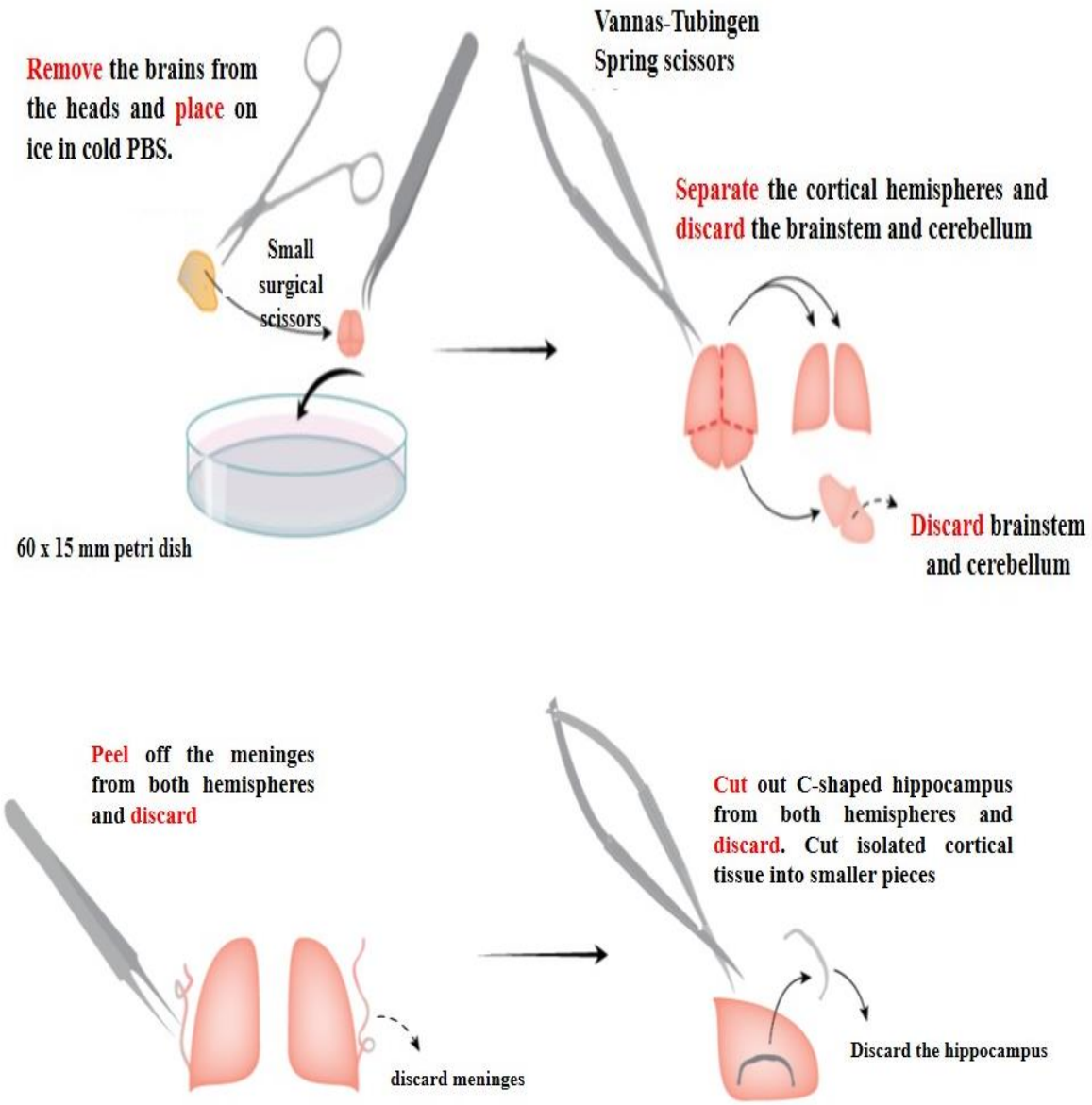

Figure (3.12): Illustration the steps of dissection of the cortical tissue

3.8.1.4 Dissociation and culturing of the cortical neurons.

1- Use a conical tube (15 mL), and mix Papain (20 U/mL) and DNase I (100 U/mL) in 5 mL of EBSS. Keep the solution in a humidified incubator with 37 ^{0}C and 5%CO_2 for 10 minutes.

2- Transfer the prepared tissue to the conical tube which contains the warmed solution. Keep the conical tube in a 37 ^{0}C, 5% CO_2 humidified incubator for 20 -30 minutes.

3- Triturate the prepared tissue by using a pipette fire-polished about 10-15 times until the solution is homogeneous.
4- The next step was a centrifuge at 200 g at room temperature for 5 minutes and then decant the solution.
5- Resuspend the prepared cells in the previous step with EBSS (5 mL) which contains about 1 µg/mL of Ovomucoid protease inhibitor with BSA as shown in Figure (3.13).
6- Centrifuge the solution in step 5 at 200 g at room temperature for 4 – 6 minutes and then decant the solution.
7- By using Neuron Base media, wash the cells twice in 10 mL and then centrifuge at 200 g at room temperature for 5 minutes and then decant the media.
8- Resuspend the prepared cells in Cortical Neuron Cultured Media about 10 mL with warmed completely. Mixing about 10 µL of the suspension cell with about 10 µL of Trypan blue (0.4%) and then counting the live cells.
9- The next step includes adding the neurons to the prepared plasmonic chip.
10- Keep the samples until use in a humidified incubator at 37 ^{0}C, (5%) CO_2.

These samples can maintain for up to 4 weeks by exchanging the media every 3-4 days.

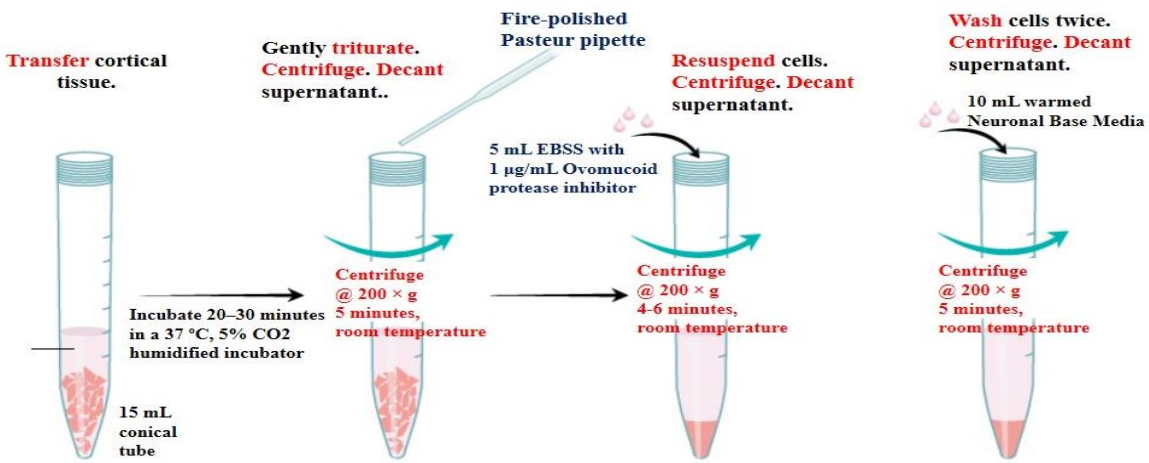

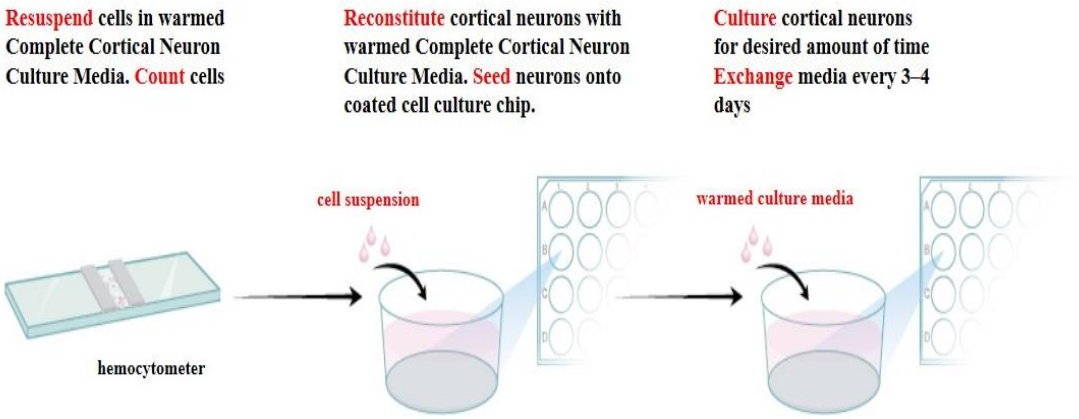

Figure (3.13): Explain the dissociation and culturing of the cortical neurons.

After culturing the neuron cells successfully and when the chips are ready to recording the cells activity, the chips will bring to the plasmonic lab as shown in Figure (3.14).

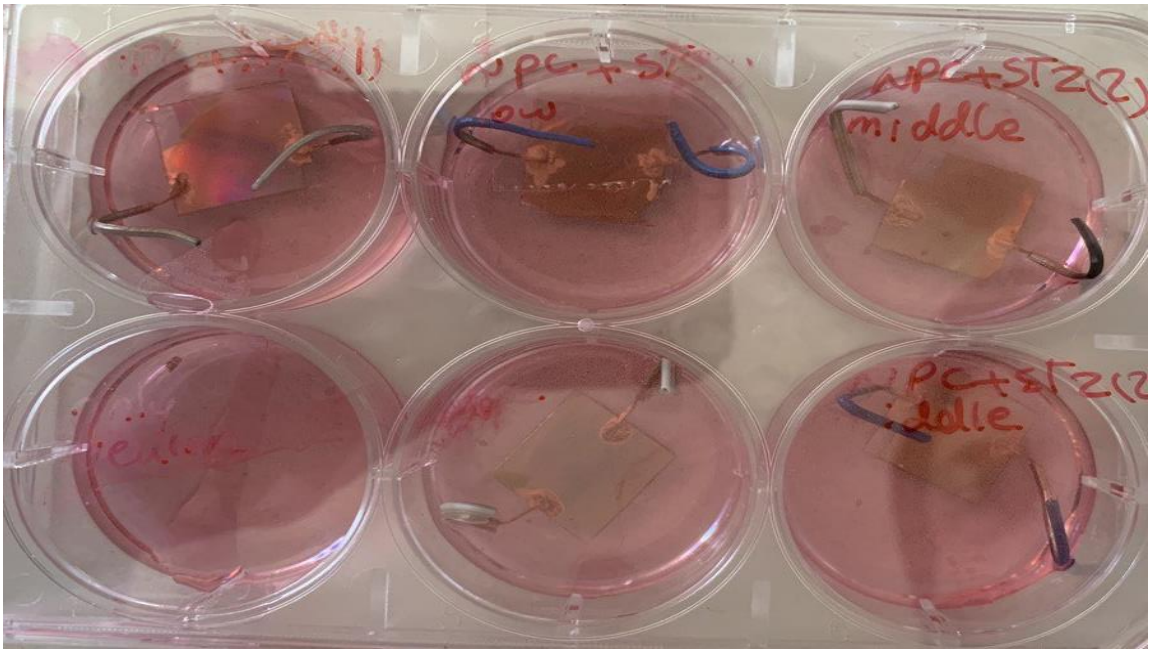

Figure (3.14): Illustration a real image of the samples

The electro-plasmonic chip was taken out from the container and placed in the homemade chamber. Furthermore, there is less than one hour to complete all the measurements. The measurement includes measuring each sample three times in different samples to be sure about the accuracy of our measurements.

Chapter Four

Results and Discussion

4.1Introduction

In this chapter, the characterization of the proposed one-dimensional nanograting electro-plasmonic chip was measured and the results show a nice physical phenomenon known as tunable plasmonic induce transparency. This phenomenon is used to enhance sensor sensitivity by increasing the external applying voltage.

The electro-plasmonic chip was tested with dopamine as a new kind of neurotransmitter sensor. The results show an excellent sensing performance to the different concentrations of dopamine. Also, with the minimum concentration of dopamine that equal to 0.5mM, the measurement indicates to the high efficiency of the prepared chip to sense the low concentrations of dopamine.

The next step includes the culturing of the plasmonic chip with neuron cells extracted from rats and measuring the cell's activity. Adding dopamine as a chemical stimulus to the cultured neuron cells and measuring the cell's activity. The results indicate to the high efficiency of the plasmonic sensor to detect and measured the cells activity.

Finally, culturing the prepared chip with HNPC cells and then adding streptozotocin in different concentrations to generate Alzheimer's disease. The results show the inhibition of the cells activity with increasing the dose of STZ. All these results are shown in detail in this chapter and discussed these results.

The experiments and the measurements of the result were done in the "magneto-plasmonic Lab, Laser and Plasma Research Institute, Shahid Beheshti University, Tehran, Iran."

4.2The characterization of the chip

After completing the setup steps and the SPPs excitation for the plasmonic sample by illuminating with a light source from 400 to 900 nm. The waveguide mode was excited using gold grating, and within the structure, the distribution of the electric field was concentrated, which refers to the existing of a narrow transmission window as shown in Figure (4.1). These metallic nanowires might be the simplest SPP resonators by absorption loss which can produce a relatively large bandwidth in a transparent window. Furthermore, as shown in Figure (4.1 a), the symmetry of the field patterns into the grooves from each nanowire approves the relation between bright and dark plasmonic modes and their decay rates. Any change in the modulation depth and thus decay rates relates to their ohmic absorption losses and thus controls the SPP properties in the PIT mechanism. The plasmon resonance was generated by exciting the gold nanowires directly by the incident light with TM polarization. A narrow-band subradiant resonance state would appear due to the incident light's mismatch with the gold grating's waveguide mode. These wide-band modes and the narrow-band waveguide modes would be strongly destructively coupled, and this would result in the formation of PIT. To study the linear transmission of one-dimensional electro-plasmonic lattice nano gold grooves, we measured the transmission spectrum at first with P-polarization and then changed to S-polarization without applying an external voltage, where a sharp transmission window in each polarization was clearly revealed resulting in a Fano resonance due to bright and dark plasmon modes. Accordingly, the dips' depth introduces incoherent loss terms in the structure or radiative scattering contributions of the dipole moment of the dark mode. A transparency window could be created, when the spacing between any two adjacent nanocavities is equal to the integer half wavelength of the guided SPPs mode. By comparing the results of measuring the P-polarization and S-

polarization, at first glance, tunability was found between the central parts of 500–600 nm by different polarization states respectively. As shown in Figure (4.1 b), the sharp peak window with P-polarization was better than that with S-polarization.

4.2.1 The tunable plasmonic induce transparency.

To study the tunable transparency properties of one-dimensional electro-plasmonic lattice grooves, spectroscopy was used to record the transmission spectrum of 1D electro-plasmonic grading chip and apply external voltage at three cases with 1 V, 2 V, and 3 V. The results confirm high peaks in the transmission spectrum with increasing the applying voltage from 1 V to 3 V. These sharp peaks refer to the formation of transparency windows and the sharp windows in P-polarization. Correspondingly, the plasmonic modulation by increasing voltage appeared in Figure (4.1 c), which indicates the realization of electro-plasmonic induced transparency in our plasmonic sample.

The intensity increases with the elevation of the applied voltage and the resonance shift to a shorter wavelength. Furthermore, the depth of modulation drops with increasing the applied voltage, from 0.5485 at 1 V to 0.2831 at 2 V and 0.1436 at 3 V applied voltages, suggesting tunable electro-plasmonic induce transparency.

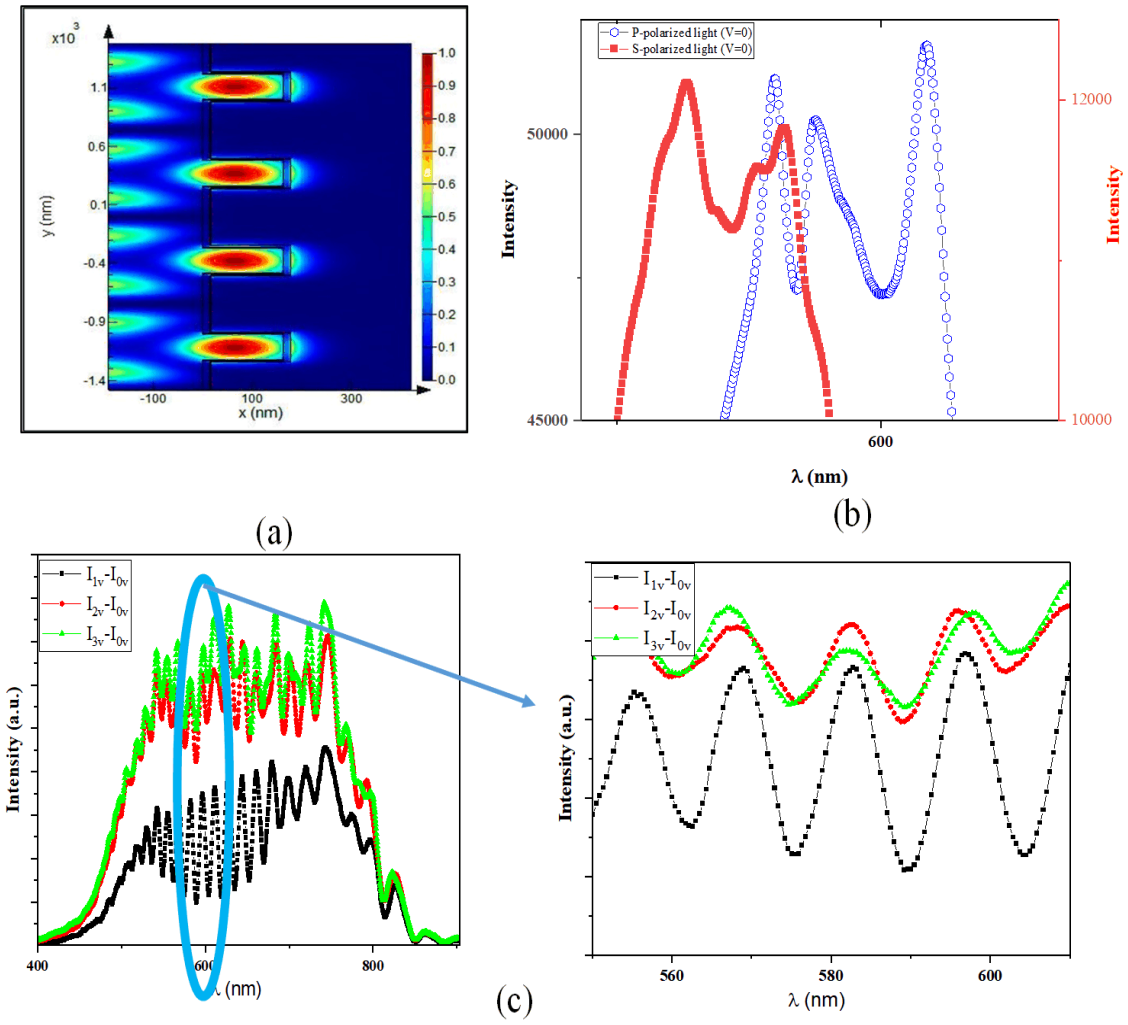

Figure (4.1): Electric field distribution of one-dimensional plasmonic grating, (b) Transmission spectrum of the sample without any voltage under two different polarizations, and (c) Modulation for plasmonic waves with different voltage for P-polarization.

4.2.2 Sensing of dopamine.

The sensitivity of the electro-plasmonic sensor was investigated for dopamine concentration detection using P-polarization with three different voltage levels. Upon increasing the voltage level, the oscillation of the transmission spectrum diminished while the linearity increased, which is very clear within the wavelength 550 – 650 nm. Also, with the elevation of the dopamine concentration from S1 to S3, the spectrum would change

completely, facilitating recognition of the dopamine concentration from the spectrum shape. Applying an electric potential that changes the properties of the dielectric in the vicinity of the metal-dielectric interface alters the SPR signal by applying external force onto the gold ions in the plasmonic substance.

In dopamine as a neurotransmitter, there is an important ion (K^+, Na^+) to induce the interaction between the ions and gold atoms that changes the SPR signal.

Any ionic force acting on the electrons in a gold thin grating causes a change in the average dipole moment of the molecules in the metallic layers. These changes occur at a frequency lower than the electric field produced by the surface plasmons resulting in producing light in each nanowire in the grating. The influence of the electric potential on the measurement with SPR sensors yields better spatial and temporal resolutions for utilization in bioscience applications. Now, the promotion of the voltage applied to the surface of the biosensor chip can enhance the sensitivity to dopamine concentration. The relative intensity of samples with and without applied voltages at different concentrations of dopamine are revealed in Figure (4.2). At first glance, one can see a blue shift (some main modes are shown by blue dash lines in this figure) by enhancing dopamine in the relative transmission of the sample. Furthermore, by elevating the applied voltage, some main electro-plasmonic modes' depth has decreased. In addition, we have some mode overlaps in the maximum amount of applied voltage as well as in ascending trend of dopamine concentrations.

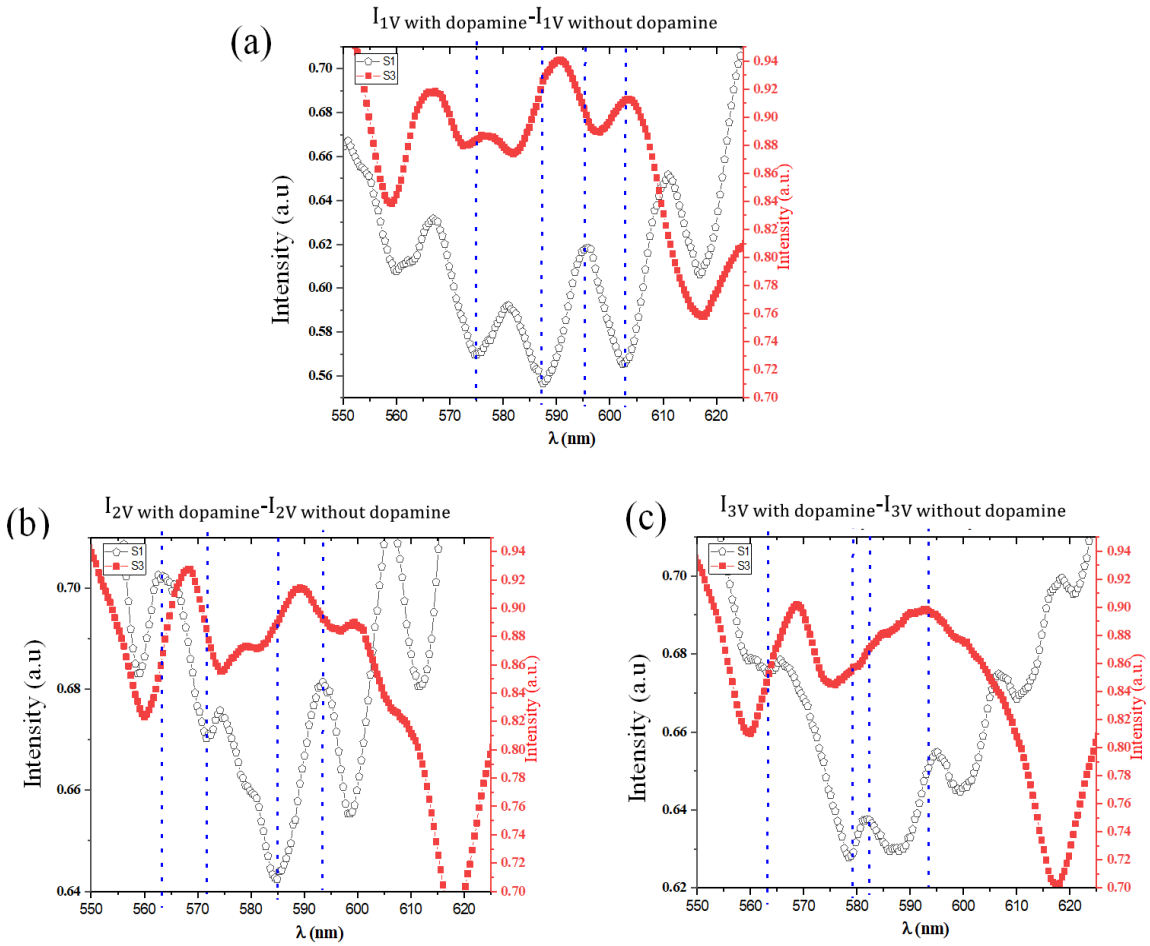

Figure (4.2): Change in electro-plasmonic modes for P-polarization and two dopamine concentrations of 3 mg/ml (S1) and 7 mg/ml (S3) samples under three different applied voltages as (a) 1 v, (b) 2 v and (c) 3 volts.

In this measurement with P-polarization and dopamine concentrations, (3 mg/ml) for S1 and (7 mg/ml) for S3, the transmission spectrum has become more linear with the elevation of the applied voltage within the wavelength 550 – 650 nm. Also, the depth width of the spectrum dropped, and so did the peak intensity with increasing the applied voltage and the dopamine concentration. This electro-plasmonic sensor can sense different dopamine concentrations, as a neurotransmitter, in the transient process of an electrical signal between neurons with the next one by chemical action. The sensing diagram of the sensor can plot in all of the main modes such as 602 nm. By increase in the neurotransmitter concentrations from S1 to S3 and thus

enhance in the decay rate of plasmonic dark mode, we must have a different slope in the sensing diagram due to the main SPP wave in our plasmonic 1D-grating chip. Inversely in 580 nm, this slope gets the opposite sign from S1 to S3 concentrations and so ones in different modes depend on the asymmetric or symmetric distribution of modes in the groves. These neurotransmitters can bind to five branches of receptors in two main classifications as D1-like and D2-like. We utilized electrically modulated plasmon in the substrate to drift dopamine binding to the neurons because binding of dopamine to these receptors initiates cascades of signals that are responsible for triggering activities in the brain. The dopamine binding to D1-like receptors would excite the neurons by doping of Na^+ channels or inhibits via the K^+ channels opening, where the refractive index of the medium onto the plasmonic surface changes, and new modes are obtained on the plasmonic side.

4.2.3 The result discussion

The characterization of the proposed electro-plasmonic chip was investigated.

1- The tunable electro-plasmon-induced transparency in one-dimensional gold nano-grating based on applying external volt with S and P polarizations. The appearance of high peaks in the transmission spectrum with alteration of the applied voltage indicated the formation of electro-plasmonic induced transparency in our plasmonic sample. Also, the results showed that the PIT and electro-plasmonic sensing with P-polarization was better than through S-polarization.
2- The results of sensing dopamine with different concentrations by this electro-plasmonic chip indicated the achievement of a new kind of neuro-plasmonic sensor that can be used in the future with neuron activation sensing.

4.3 Cultured the plasmonic chip by neuron cells.

Neuron cells obtained from the rat cortex were cultured on the plasmonic nanograting platform. As the first result of cultured neuron cells, scanning electron microscopy (SEM) of cultured cells onto the plasmonic chip was recorded as indicated in Figure (4.3). Plasmonic chip periodic manner with 780 nm in unit cell size is shown in this figure in the spite of cultured cells.

As explained earlier, the activity of the cultured neuron cells without the effect of dopamine was measured as shown in Figure (4.4 a).

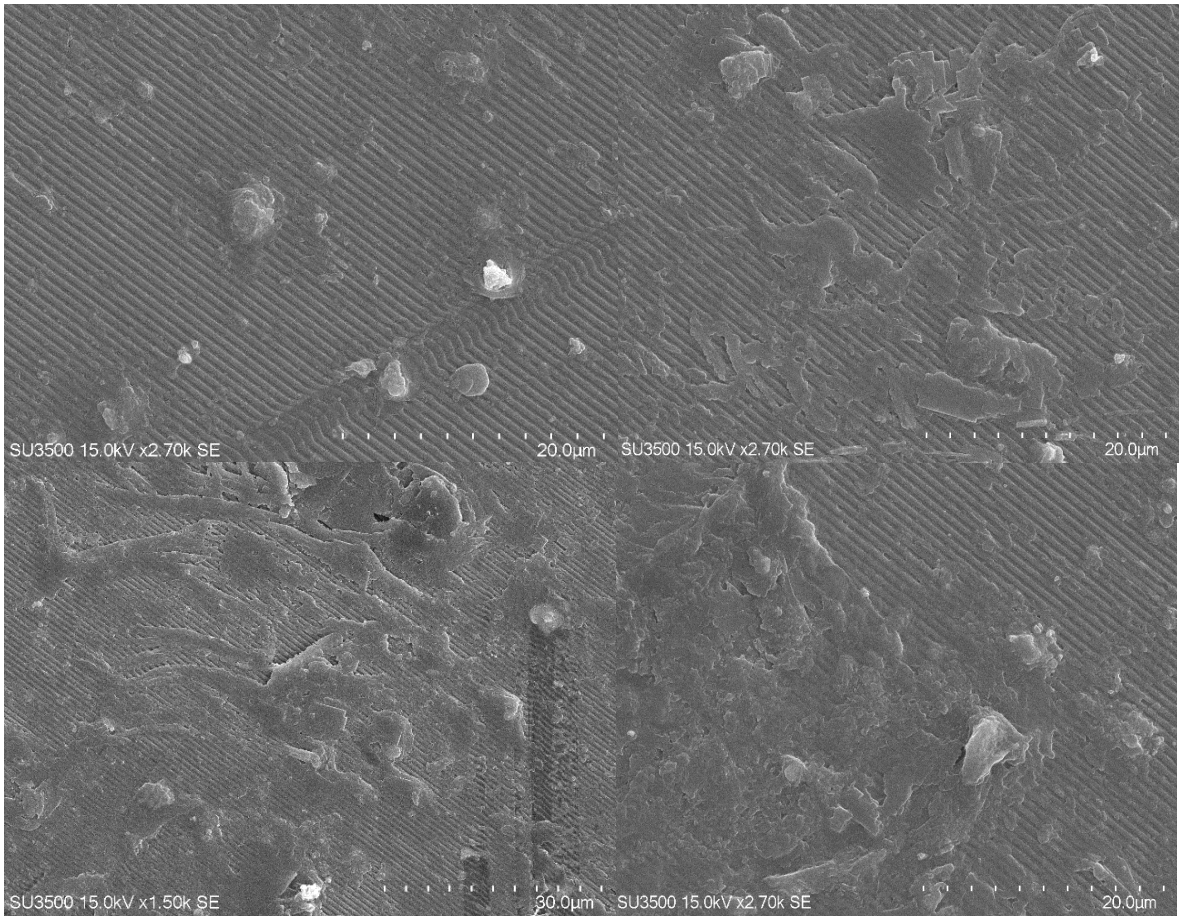

Figure (4.3): Scanning electron microscopy (SEM) image shows the neuron cells were successfully cultured on the plasmonic grating chip

4.3.1 Adding dopamine to the cultured neuron cells.

In the first step, dopamine as a chemical stimulus with a concentration of 300 ppm (S1) was added to the cultured cells. The results showed there is a significant contrast between the rest state without dopamine and the stimulated state with dopamine. By repeating the previous step with 400 ppm (S2) and 500 ppm (S3) concentrations of dopamine, as expected, the main plasmonic mode appeared in the red spectral region and some other modes on the left and right sides of that one. These main modes have been changed by variations in the activity of the neuron cells under the effect of three different concentrations of dopamine (DA) as depicted in Figure (4.4). (b).

These spectra indicate that in p polarization, before the main plasmonic mode in 620 nm, we have a slightly blue shift with dopamine concentration enhancement as well as the plasmonic induced transparency by this enhancement in stimulant concentrations. The mentioned blue shift repeated on the right-hand side of the main resonance wavelength also has the main difference which appears as plasmonic-induced opaque. In S polarization (Figure (4.4). (c)), in spite of the non-logic manner in a red or blue shift as well as in the transparency or opaque states, we lose some main modes and thus we continue our measurement with P polarization in all of our measurements.

It is well known that in the vicinity of the plasmonic chip and the neural tissue or cells, there is stern layer voltage, and thus electrical double layer consists of Thomas-Fermi screening length in the metallic layer and stern layer thickness in the electrolyte. Any change in the potassium or sodium concentrations in the neural region can affect these double layers, and thus plasmonic modes changes.

In our measurement of dopamine concentrations, we have a famous neurotransmitter to transient an electrical signal from neuron to the neighbor by chemical action. These neurotransmitters can bind to five different receptor subtypes in two main classifications D1-like and D2-like. This is due to the fact that the association of dopamine to all these receptors initiates signaling cascades that activate brain activities. The binding of dopamine to D1-like receptors would excite the neurons by doping of Na^+ channels or inhibits via the K^+ channels opening. These changes in K^+ and Na^+ in the neurons mainly affect the electrical double layer and thus act as the main modulation origin of neurons and neural activity.

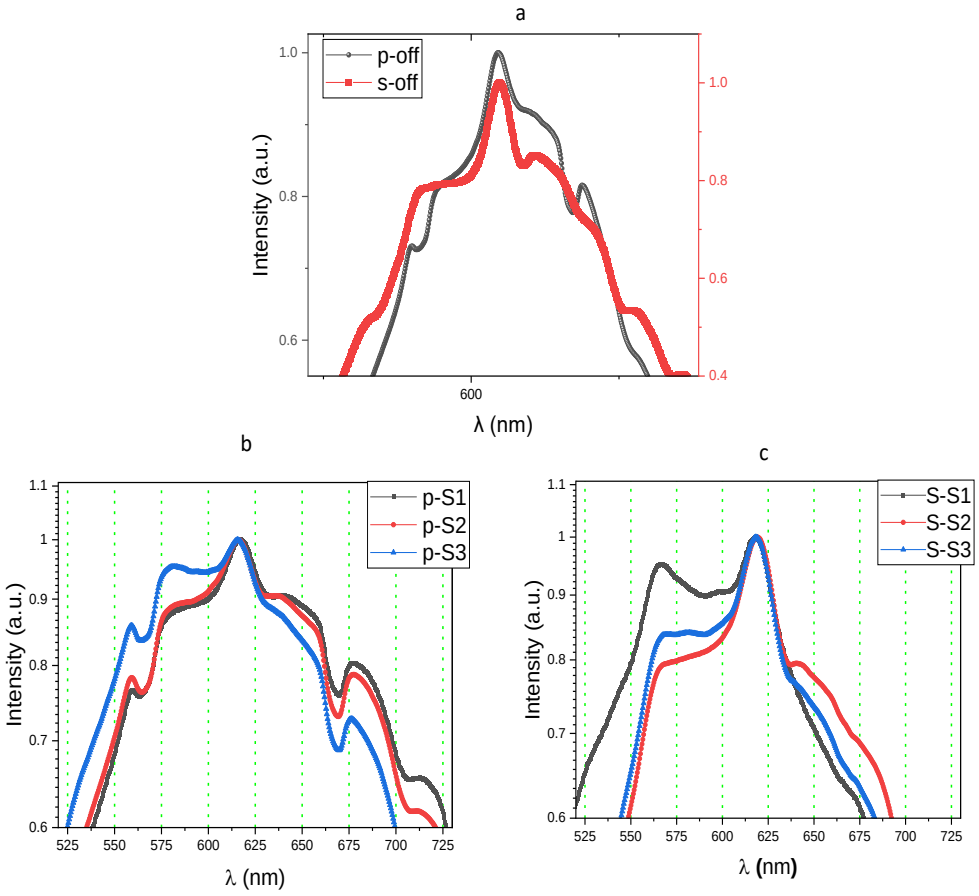

Figure (4.4): (a) the spectrum of the cell's activity in P & S polarization, the spectrum of the cell's activity with three different concentrations in (b) P polarization and (c) S polarization.

This means the neuron cells respond to the dopamine stimulation and the plasmonic sensor measuring this signal. These measurements refer to the high sensitivity of the one-dimensional gold nanograting sensor to the neuron cell's activities. The second test of the neuroplasmonic sensor was done by reducing the dopamine concentration to 0.5 ppm and 10 ppm. The results show the ability of this sensor to sense the effect of these concentrations of dopamine on the cell's activity, suggesting the high sensitivity of the suggested neuroplasmonic sensor.

4.3.2 Measure the cell's activity with different minutes

To measure the effect of dopamine on the activity of the cells with a low concentration of dopamine (0.5 ppm), Figure (4.5) shows significant contrast between the rest state without dopamine and the stimulated state with dopamine at 2, 5, and 10 minutes using P polarization.

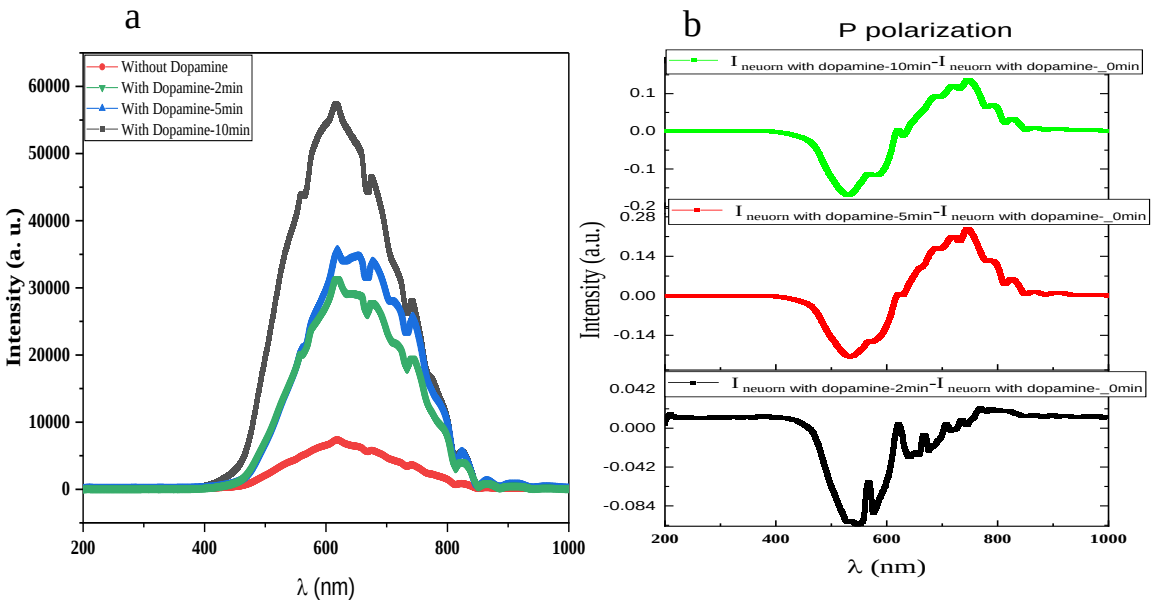

Figure (4.5): (a) sensing of food, and dopamine at zero, two, and ten minutes, (b) the effect of dopamine on the activity of the cells in P polarization after 2, 5, and 10 min

To further examine the effect of dopamine, a new graph has been drawn in Figure (4.5 b) as the comparison between neuron cells under dopamine effect

and without any stimulants in 2, 5, and 10 minutes. Notably, the main plasmonic modes in the bottom row with the 2-minute effect of dopamine stimulant disappeared in the other two rows under longer stimulation times which confirms neuron activity changes under this neurotransmitter.

Figure (4.6) reveals that the spectrum intensity changes over time, which confirms that variations in the spectrum amplitude do not depend on changing the refractive index of adding dopamine or food. In other words, adding the chemical stimulus dopamine (DA) under the effecting of plasmonic led to a change in the distribution of ions as explained before as double-layer formation and change, as a result, the plasmonic interface was affected and the activity of the cells is increasing with the time increase. Thus, changing the amplitude of the spectrum could be investigated in the cell's membrane depolarization. Lipid membranes surround cells and are naturally impermeable to ions, requiring transmembrane proteins to transport ions through them. In the extracellular space, sodium (Na^+) and chloride (Cl^-) ions are more concentrated, and inside the cells, the potassium (K^+) and organic anions (proteins and amino acids) exist. The sodium-potassium pump family actively couples the efflux of three ions of Na^+ with the influx of two ions of K^+ depending on an ATP manner, while the chloride symporter by gradient k^+ could be a couple of the efflux Cl^- and K^+ against the gradient concentration of Cl^- without using ATP. These gradients concentration with protein activities produce the steady state which is represented by negatively charged intracellular compared to the extracellular.

Because of the cellular membranes' selective permeability to ions and the negatively charged intracellular environment, an increase in extracellular K^+ changes the ion gradient, reversing K^+ outflow and boosting permeability to Na^+ (voltage-gated channels). This results in membrane depolarization

which has been frequently utilized to research electrical activity-dependent alterations in neuron cells.

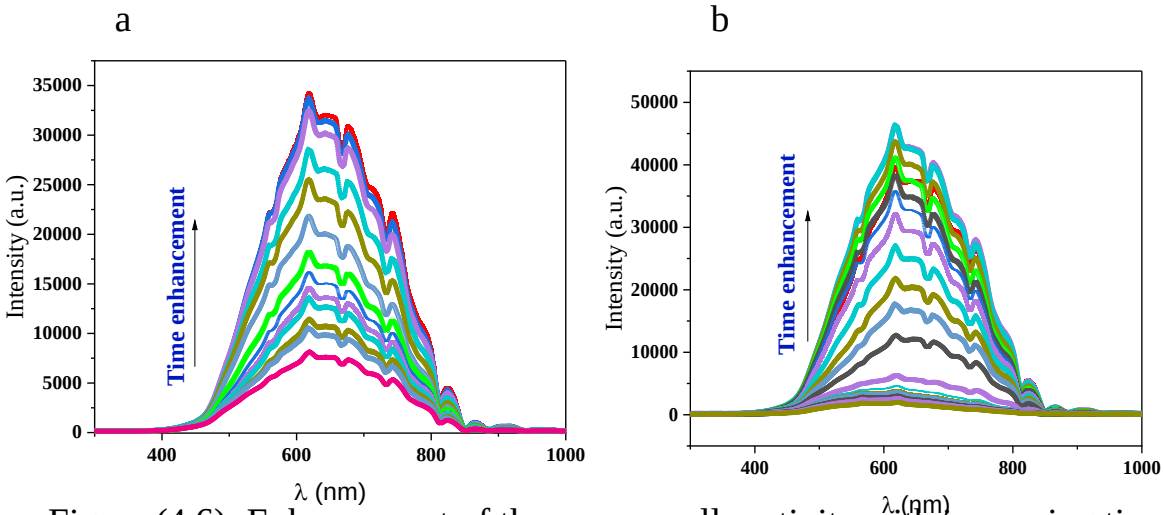

Figure (4.6): Enhancement of the neuron cells activity with increasing time to 10 minutes with dopamine concentration about (a) 0.5 ppm and (b) 10 ppm.

4.3.3 The result discussion

The ability of the one-dimensional plasmonics chip to measure neuron cell activity under the effect of dopamine was investigated.

1- Regardless of the little difference in the measurement spectrum with different concentrations of dopamine, the spectrum amplitude rose with increasing time to 10 minutes. This means that the changes in the measured spectrum were caused by the cell's depolarization as well as changes in the ion distribution of the cultured cells that would affect the plasmons interface.

2- When the plasmons interface changes that lead to changing the refractive index because the contrast of the cells is changed.

3- The results indicate the high sensitivity of the one-dimensional nanograting gold sensor with different concentrations of dopamine to stimulate neuron cells and the results refer to getting a new kind of neuron cells sensor.

4.4 Streptozotocin-induced Alzheimer's disease

The tunable electro-plasmonic chip was cultured with HNPC cells and investigated the ability of STZ to induce AD. The neuron cells are successfully cultured on the electro-plasmonic chip and injected with STZ in different concentrations. The c image of the cultured cells is illustrated in Figure (4.7).

The experiment steps included several samples without and with STZ in different concentrations (0.5, 1, 2 mM). Also, the measurement procedures included applying different voltage levels (1, 2, 2.5, and 3) V on the chip and using S and P polarizations.

The first step is measuring the neuron cell's activities without STZ and applying external voltage with P and S polarizations. The results are shown in Figure (4.8).

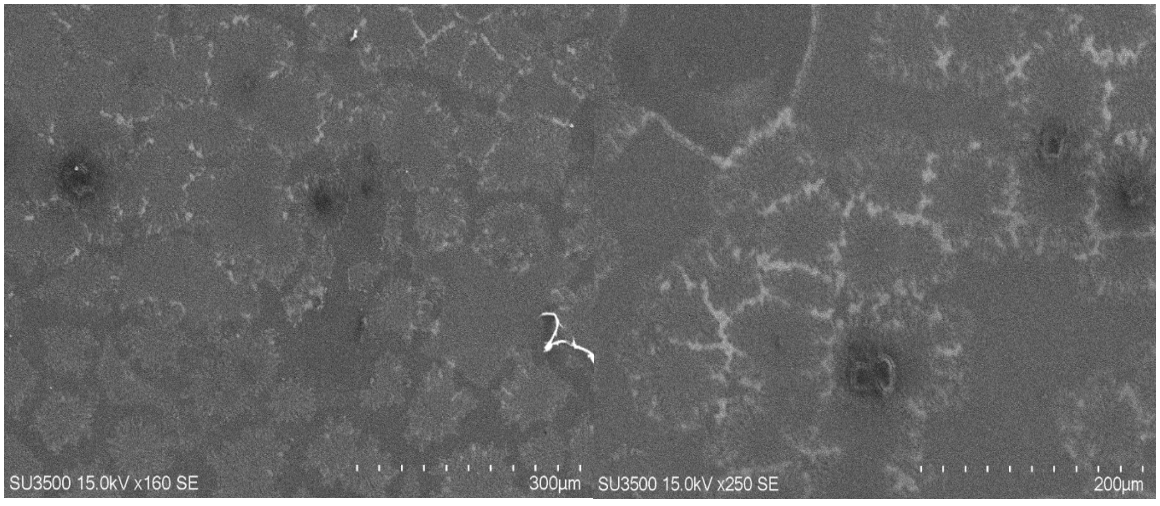

Figure (4.7): Scanning electron microscopy (SEM) image shows the neuron cells were successfully cultured on the plasmonic grating chip

The results show that we have successfully investigated the tunable electro-plasmonic sensor. The sensitivity of the sensor has been increased by increasing the applied voltage from 1V to 3V. The plasmonic mode of the spectrum intensity in P polarization has a clear shifting at 520nm and 620nm with increasing applied voltage. Also, it shows that the sensing performance with P polarization is better than with S polarization. In S polarization as shown in Figure (4.8 b), the results show the same spectrum at 520nm with different applied voltages, and also the other measurements show that the spectrum intensity has a clear contrast between several modes in P

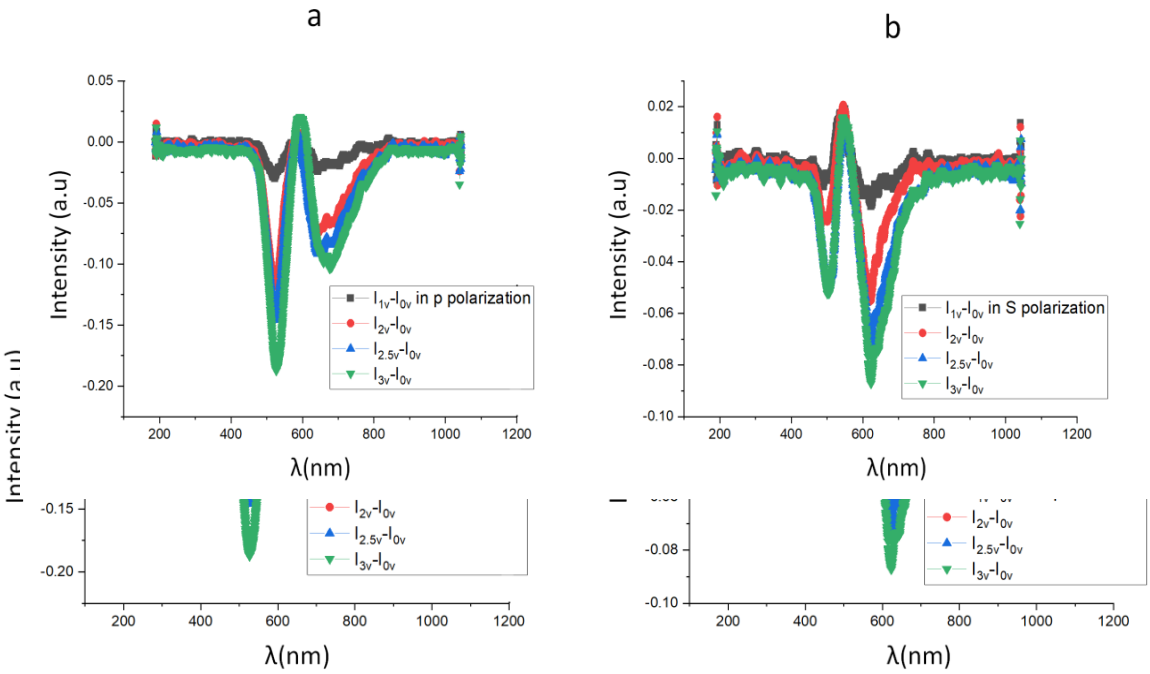

(a) with P polarization (b) with S polarization

It is widely known that stern layer voltage is close to the plasmonic chip and the neural tissue. Therefore, there is stern layer voltage, and thus electrical double layer consists of Thomas–Fermi screening length in the metallic layer and stern layer thickness in the electrolyte. These double layers are sensitive to variations in the potassium or sodium levels in the neural area, which results in plasmonic mode alterations.

As mentioned early in chapter 2 Figure (2.4), pancreatic beta cells are affected by STZ and usually GLUT-2. So, STZ induced deregulation of

insulin and glucose in the cultured cells model. The GLUT-2 is the main glucose transporter in pancreatic beta cells and plays an important role in insulin secretion from beta cells. The insulin receptor (IR) and the Insulin-like growth factor-1 receptor (IGF-1R) signaling (IIR) are markedly disturbed in the CNS of AD patients. Moreover, the injection of STZ will decrease GLUT-2 that cause to reduce the insulin receptor and then decrease the phosphorylated levels (GSK-3β) and induce insulin resistance. Insulin resistance develops when the tissues of the cell don't react to the insulin. Moreover, binding the STZ to the insulin receptor will decrease the neuron's activity. The neuron activity is done by doping Na^+ channels or inhibits via the K^+ channels opening. Since the electrical double layer is primarily affected by these variations in K^+ and Na^+ in neurons, it serves as the primary modulation source for neurons and neural activity. These activities will reduce because of the effect of STZ as mentioned above.

4.4.1 Measuring the effecting of streptozotocin on cultured neuron cells.

Figure (4.9) shows the spectrum measurement of the neuron activity under the different concentrations of STZ. The results refer to the response of the cultured neuron cell's activity to the effecting of STZ. Figure (5 (a, b, c)) shows that increasing the applied voltage from 0V to 3V in P polarization will increase the sensor sensitivity. Also, these measurements show the high sensitivity of the electro-plasmonics sensor to the neuron cell's activities and the performance enhances by increasing the applied voltage to 3V.

The second measurement is shown in Figure (5 (d, e, f)), which appear the effect of different concentrations of STZ on the cell's activity. Furthermore, increasing the concentration of the STZ to the middle (1mM) and then to a high concentration (2mM). The results show high accuracy in measuring the activity of the cells under the effecting of STZ in P polarization and enhancing the performance of sensing by increasing the applied voltage.

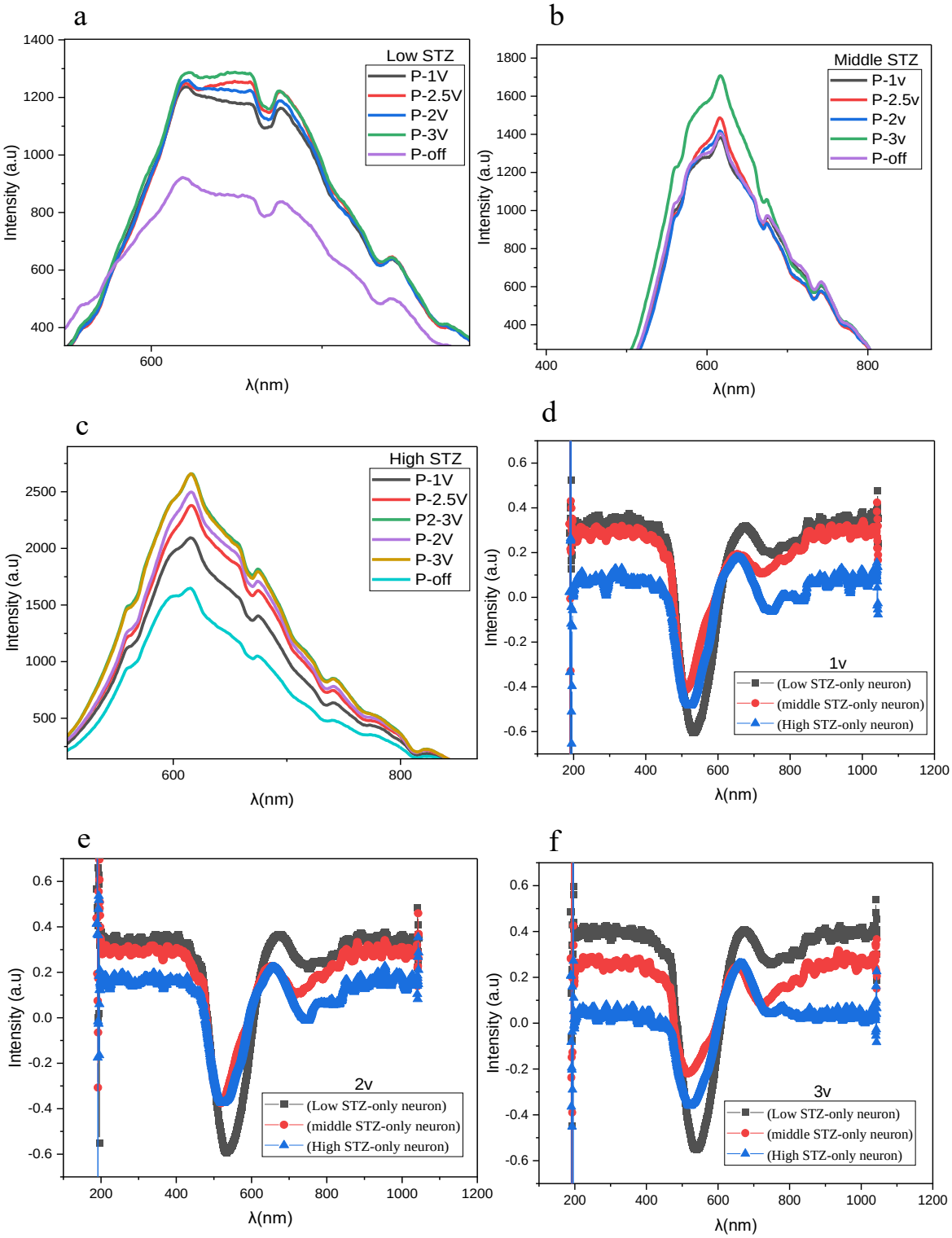

Figure (4.9): Show the activity of the cells under P polarization by applying an external voltage (a) With a low concentration of STZ, (b) With a middle concentration of STZ, (c) With a high concentration of STZ, (d) with applying 1V and different concentration of STZ, (e) with applying 2V and

different concentration of STZ, (f) with applying 3V and different concentration of STZ.

Also, the results show the ability of the electro-plasmonics sensor to sense the inhibits of the cells under different dose of STZ by applying external voltage from 1V, 2V, and 3V respectively. The results show that the spectrum intensity reduces with increasing the concentration of STZ at the wavelength 520nm and 620nm. The results refer to the electro-plasmonics sensor having good performance for sensing the stimulation and inhabitation (under the effecting of STZ) of the neuron cells.

In the other words, adding the STZ to the cultured neuron cells led to a change in the distribution of ions as explained before as double-layer formation and change, as a result, the plasmonic interface was affected and the activity of the cells decreased with increasing the STZ concentration to 2mM.

This electro-plasmonic sensor can sense the different effecting concentrations of STZ on the cells inhibits. The sensing diagram of the sensor can plot in all of the main modes such as 620 nm as shown in Figure (4.10). The modulation depth shows the clear difference between the different concentrations.

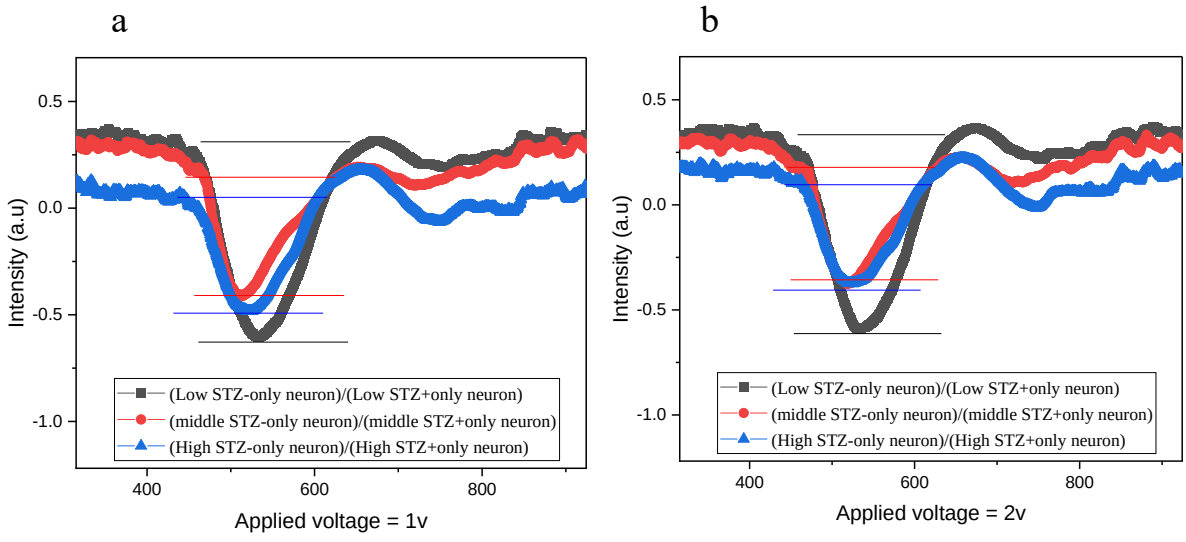

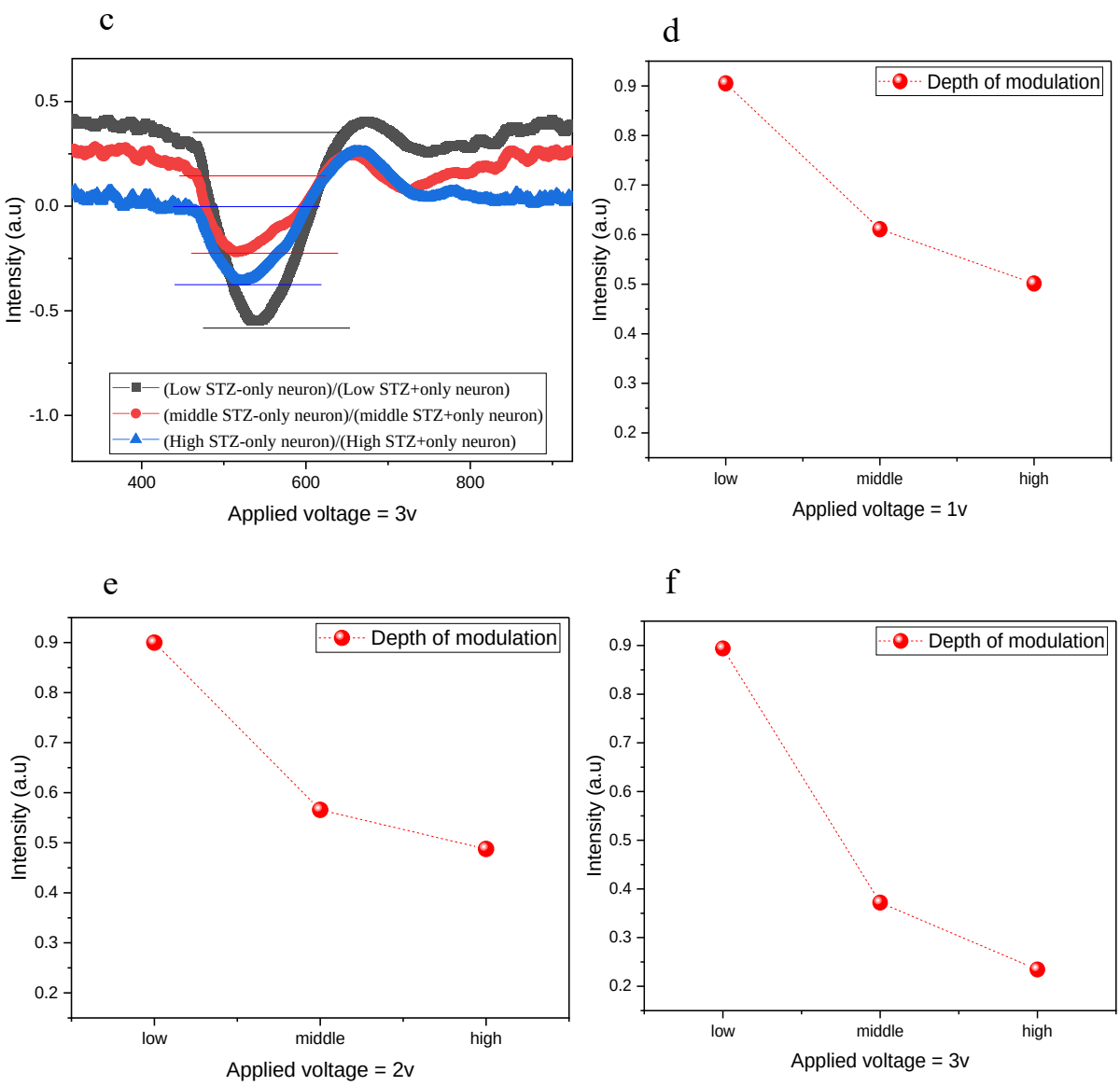

Figure (4.10): Sensing diagram of the samples under low, middle, and high concentrations of STZ in 620 nm as one of the main modes

The spectrum amplitude depends on changes in the refractive index of the cultured neuron cells. The change in the refractive index occurs from the activity of the cultured neuron cells. In the extracellular space, sodium (Na^+) and chloride (Cl^-) ions are more concentrated, and inside the cells, the potassium (K^+) and organic anions (proteins and amino acids) exist. The sodium-potassium pump family actively couples the efflux of three ions of Na^+ with the influx of two ions of K^+ depending on an ATP manner, while the chloride symporter by gradient k^+ could be a couple of the efflux Cl^- and

K^+ against the gradient concentration of Cl^- without using ATP. These gradients concentration with protein activities produce the steady state which is represented by negatively charged intracellular compared to the extracellular. Because of the cellular membranes' selective permeability to ions and the negatively charged intracellular environment, an increase in extracellular K^+ changes the ion gradient, reversing K^+ outflow and boosting permeability to Na^+ (voltage-gated channels). This results in membrane depolarization which has been frequently utilized to research electrical activity-dependent alterations in neuron cells.

4.4.2 Measuring the surrounding temperature.

One of the main challenges in dealing with neuron cells is the temperature. Because increasing the temperature will lead to damage to the cultured neuron cells. So, for this reason, using an IR camera to measure the temperature of the cultured neuron cells which shows normal temperature and it's in a safety to keep the cell's activities as shown in Fig. (4.11).

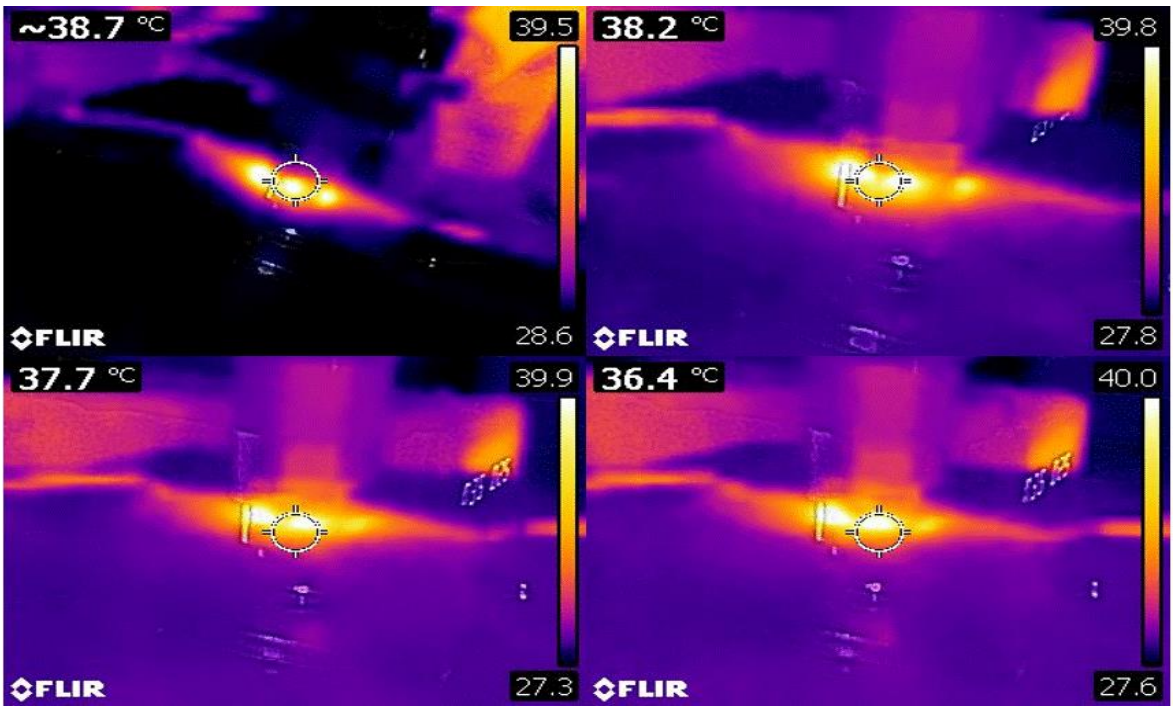

Figure (4.11): Illustrate the temperature of the cultured cells under the effect of plasmonic taken by an IR camera

Furthermore, the plasmonic place where the cultured cells were found was about 39 ^{0}C and the surrounding reign was more than 27 ^{0}C. This temperature range is safe to keep the cultured cells alive until to complete the experimental measurements.

4.4.3 The result discussion

The ability of the electro-plasmonics chip to sense the effect of the STZ on neuron cell activity using a one-dimensional gold nano grating chip by applying an external voltage with P polarization was investigated.

1- The results show a high ability of the electro-plasmonic chip to sense the activity of the cultured neuron cells. The sensitivity performance will increase by increasing the externally applied voltage to 3 V. In addition, it has a high ability to measure the degradation in neuronal activity caused by the addition of STZ.

2- The change in the measured spectrum comes from the cell's depolarization as well as changes in the ion distribution of the cultured cells that would affect the plasmons interface. When the plasmon interface changes, the refractive index changes because the contrast of the cells changes.

3- The results indicate the high sensitivity of the electro-plasmonic one-dimensional nanograting gold sensor to sense the cultured neuron activates with different doses of STZ. Moreover, the suggested electro-plasmonic chip is a promising sensor for future cultured neuron cell experiments. It could be used in a biomedical research laboratory to measure the effectiveness of suggested drugs on the neuron cell's activity.

Chapter Five

5.1 Conclusions

The important point that can be concluded from this thesis are presented in the following point:-

1- Investigated the characterization of the proposed electro-plasmonics one-dimensional gold nano-grating chip by applying an external volt from 1V to 3V with changing S and P polarizations. The results show high peaks in the transmission spectrum and the amplitude increased with the increase in the applied voltage (1V – 3V) which indicates the formation of electro-plasmonic induced transparency in our plasmonic chip. Also, the results showed that the tunable plasmonic induce transparency (T-PIT) in P-polarization was better than through S-polarization in the proposed electro-plasmonic chip.

2- Investigating the ability of the electro-plasmonics chip to sense a different concentration of dopamine. The results indicate the high ability of the proposed electro-plasmonic chip to sense the different concentrations of dopamine. Also, with a low concentration of about 0.5mM of dopamine. This refers to the successful design of a new kind of neurotransmitter sensor that can be used to measure dopamine concentration in cultured neuron cells.

3- The results show the high ability of the one-dimensional plasmonics chip to measure the activity of the neuron cells under the effect of dopamine.

4- When the plasmons interface changes that lead to changing the refractive index because the contrast of the cells is changed. The results indicate the high sensitivity of the one-dimensional nanograting gold sensor with different concentrations of dopamine to

stimulate neuron cells and the results refer to getting a new kind of neuron cells sensor.

5- Investigates the ability of the electro-plasmonics chip to sense the effect of the STZ on neuron cell activity using a one-dimensional gold nano grating chip by applying an external voltage with P polarization. The results show a high ability of the electro-plasmonic chip to sense the activity of the cultured neuron cells.

6- High ability to measure the degradation in the activity of the neuron cells caused by adding the STZ. The change in the measured spectrum comes from the cell's depolarization as well as changes in the ion distribution of the cultured cells that would affect the plasmons interface. When the plasmon interface changes, the refractive index changes because the contrast of the cells changes.

5.2 Future Work

1- Investigate the ability of the electro-plasmonics chip to sense the activity of the cells with another brain dementia such as Parkinson’s or schizophrenia

2- Investigate the ability of any suggested drugs to the neuron cell's activity, possibly with high accuracy by using one-dimensional electro plasmonic chip cultured with neuron cells and checking the effect of the drugs on the activity of the cells.

References

1. Gonzalez, Armijo, Bravo-Alegria, Becerra-Calixto, Mays, & Soto. "Modeling amyloid beta and tau pathology in human cerebral organoids." *Molecular psychiatry* 23.12 (2018): 2363-2374.
2. Sohrabi, Foozieh, and Seyedeh Mehri Hamidi. "Optical detection of brain activity using plasmonic ellipsometry technique." *Sensors and Actuators B: Chemical* 251 (2017): 153-163.
3. Benounis, M., et al. "High sensitive surface plasmon resonance (SPR) sensor based on modified calix (4) arene self-assembled monolayer for cadmium ions detection." *Materials Transactions* 56.4 (2015): 539-544.
4. Shuxian Chen, Junyi Li, Zicong Guo, Li Chen, Kunhua Wen, Pengbai Xu, Jun Yang and Yuwen Qin "Dynamically tunable plasmon-induced transparency effect based on graphene metasurfaces." *Journal of Physics D: Applied Physics* 55.11 (2021): 115105.
5. Do, Yun Seon. "Efficient Design Method for Plasmonic Filter for Tuning Spectral Selectivity." *Crystals* 10.6 (2020): 531.
6. Butt, Muhammad Ali, Nikolay Lvovich Kazanskiy, and Svetlana Nikolaevna Khonina. "Highly sensitive refractive index sensor based on plasmonic bow tie configuration." *Photonic sensors* 10.3 (2020): 223-232.
7. Matthew Klein, Bekele H. Badada, Rolf Binder, Adam Alfrey, Max McKie, Michael R. Koehler, David G. Mandrus, Takashi Taniguchi, Kenji Watanabe, Brian J. LeRoy & John R. Schaibley "2D semiconductor nonlinear plasmonic modulators." *Nature communications* 10.1 (2019): 1-7.
8. Hekmatnia, Banafsheh, Mohammad Naser-Moghadasi, and Mehdi Khatir. "Propagation length enhancement in a magneto optic

plasmonic Mach–Zehnder isolator using graphene." *Optical and Quantum Electronics* 52.1 (2020): 1-12.

9. Jianxing Zhao, Jianlin Song, Yao Zhou, Ruilong Zhao, And Jianhong Zhou. "Tunable multiple plasmon-induced transparency in a simple terahertz Dirac semimetal-based metamaterial." *Optical Materials Express* 9.8 (2019): 3325-3332.
10. Wei, W., Yan, X., Shen, B. & Zhang, X. "Plasmon-induced transparency in an asymmetric bowtie structure." *Nanoscale Research Letters* 14.1 (2019): 1-7.
11. Z. Jia, L. Huang, J. Su, and B. Tang, "Tunable electromagnetically induced transparency-like in graphene metasurfacesand its application as a refractive index sensor," *J. Lightwave Technol*. **39**(5), 1544–1549 (2021).
12. Shuxian Chen, Junyi Li, Zicong Guo, Li Chen, Kunhua Wen, Pengbai Xu, Jun Yang and Yuwen Qin. "Dynamically tunable plasmon-induced transparency effect based on graphene metasurfaces." *Journal of Physics D: Applied Physics* 55.11 (2021): 115105.
13. Zhao Chen, Yaolun Yu, Yilin Wang, Zhiling Hou, and Li Yu. "Plasmon-Induced Transparency for Tunable Atom Trapping in a Chiral Metamaterial Structure." *Nanomaterials* 12.3 (2022): 516.
14. Sohrabi, Foozieh, and Seyedeh Mehri Hamidi. "Neuroplasmonics: from Kretschmann configuration to plasmonic crystals." *The European Physical Journal Plus* 131.7 (2016): 1-15.
15. Sohrabi, Foozieh, and Seyedeh Mehri Hamidi. "Neuroplasmonics: From Kretschmann configuration to plasmonic crystals." *The European Physical Journal Plus* 131 (2016): 1-15.
16. Prince MJ, Wimo A, Guerchet MM, Ali GC, Wu Y-T, Prina M. World Alzheimer Report 2015 - The Global Impact of Dementia: An analysis

of prevalence, incidence, cost and trends. London: Alzheimer's Disease International, 2015. 84 p.

17. Xiao, Lan, Sangeetha Hareendran, and Y. Peng Loh. "Function of exosomes in neurological disorders and brain tumors." *Extracellular vesicles and circulating nucleic acids* 2 (2021): 55.
18. Canevelli M, Lacorte E, Cova I, Zaccaria V, Valletta M, Raganato R, et al. Estimating dementia cases amongst migrants living in Europe. Eur J Neurol. 2019; 26:1191–9.
19. Santiago, João CP, and Manfred Hallschmid. "Outcomes and clinical implications of intranasal insulin administration to the central nervous system." *Experimental Neurology* 317 (2019): 180-190.
20. Bagaméry, Fruzsina, et al. "Lack of insulin resistance in response to streptozotocin treatment in neuronal SH-SY5Y cell line." *Journal of Neural Transmission* 127.1 (2020): 71-80.
21. Baac, Hyoungwon, et al. "Extracellular optical recording configuration for neuronal action potential detection by using surface plasmon resonance: Preliminary experiment." *Conference Proceedings. 2nd International IEEE EMBS Conference on Neural Engineering, 2005.* IEEE, 2005.
22. Kim, Shin Ae, et al. "Optical measurement of neural activity using surface plasmon resonance." *Optics letters* 33.9 (2008): 914-916.
23. Zhang, Jiayi, Tolga Atay, and Arto V. Nurmikko. "Optical detection of brain cell activity using plasmonic gold nanoparticles." *Nano letters* 9.2 (2009): 519-524.
24. Moirangthem, Rakesh Singh, et al. "Surface plasmon resonance ellipsometry based sensor for studying biomolecular interaction." *Biosensors and Bioelectronics* 25.12 (2010): 2633-2638.
25. Choi, Seung Ho, et al. "Quantitative model for the change of optical resonance in neural activity detection systems based on surface

plasmon resonance." *Optics & Laser Technology* 43.5 (2011): 938-948.

26. Kim, Shin Ae, et al. "In vivo optical neural recording using fiber-based surface plasmon resonance." *Optics letters* 37.4 (2012): 614-616.
27. Yasui, Chikara, et al. "Sensitive fluorescence microscopy of neurons cultured on a plasmonic chip." *Japanese Journal of Applied Physics* 51.6S (2012): 06FK10.
28. Huang, Yu, et al. "Theoretical analysis of voltage-dependent fiber optic surface plasmon resonance sensor." *Optics Communications* 308 (2013): 109-114.
29. Le, An-Phong, et al. "Quantitative reflection imaging of fixed Aplysia californica pedal ganglion neurons on nanostructured plasmonic crystals." *The Journal of Physical Chemistry B* 117.42 (2013): 13069-13081.
30. Choi, Jong Min, et al. "Multi-color fluorescence imaging based on plasmonic wavelength selection and double illumination by white light." *Optics Express* 22.5 (2014): 5977-5985.
31. Eom, Kyungsik, et al. "Enhanced infrared neural stimulation using localized surface plasmon resonance of gold nanorods." *Small* 10.19 (2014): 3853-3857.
32. Sohrabi, Foozieh, and Seyedeh Mehri Hamidi. "Optical detection of brain activity using plasmonic ellipsometry technique." *Sensors and Actuators B: Chemical* 251 (2017): 153-163.
33. Saeidifard, Sajede, et al. "Two-dimensional plasmonic biosensing platform: Cellular activity detection under laser stimulation." *Journal of applied physics* 126.10 (2019): 104701.
34. Sohrabi, Foozieh, et al. "Membrane activity detection in cultured cells using phase-sensitive plasmonics." *Optics Express* 28.24 (2020): 36643-36655.

35. Akbari, S., et al. "Thermoplasmonic effect onto Toad physiology signals by plasmonic microchip structure." *Scientific Reports* 11.1 (2021): 17287.
36. Chemerkouh, Mohammad Javad Haji Najafi, Seyedeh Bita Saadatmand, and Seyedeh Mehri Hamidi. "Ultra-high-sensitive biosensor based on SrTiO 3 and two-dimensional materials: ellipsometric concepts." Optical Materials Express 12.7 (2022): 2609-2622
37. Bohm, David. "A suggested interpretation of the quantum theory in terms of" hidden" variables. I." *Physical review* 85.2 (1952): 166.
38. Raether, Heinz. "Surface plasmons on smooth surfaces." *Surface plasmons on smooth and rough surfaces and on gratings* (1988): 4-39.
39. Maier, Stefan A. *Plasmonics: fundamentals and applications*. Vol. 1. New York: springer, 2007.
40. Yu, Huakang, et al. "Plasmon-enhanced light–matter interactions and applications." *npj Computational Materials* 5.1 (2019): 1-14.
41. Zia, Rashid, et al. "Plasmonics: the next chip-scale technology." *Materials today* 9.7-8 (2006): 20-27.
42. Chen, Shuxian, et al. "Dynamically tunable plasmon-induced transparency effect based on graphene metasurfaces." *Journal of Physics D: Applied Physics* 55.11 (2021): 115105.
43. Do, Yun Seon. "Efficient Design Method for Plasmonic Filter for Tuning Spectral Selectivity." *Crystals* 10.6 (2020): 531.
44. Butt, Muhammad Ali, Nikolay Lvovich Kazanskiy, and Svetlana Nikolaevna Khonina. "Highly sensitive refractive index sensor based on plasmonic bow tie configuration." *Photonic sensors* 10.3 (2020): 223-232.

45. Yu, X. Q., and S. N. Zhu. "Wavelength division multiplexer of surface plasmon polaritons using dual-periodical arranged metal gap waveguide." *2010 3rd International Nanoelectronics Conference (INEC)*. IEEE, 2010.
46. Klein, Matthew, et al. "2D semiconductor nonlinear plasmonic modulators." *Nature communications* 10.1 (2019): 1-7.
47. Hekmatnia, Banafsheh, Mohammad Naser-Moghadasi, and Mehdi Khatir. "Propagation length enhancement in a magneto optic plasmonic Mach–Zehnder isolator using graphene." *Optical and Quantum Electronics* 52.1 (2020): 1-12.
48. Shuwen Zeng, Dominique Baillargeat, Ho-Pui Ho, Ken-Tye Yong, Nanomaterials enhanced surface plasmon resonance for biological and chemical sensing applications. Chem. Soc. Rev. 43 (10) (2014) 3426–3452.
49. Seron, Bruna Barboza, Gustavo Aires de Arruda, and Márcia Greguol. "Facilitadores e barreiras percebidas para a prática de atividade física por pessoas com deficiência motora." *Revista Brasileira de Ciências do Esporte* 37 (2015): 214-221.
50. Wood, R. W. "On a lemarkable case of uneven distribution of Ught in a difraction grating specmma." *Proceedings of the Royal Society ofLondon*. Vol. 18. No. 1. 1902.
51. Kretschmann, Erwin, and Heinz Raether. "Radiative decay of non radiative surface plasmons excited by light." *Zeitschrift für Naturforschung A* 23.12 (1968): 2135-2136.
52. Bauman, Stephen J. *Fabrication of sub-10 nm metallic structures via nanomasking technique for plasmonic enhancement applications*. University of Arkansas, 2015.

53. Liedberg, Bo, Claes Nylander, and Ingemar Lunström. "Surface plasmon resonance for gas detection and biosensing." *Sensors and actuators* 4 (1983): 299-304.
54. Gupta, Banshi D., Anand M. Shrivastav, and Sruthi P. Usha. "Surface plasmon resonance-based fiber optic sensors utilizing molecular imprinting." *Sensors* 16.9 (2016): 1381.
55. A. D. Boardman, Electromagnetic surface modes: John Wiley & Sons, United States, 1982.
56. Maier, Stefan A. *Plasmonics: fundamentals and applications*. Vol. 1. New York: springer, 2007.
57. Shnan, N. S., N. Roostaei, and S. M. Hamidi. "Tunable and reversible thermo-plasmonic hot spot imaging for temperature confinement." *Journal of Theoretical and Applied Physics* 14 (2020): 367-376.
58. Melentiev, P. N., et al. "Plasmonic sensor based on the Ebbesen effect." *arXiv preprint arXiv:1809.06356* (2018).
59. Sohrabi, Foozieh, and Seyedeh Mehri Hamidi. "Neuroplasmonics: from Kretschmann configuration to plasmonic crystals." *The European Physical Journal Plus* 131.7 (2016): 1-15.
60. Benounis, M., et al. "High sensitive surface plasmon resonance (SPR) sensor based on modified calix (4) arene self-assembled monolayer for cadmium ions detection." *Materials Transactions* 56.4 (2015): 539-544.
61. S. H. Choi, S. J. Kim, C.-H. Im, S. A. Kim, and D. Kim, “Quantitative model for the change of optical resonance in neural activity detection systems based on surface plasmon resonance,” Opt. Laser Technol. 43(5), 938–948 (2011).

62. Knoll, Wolfgang. "Interfaces and thin films as seen by bound electromagnetic waves." *Annual review of physical chemistry* 49.1 (1998): 569-638.
63. Raether, Heinz. "Surface plasmons on gratings." *Surface plasmons on smooth and rough surfaces and on gratings*. Springer, Berlin, Heidelberg, 1988. 91-116.
64. Huang, Yu, et al. "Theoretical analysis of voltage-dependent fiber optic surface plasmon resonance sensor." *Optics Communications* 308 (2013): 109-114.
65. Kim, Shin Ae, et al. "In vivo optical neural recording using fiber-based surface plasmon resonance." *Optics letters* 37.4 (2012): 614-616.
66. Kim, Shin Ae, et al. "Optical measurement of neural activity using surface plasmon resonance." *Optics letters* 33.9 (2008): 914-916.
67. Zhang, Jiayi, Tolga Atay, and Arto V. Nurmikko. "Optical detection of brain cell activity using plasmonic gold nanoparticles." *Nano letters* 9.2 (2009): 519-524.
68. Choi, Seung Ho, et al. "Quantitative model for the change of optical resonance in neural activity detection systems based on surface plasmon resonance." *Optics & Laser Technology* 43.5 (2011): 938-948.
69. Stepnoski, R. A., et al. "Noninvasive detection of changes in membrane potential in cultured neurons by light scattering." *Proceedings of the National Academy of Sciences* 88.21 (1991): 9382-9386.
70. Cohen, Laurence B., R. D. Keynes, and Bertil Hille. "Light scattering and birefringence changes during nerve activity." *Nature* 218.5140 (1968): 438-441.

71. Foust, Amanda J., and David M. Rector. "Optically teasing apart neural swelling and depolarization." *Neuroscience* 145.3 (2007): 887-899.
72. Teramura, Yuji, Yusuke Arima, and Hiroo Iwata. "Surface plasmon resonance-based highly sensitive immunosensing for brain natriuretic peptide using nanobeads for signal amplification." *Analytical biochemistry* 357.2 (2006): 208-215.
73. Le, An-Phong, et al. "Quantitative reflection imaging of fixed Aplysia californica pedal ganglion neurons on nanostructured plasmonic crystals." *The Journal of Physical Chemistry B* 117.42 (2013): 13069-13081.
74. Hirata, Isao, et al. "Deposition of complement protein C3b on mixed self-assembled monolayers carrying surface hydroxyl and methyl groups studied by surface plasmon resonance." *Journal of Biomedical Materials Research Part A: An Official Journal of The Society for Biomaterials, The Japanese Society for Biomaterials, and The Australian Society for Biomaterials and the Korean Society for Biomaterials* 66.3 (2003): 669-676.
75. Hirata, Isao, et al. "Study of complement activation on well-defined surfaces using surface plasmon resonance." *Colloids and Surfaces B: Biointerfaces* 18.3-4 (2000): 285-292.
76. Iwasaki, Yuzuru, Tsutomu Horiuchi, and Osamu Niwa. "Detection of electrochemical enzymatic reactions by surface plasmon resonance measurement." *Analytical chemistry* 73.7 (2001): 1595-1598.
77. Zhou, M., et al. "Real-time measurements of kinetics of EGF binding to soluble EGF receptor monomers and dimers support the dimerization model for receptor activation." *Biochemistry* 32.32 (1993): 8193-8198.

78. Zhang, Jiayi, Tolga Atay, and Arto V. Nurmikko. "Optical detection of brain cell activity using plasmonic gold nanoparticles." *Nano letters* 9.2 (2009): 519-524.
79. Huang, Yu, et al. "Theoretical analysis of voltage-dependent fiber optic surface plasmon resonance sensor." *Optics Communications* 308 (2013): 109-114.
80. Hamidi, S. M., H. Goudarzi, and S. Sadeghi. "Surface plasmon resonance magneto-optical kerr effect in Au/Co/Au magneto-plasmonic multilayer." *Journal of Superconductivity and Novel Magnetism* 28.5 (2015): 1565-1569.
81. Sturm, Volker, et al. "The nucleus accumbens: a target for deep brain stimulation in obsessive–compulsive-and anxiety-disorders." *Journal of chemical neuroanatomy* 26.4 (2003): 293-299.
82. Belmonte, Matthew K., et al. "Autism and abnormal development of brain connectivity." *Journal of Neuroscience* 24.42 (2004): 9228-9231.
83. Viventi, Jonathan, et al. "Flexible, foldable, actively multiplexed, high-density electrode array for mapping brain activity in vivo." *Nature neuroscience* 14.12 (2011): 1599-1605.
84. Bahar, Sonya, et al. "Intrinsic optical signal imaging of neocortical seizures: the 'epileptic dip'." *Neuroreport* 17.5 (2006): 499-503.
85. Packer, Adam M., Botond Roska, and Michael Häusser. "Targeting neurons and photons for optogenetics." *Nature neuroscience* 16.7 (2013): 805-815.
86. Kim, Shin Ae, et al. "Optical measurement of neural activity using surface plasmon resonance." *Optics letters* 33.9 (2008): 914-916.
87. Kim, Shin Ae, et al. "In vivo optical neural recording using fiber-based surface plasmon resonance." *Optics letters* 37.4 (2012): 614-616.

88. Kim, Shin Ae, and Sang Beom Jun. "In-vivo optical measurement of neural activity in the brain." *Experimental neurobiology* 22.3 (2013): 158.
89. Grienberger, Christine, and Arthur Konnerth. "Imaging calcium in neurons." *Neuron* 73.5 (2012): 862-885.
90. Mutoh, Hiroki, et al. "Optogenetic monitoring of membrane potentials." *Experimental physiology* 96.1 (2011): 13-18.
91. Cao, Guan, et al. "Genetically targeted optical electrophysiology in intact neural circuits." *Cell* 154.4 (2013): 904-913.
92. Le, An-Phong, et al. "Quantitative reflection imaging of fixed Aplysia californica pedal ganglion neurons on nanostructured plasmonic crystals." *The Journal of Physical Chemistry B* 117.42 (2013): 13069-13081.
93. Curtis, A. S. "Cell reactions with biomaterials: the microscopies." *Eur Cell Mater* 1 (2001): 59-65.
94. Wessels, JTea, et al. "In vivo imaging in experimental preclinical tumor research–a review." *Cytometry Part A: the journal of the International Society for Analytical Cytology* 71.8 (2007): 542-549.
95. Yasui, Chikara, et al. "Sensitive fluorescence microscopy of neurons cultured on a plasmonic chip." *Japanese Journal of Applied Physics* 51.6S (2012): 06FK10.
96. Giepmans, Ben NG, et al. "The fluorescent toolbox for assessing protein location and function." *science* 312.5771 (2006): 217-224.
97. Hu, C. D., and T. K. Kerppola. "Simultaneous visualization of interactions between multiple proteins in living cells using multicolor bimolecular fluorescence complementation analysis." *Nat Biotechnol* 21 (2003): 539-545.

98. Wells, Jonathon, et al. "Pulsed laser versus electrical energy for peripheral nerve stimulation." *Journal of neuroscience methods* 163.2 (2007): 326-337.
99. Richter, Claus-Peter, et al. "Optical stimulation of auditory neurons: effects of acute and chronic deafening." *Hearing research* 242.1-2 (2008): 42-51.
100. Shapiro, Mikhail G., et al. "Infrared light excites cells by changing their electrical capacitance." *Nature communications* 3.1 (2012): 1-11.
101. Richter, C-P., et al. "Neural stimulation with optical radiation." *Laser & photonics reviews* 5.1 (2011): 68-80.
102. Katz, Elizabeth J., et al. "Excitation of primary afferent neurons by near-infrared light in vitro." *Neuroreport* 21.9 (2010): 662-666.
103. Paviolo, Chiara, et al. "Laser exposure of gold nanorods can increase neuronal cell outgrowth." *Biotechnology and bioengineering* 110.8 (2013): 2277-2291.
104. Sohrabi, Foozieh, and Seyedeh Mehri Hamidi. "Neuroplasmonics: from Kretschmann configuration to plasmonic crystals." *The European Physical Journal Plus* 131.7 (2016): 1-15.
105. Roy, Indrajit, et al. "Optical tracking of organically modified silica nanoparticles as DNA carriers: a nonviral, nanomedicine approach for gene delivery." *Proceedings of the National Academy of Sciences* 102.2 (2005): 279-284.
106. Tamaru, Hiroharu, et al. "Resonant light scattering from individual Ag nanoparticles and particle pairs." *Applied Physics Letters* 80.10 (2002): 1826-1828.
107. Atay, Tolga, Jung-Hoon Song, and Arto V. Nurmikko. "Strongly interacting plasmon nanoparticle pairs: from dipole− dipole interaction to conductively coupled regime." *Nano letters* 4.9 (2004): 1627-1631.

108. Lal, Surbhi, et al. "Profiling the near field of a plasmonic nanoparticle with Raman-based molecular rulers." *Nano letters* 6.10 (2006): 2338-2343.
109. Talley, Chad E., et al. "Surface-enhanced Raman scattering from individual Au nanoparticles and nanoparticle dimer substrates." *Nano letters* 5.8 (2005): 1569-1574.
110. Taton, T. Andrew, Chad A. Mirkin, and Robert L. Letsinger. "Scanometric DNA array detection with nanoparticle probes." *Science* 289.5485 (2000): 1757-1760.
111. Zhang, Jiayi, Tolga Atay, and Arto V. Nurmikko. "Optical detection of brain cell activity using plasmonic gold nanoparticles." *Nano letters* 9.2 (2009): 519-524.
112. Liao, Hongwei, Colleen L. Nehl, and Jason H. Hafner. "Biomedical applications of plasmon resonant metal nanoparticles." (2006): 201-208.
113. Haes, Amanda J., et al. "Localized surface plasmon resonance spectroscopy near molecular resonances." *Journal of the American Chemical Society* 128.33 (2006): 10905-10914.
114. Smythe, Elizabeth J., Ertugrul Cubukcu, and Federico Capasso. "Optical properties of surface plasmon resonances of coupled metallic nanorods." *Optics Express* 15.12 (2007): 7439-7447.
115. Le, An-Phong, et al. "Quantitative reflection imaging of fixed Aplysia californica pedal ganglion neurons on nanostructured plasmonic crystals." *The Journal of Physical Chemistry B* 117.42 (2013): 13069-13081.
116. Rodrigo, Sergio G., Fernando de Leon-Perez, and Luis Martin-Moreno. "Extraordinary optical transmission: fundamentals and applications. " *Proceedings of the IEEE* 104.12 (2016): 2288-2306.

117. Tao, Long, et al. "Gate-tunable plasmon-induced transparency modulator based on stub-resonator waveguide with epsilon-near-zero materials." *Scientific reports* 9.1 (2019): 1-8.
118. Kim, Shin Ae, et al. "Optical measurement of neural activity using surface plasmon resonance." *Optics Letters* 33.9 (2008): 914-916
119. Koepsell, Hermann. "Glucose transporters in brain in health and disease." *Pflügers Archiv-European Journal of Physiology* 472.9 (2020): 1299-1343.
120. Kullmann, Stephanie, et al. "Brain insulin resistance at the crossroads of metabolic and cognitive disorders in humans." *Physiological reviews* 96.4 (2016): 1169-1209.
121. Santiago, João CP, and Manfred Hallschmid. "Outcomes and clinical implications of intranasal insulin administration to the central nervous system." *Experimental Neurology* 317 (2019): 180-190.
122. Bagaméry, Fruzsina, et al. "Lack of insulin resistance in response to streptozotocin treatment in neuronal SH-SY5Y cell line." *Journal of Neural Transmission* 127.1 (2020): 71-80.
123. Hu, Wanjun, et al. "Highly sensitive detection of dopamine using a graphene functionalized plasmonic fiber-optic sensor with aptamer conformational amplification." *Sensors and Actuators B: Chemical* 264 (2018): 440-447.
124. Prince MJ, Wimo A, Guerchet MM, Ali GC, Wu Y-T, Prina M. World Alzheimer Report 2015 - The Global Impact of Dementia: An analysis of prevalence, incidence, cost and trends. London: Alzheimer's disease International, 2015. 84 p.
125. Alzheimer’s disease facts and figures. "Alzheimers Dement." (2020): 391-460.

126. Canevelli M, Lacorte E, Cova I, Zaccaria V, Valletta M, Raganato R, et al. Estimating dementia cases amongst migrants living in Europe. Eur J Neurol. 2019; 26:1191–9.
127. Masters, C. L. & Selkoe, D. J. Biochemistry of amyloid β-protein and amyloid deposits in Alzheimer disease. Cold Spring Harb. Perspect. Med. 2, a006262 (2012).
128. Amini, Morteza, et al. "Plasmonics Optoelectronics Nanobiosensors for Detection of Alzheimer's Disease Biomarker via Amyloid-Beta (Aβ) in Near-Infrared."*Plasmonics* 17.3 (2022): 1191-1201.
129. Sotiropoulos, Ioannis, et al. "Atypical, non-standard functions of the microtubule associated Tau protein." *Acta neuropathologica communications* 5.1 (2017): 1-11.
130. Kamat, Pradip Kumar. "Streptozotocin induced Alzheimer's disease like changes and the underlying neural degeneration and regeneration mechanism." *Neural regeneration research* 10.7 (2015): 1050.
131. Salkovic-Petrisic, Melita, and Siegfried Hoyer. "Central insulin resistance as a trigger for sporadic Alzheimer-like pathology: an experimental approach."*Neuropsychiatric disorders an integrative approach* (2007): 217-233.
132. Wu, Jinzi, and Liang-Jun Yan. "Streptozotocin-induced type 1 diabetes in rodents as a model for studying mitochondrial mechanisms of diabetic β cell glucotoxicity." *Diabetes, metabolic syndrome and obesity: targets and therapy* 8 (2015): 181.
133. Wang, Zhiyong, and Helga Gleichmann. "GLUT2 in pancreatic islets: crucial target molecule in diabetes induced with multiple low doses of streptozotocin in mice." *Diabetes* 47.1 (1998): 50-56.
134. Zhang, Yonglan, et al. "Geniposide attenuates insulin-deficiency-induced acceleration of β-amyloidosis in an APP/PS1 transgenic model of Alzheimer's disease." *Neurochemistry international* 89 (2015): 7-16.

135. Plaschke, Konstanze, and Jürgen Kopitz. "In vitro streptozotocin model for modeling Alzheimer-like changes: effect on amyloid precursor protein secretases and glycogen synthase kinase-3." *Journal of neural transmission* 122.4 (2015): 551-557.
136. Guo, Xiao-dan, et al. "Small molecule LX2343 ameliorates cognitive deficits in AD model mice by targeting both amyloid β production and clearance." *Acta Pharmacologica Sinica* 37.10 (2016): 1281-1297.
137. Zhang, Zhengren, et al. "Plasmon induced transparency in a surface plasmon polariton waveguide with a comb line slot and rectangle cavity." *Applied Physics Letters* 104.23 (2014): 231114
138. Shepardson, Dylan. *Algorithms for inverting Hodgkin-Huxley type neuron models*. Georgia Institute of Technology, 2009.

الخلاصة

يحتوي دماغ الإنسان على بلايين من الخلايا العصبية التي تتحكم في الجهاز العصبي المركزي. العديد من التقنيات تم استخدامها لتسجيل أنشطة الخلايا العصبية وتصويرها مثل تقنية تخطيط الدماغ (EEG) ، تقنيات التصوير بالرنين المغناطيسي(MEG, MRI, fMRI) ،والتقنيات الضوئية ... إلخ. يعد تسجيل النشاط العصبي مع دقة مكانية وزمانية عالية في مجال أنسجة الدماغ هو التحدي الأكثر صعوبة لجميع تلك الأساليب. لذلك ، تطلبت هذه التحديات تقنيات جديدة لتسجيل انشطة الخلاليا العصبية في مجال البصريات والإلكترونيات وغيرها من التقنيات لزيادة الدقة الزمانية والمكانية.

إحدى التقنيات الحديثة لاستشعار نشاط الخلايا العصبية ذات الدقة المكانية والزمانية العالية هي تقنية البلازمونيك. تستخدم هذه التقنية استشعار رنين البلازمون السطحي (SPR) لاكتشاف نشاط الخلايا العصبية. يُطلق على استخدام تقنية البلازمونك مع استشعار الخلايا العصبية تقنية النيوروبلازمونك (Neuroplasmonics). تجمع هذه التقنية بين الاستشعار البيولوجي وتقنيات النانو علاوة على ذلك ، فإنها توفرعدة مزايا مثل الكشف الغير مقيد او ما يعرف بـ(label free) , التحليل الآني, التوافق الحيوي مع الخلايا, صغر حجم الشريحة, الامكانية العالية على كشف النشاط العصبي مع جودة الاشارة المستلمة.

في هذه الأطروحة، تم تصنيع رقاقة كهروبلازمونية احاية الأبعاد (1D) تتكون من طبقة عازلة من مادة البولي كاربونات. هذه الطبقة تم طلائها بطبقة نانوية من الذهب (٣٥ نانومتر). تم توصيل الشريحة بسلكين عن طريق اطراف الشريحة لتسليط جهد خارجي. تضمنت الخطوة الأولى تقييم كفاءة هذه الشريحة في مختبر البلازمونك للعمل كمتحسس بلازموني ومن ثم قياس تراكيز مختلفة للناقل العصبي الدوبامين. اما الخطوة الثانية فكانت بزراعة الشريحة الكهروبلازمونية بخلايا عصبية مستخرجة من دماغ الفئران وتحفيزها بواسطة الدوبامين. كانت الغاية من هذه الخطوة هي لتقييم قدرة الشريحة الكهروبلازمونية للكشف عن نشاط الخلايا العصبية المستزرعة. أخيرًا ، تمت زراعة الشريحة الكهروبلازمونية بخلايا النواة اللبية البشرية (HNPC) ومن ثم حقنها بالستربتوزوتوسين (STZ). كانت هذه الخطوة لتقييم قدرة الشريحة المقترحة على استشعار تثبيط الخلايا العصبية المستزرعة.

أظهرت النتائج ظاهرة فيزيائية لطيفة تُعرف بالتحريض البلازموني للشفافية (PIT). تنتج هذه الظاهرة الفيزيائية مع ظاهرة الرنين البلازمون السطحي (SPR) وهي مناسبة لاستشعار نشاط الخلايا العصبية. عند تسليط جهد تيار مستمر خارجي لوحظ ازدياد سعة شدة الضوء ، مما يشير الى امكانية زيادة مقدار الشفافية وبالتالي زيادة حساسية الشريحة المقترحة.

كما أظهرت الرقاقة المقترحة نتائج ممتازة لاستشعار التراكيز المختلفة من الدوبامين (٣٠٠ و ٧٠٠ جزء في المليون). لوحظ اختلاف واضح للغاية في قراءة جهاز المطياف الضوئي وخاصة ضمن الطول الموجي من ٥٨٠ نانومتر إلى ٦٠٠ نانومتر.

الخطوة التالية تضمنت زراعة اثني عشر عينة بخلايا عصبية (الفئران) ثم تم تحفيزها بتراكز مختلفة من الدوبامين. أظهرت النتائج القدرة العالية للرقاقة المقترحة لاستشعار نشاط الخلايا العصبية بتركيز عالٍ (٧٠٠ جزء في المليون) وتركيز منخفض حوالي ٠,٥ جزء في المليون. أيضًا ، قد تشير الحساسية العالية مع التركيز المنخفض من ٢ إلى ١٠ دقائق إلى احتمال وجود ظاهرة (EOT).

أما الخطوة الأخيرة ، فتمت زراعة مجموعة عينات من الشريحة المصنعة (٨ عينات) بخلايا بشرية تعرف ب (HNPC) وحقنها بمادة الستربتوزوتوسين (STZ) في ثلاثة تراكيز مختلفة (٠,٥ ، ١ ، ٢ ملي مول). كان الهدف من ذلك هو إحداث مرض الزهايمر وقياس مقدار تثبيط الخلية. أظهرت النتائج أن نشاط الخلية انخفض (تثبيط) مع زيادة جرعة STZ. واشارت هذه إلى الحساسية العالية للرقاقة الكهروبلازمونية لامكانية استشعار نشاط الخلايا العصبية المثبطة بعد اصابتها بمرض الزهايمر.

جمهورية العـراق
وزارة التعليم العالي والبحث العلمي
جامعــة بابـل/ كليـــــة الهندســـة
قسم الهندسة الكهربائية

تنفيذ شريحة البلازومينيك الكهربائية للكشف عن مرض الزهايمر

اطروحة

مقدمة إلى جامعة بابل - كلية الهندسة وهي جزء من متطلبات الحصول على درجة الدكتوراه فلسفة في الهندسة / الهندسة الكهربائية / الكترونيك واتصالات

من قبـل

حسام جواد كاظم عبود الجنابي

بإشـراف

أ.م.د.حيدر صاحب المؤمن

أ.م.د.حسين هادي ناهي

١٤٤٤هـ ٢٠٢٣م